THE EVOLUTION OF A FOSFOMYCIN RESISTANCE ENZYME, FOSA, FROM *Pseudomonas aeruginosa* AND THE DEVELOPMENT OF A HIGH-THROUGHPUT SCREEN FOR THE DISCOVERY OF BIOACTIVE INHIBITORS

By

Daniel Wade Brown

Dissertation

Submitted to the Faculty of the

Graduate School of Vanderbilt University

in partial fulfillment of the requirements

for the degree of

DOCTOR OF PHILOSOPHY

in

Chemistry

August, 2010

Nashville, TN

Approved:

Professor Richard N. Armstrong

Professor Brian O. Bachmann

Professor David W. Wright

Professor Alan R. Brash

Professor F. Peter Guengerich

ACKNOWLEDGEMENTS

Firstly, I have to thank my wonderful wife who pushed me for all of these years and never gave up in her belief in me. I could never have done this without her love and support. I would like to thank my parents for teaching me to love knowledge and training me to be a student. Their support throughout my life has been invaluable in allowing me to write this document. A big thank you goes to Dr. Sarath Gunasekera and the Drug Discovery Program at Harbor Branch Oceanographic Institute for the opportunity to do my first real drug discovery research.

I have to really thank Emily, Michelle, and Dan in the High Throughput Screening core. Without their help and the guidance of the HTS Core director Dave Weaver, the main part of this thesis would have never gotten off the ground. Thanks go to Dr. Wright for getting me in to graduate school in the first place and then for serving on my committee as well. I would like to thank Dr. Bachmann, Dr. Brash, and Dr. Guengerich for serving on my committee as well and helping guide me through my research.

Finally, I would like to thank Dr. Armstrong for giving me the leeway to pursue a project that I thought was interesting and to let me run with it. It has been an adventure and I owe him greatly for giving me the freedom to pursue a new research avenue.

This work was supported by the National Institutes of Health (R01 AI042756 and R56 AI042756-10A) and by the Center in Molecular Toxicology Training Grant (T32 ES007028).

TABLE OF CONTENTS

LIST OF TABLES

Table Page

LIST OF FIGURES

ABBREVIATIONS

FDA	Food and Drug Administration
GSK	GlaxoSmithKline
Tn	Transposon
ED_{50}	50% Effective Dose
UDP-GlcNAc	Uridine-5'-diphospho-*N*-acetyl-D-glucosamine
PEP	Phosphoenolpyruvate
PDB	Protein Data Bank
G6P	Glucose-6-phosphate
GSH	Reduced Glutathione
BLAST	Basic Local Alignment Search Tool
MIC	Minimum Inhibitory Constant
VOC	Vicinal Oxygen Chelate
HTS	High-Throughput Screening
Pf	Phosphonoformate
mBBr	Monobromobimane
EDTA	Ethylenediamine tetraacetic acid
Tris	Tris(hydroxymethyl)aminomethane
MOPS	3-(N-morpholino)-propanesulfonic acid
HEPES	N'-(2-ethanesulfonic acid) free acid
TMA-OH	Tetramethylammonium hydroxide
LB	Luria broth

HPLC	High Performance Liquid Chromatography
DMSO	Dimethyl sulfoxide
IPTG	Isopropyl-b-D-thiogalactopyranoside
DTT	Dithiothreitol
AQC	6-aminoquinolyl-N-hydroxysuccinimidyl carbamate
HA	Hydroxyapatite
DEAE	Diethyl aminoethyl
FPLC	Fast Protein Liquid Chromatography
SDS-PAGE	Sodium dodecylsulfate polyacrylamide gel electrophoresis
NMR	Nuclear Magnetic Resonance
PCR	Polymerase Chain Reaction
UV	Ultraviolet
OD_{600}	Optical Density at 600 nm
PEG	Polyethylene glycol
CCD	Charge Coupled Device
$IC_{50,80}$	50%, 80% Inhibition Concentration
PP	Polypropylene
PS	Polystyrene
CB	ChemBridge
CD	ChemDiv
CRC	Concentration-Response Curve
VCSC	Vanderbilt Chemical Synthesis Core
NAA	Neutron Activation Analysis

HSQC	Heteronuclear Single Quantum Coherence
HMBC	Heteronuclear Multiple Bond Correlation
COSY	Correlation Spectroscopy
NOESY	Nuclear Overhauser Effect Spectroscopy
DAPBA	3-(Dansylamino)phenyl boronic acid
8-QBA	8-quinoline boronic acid
EPA	Ethylphosphonic acid
PAA	Phosphonoacetic acid
CEPA	2-carboxyethylphosphonic acid
ECP	Ethoxycarbonyl phosphate
AMP, ADP, ATP	Adenosine mono-, di-, and triphosphate
EGTA	Ethylene glycol tetraacetic acid
ADA	Alanine diacetic acid
HEDTA	Hydroxyethylethylenediaminetriacetic Acid
BAPTA	1,2-bis(o-aminophenoxy)ethane-N,N,N',N'-tetraacetic acid
PHOME	(3-Phenyl-oxiranyl)-acetic acid cyano-(6-methoxy-napthalen-2-yl)-methyl ester
RMSD	Root Mean Square Distance
GS-mB	Glutathione adducted bimane product
SAR	Structure-Activity Relationship

CHAPTER I

INTRODUCTION

Antibiotic History

In 1929 Alexander Fleming changed the future of medicine and how we treat disease.[1] The publication of the antibacterial effect of the fungus *Penicillium* upon the growth of *Bacillus influenzae* (since renamed *Haemophilus influenzae*) began the battle between man and microbe (Figure 1). The discovery and subsequent introduction of penicillin into the clinic not only opened a new field of research, but also an entirely new industry.[2] Penicillin G was approved by the FDA in 1943 and an explosion of discovery soon followed.[3] Soon after the successful introduction of penicillin, several antibiotics were introduced to the clinic in the following 25 years. This golden age of antibiotics was responsible for the introduction of streptomycin, tetracycline, methicillin, fosfomycin, and more.

After this explosion of new drugs hit the market, it took another thirty-two years for another new class of antibiotic to be introduced into the clinic (Figure 2).[4,5] The time elapsed between the introduction of trimethoprim in 1968 and the oxazolidinones in 2000 was filled with many factors that influenced the future of drug discovery and antibiotic drug discovery in particular. During this time many large pharmaceutical companies began to merge and focus on targets that would require patients to take medications over a longer period of time. Larger companies needed larger profits in order to remain stable. With the flood of antibacterial agents that hit the market in the 1950's and 1960's, market competition was fierce and research turned to new areas with higher profit potential.[6]

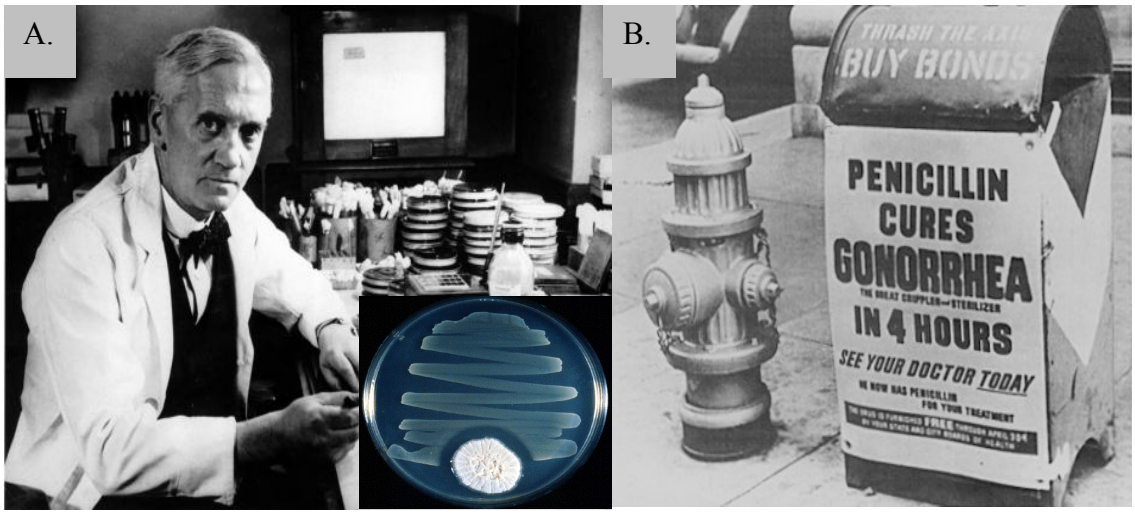

Figure 1: A) Alexander Fleming in his lab. Inset: a microplate of the fungus *Penicillium* inhibiting the growth of *E. coli*. B) Sign placard demonstrating one of the less serious, but no less meaningful, changes made in the medical establishment.

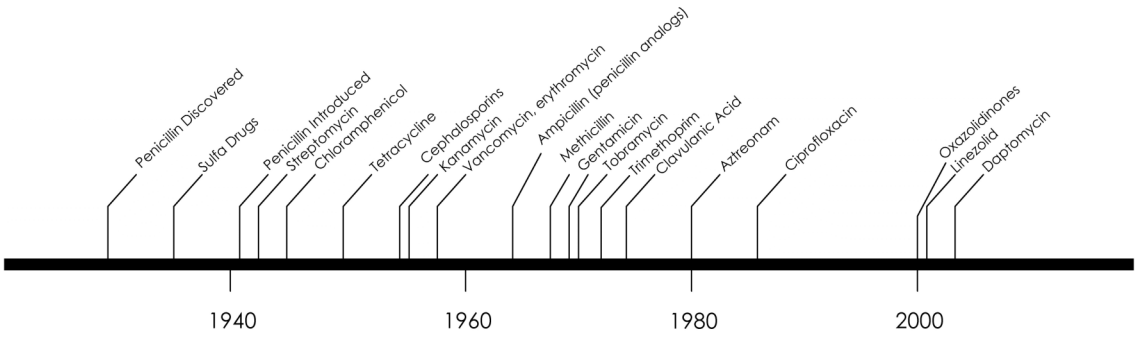

Figure 2: Cartoon timeline of antibiotic introduction to the clinic. Modified from Reference #5.

There has been a re-focusing of research into novel antibacterial agents in recent years. The last eight years has seen new classes of antibiotics hitting the markets, in the form of the oxazolidinones and lipopeptides. The discovery of a new class of antibiotic that has yet to be introduced into the clinic, platensimycin, has also been reported.[7] Much of this new research has been spurred by the increase in the number of antibiotic resistant infections being seen in the clinic. Every antibiotic introduced into the clinic has had resistance reported shortly thereafter. Antibiotic resistance was one of the factors that propagated the exit of many large companies from the antibiotic research field. However, in recent years, many smaller research firms have begun to take up the task of developing new antibiotics.[3,4,8]

Antibiotic Resistance

In 2002, the global antibiotic market value was an estimated US $25 billion and estimated to be about the same in 2005 (Figure 3). The top antibiotics totaled over US $8.5 billion in sales in the United States alone in 2005.[9,10] While they remain profitable, antibiotics are less so when compared to other drugs, such as cholesterol controlling drugs where a single drug may make in excess of US $9 billion alone.[2] Resistance also takes a major financial toll, costing an estimated US $5-20 billion a year.[11] Therefore, despite its remaining profitability and overall sales increasing yearly, the number of new drugs hitting the market is falling rapidly (Figure 4).[8]

One of the main reasons for the increase in resistance seen over the last several years is that the cellular targets of antibiotics remain rather limited. Antibiotics target

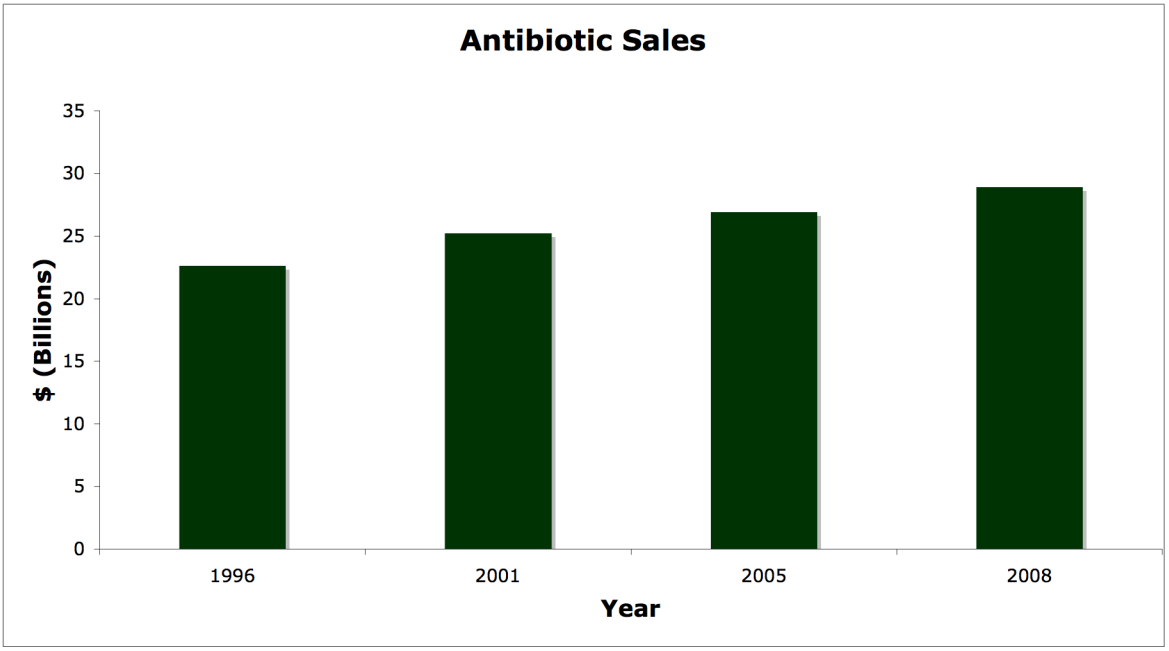

Figure 3: Sales of antibiotics from the years 1996 to 2008. Modified from Reference #8.

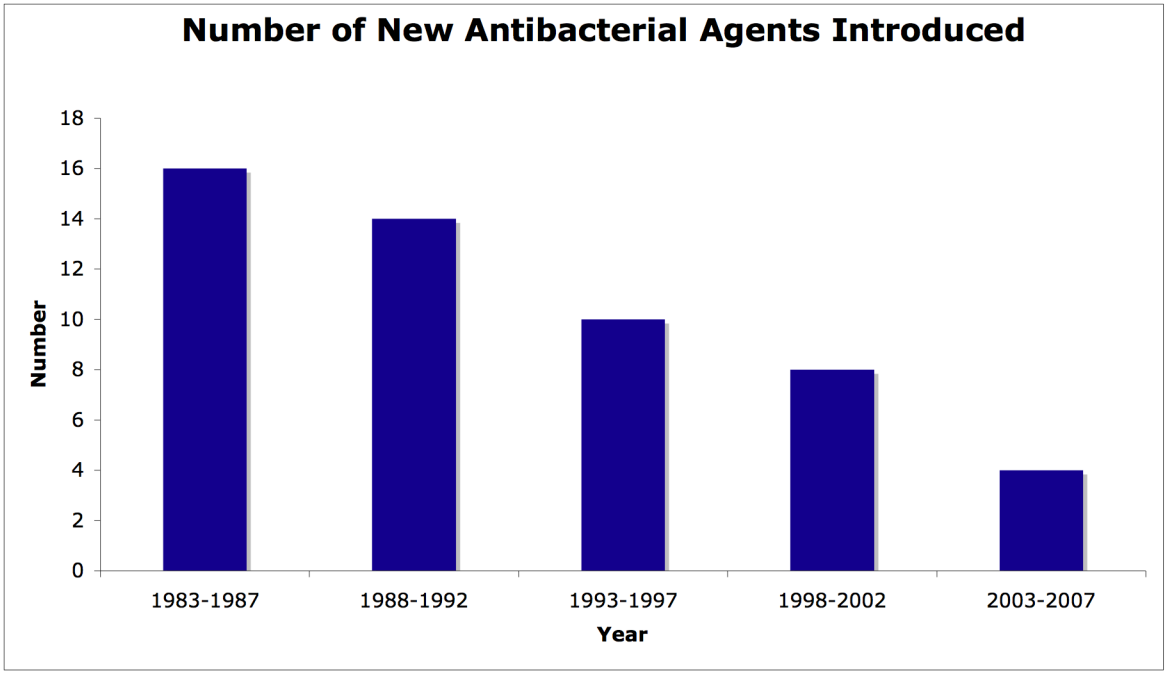

Figure 4: Number of new antibiotics on the market from 1983 to 2007. Modified from Reference #8.

only a few main cellular functions: cell wall biosynthesis, protein synthesis, nucleic acid synthesis, folate metabolism, isoprenoid biosynthesis, and cell membrane structure disruption. The actual number of targets is fewer still as companies look for the greatest reward with the fewest number of side effects. The few number of targets limits the search to those that either do not have human analogs or can be sufficiently discerned from their human analogs with adequate specificity.

Another reason for the increase in resistance is that there are several mechanisms by which a bacterium can become resistant to an antibiotic (Figure 5). In addition, once a bacterium has developed a mechanism of resistance it can be easily transferred to other bacterium. Resistance determinants can develop via mutation of genomically encoded enzymes or be taken up from the environment or via horizontal gene transfer between bacteria (Figure 6). This allows resistance determinants to quickly spread through bacterial populations and compounds problems combating antibiotic resistance.[12] In fact, it has been recently shown that antibiotic resistant determinants can be found in soil microbes from many different environments and that some bacteria are able to use current antibiotics as the sole carbon source in their diet.[13-15]

In the face of these odds it is imperative that the development of new antibiotics and maintaining the effectiveness of current antibiotics become a priority.[16] One method of looking for new drugs is to find new targets. In 2006, Payne, *et al*. from GlaxoSmithKline (GSK) published an interesting paper in which they made systematic mutations throughout the *Streptococcus pneumoniae* to determine which genes were essential for the growth and development of the bacterium. They found that 127 of the 358 genes tested were essential. These essential genes were a good starting point to

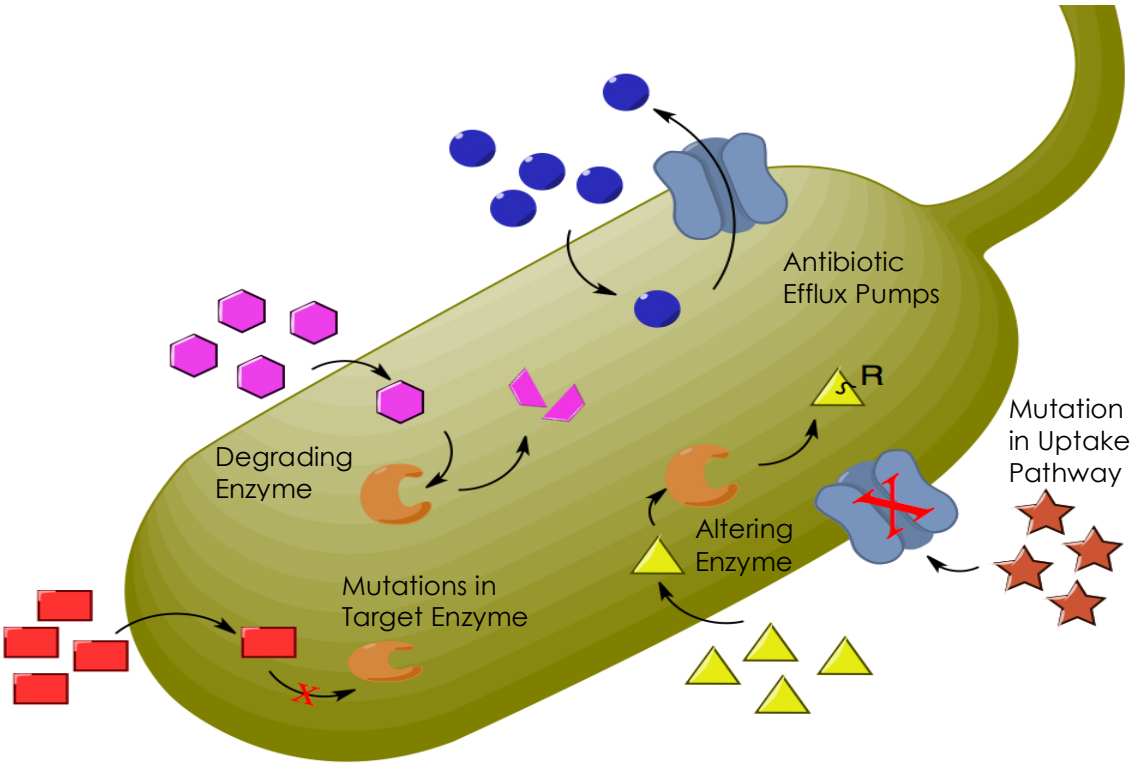

Figure 5: Cartoon depiction of the five methods of bacterial resistance to antibiotics. Modified from Reference #13.

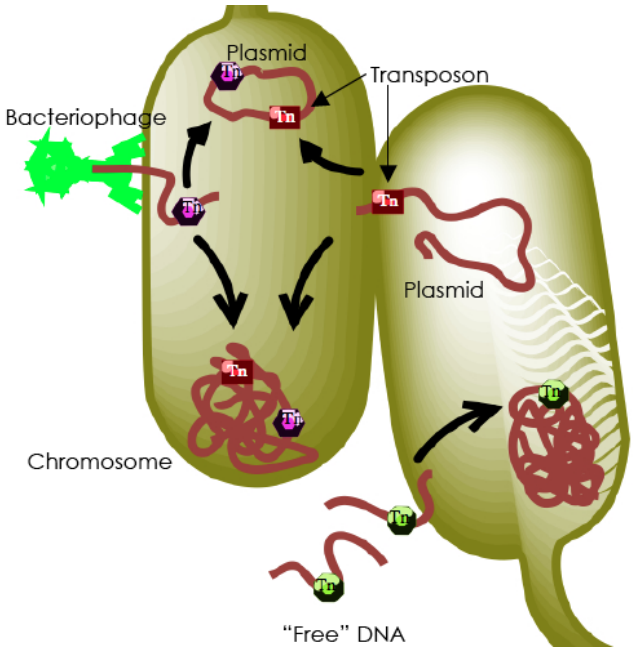

Figure 6: Cartoon depicting the many ways transposable resistance elements can be transferred among bacterial populations. Modified from Reference #13.

begin high-throughput screening campaigns for targeted enzymes as well as whole cell assays. This is just one example of a strategy to develop new antimicrobial compounds.[17]

Other strategies for combating antibiotic resistance are plentiful. These include but are not limited to: finding new compounds for already established targets, such as MurA in cell wall biosynthesis,[18] finding compounds to target new enzymes, such as platensimycin inhibition of FabF in bacterial type II fatty-acid synthesis,[7] inhibiting antibiotic resistance propagation,[19] cell-division inhibition,[20] inhibiting mechanisms involved with persistence and adaptation,[21] efflux-pump inhibitors,[22] and stress response inhibitors.[23] Many of these methods are promising and will probably lead to new antibiotics in the near future.

Until these new compounds can be clinically verified and reach the market, work is needed to maintain the effectiveness of current antibiotics. One commercially effective solution has been to find a way to inhibit enzymatic mechanisms of resistance so the antibiotic can perform its intended function. The β-lactamase inhibitors clavulanate, tazobactam, and sulbactam have been used clinically for decades to maintain the utility of β-lactam drugs, like amoxicillin.[24] Clavulanate was first discovered in 1972 and went on to be a commercial success, sold as a combination oral drug with amoxicillin as Augmentin (GSK)(Figure 7).[25] It is possible that this method could be effective in

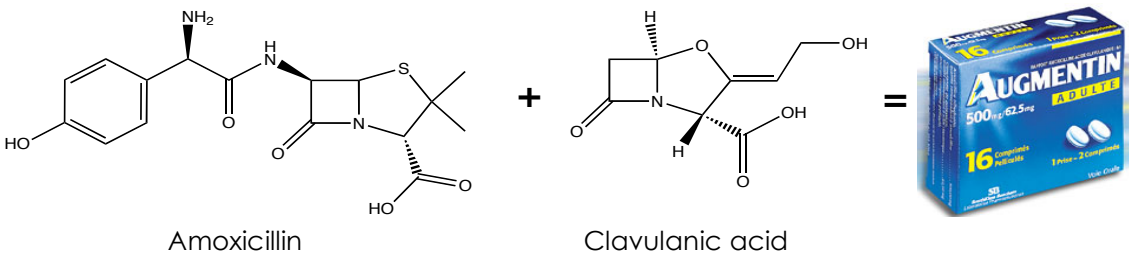

Amoxicillin Clavulanic acid

Figure 7: Molecular structures of the components of Augmentin.

preserving the activity of many antibiotics where enzymatically catalyzed resistance is a key factor. This method may also be a successful way to reintroduce old antibiotics into the clinic.

Fosfomycin

One old antibiotic that may be resuscitated is the broad-spectrum antibiotic fosfomycin, **1**. Fosfomycin was first discovered by scientists at Merck as an isolate from certain species of *Streptomyces*.[26] Its initial structure was determined by comparison to the synthetic compound.[27] Fosfomycin was found to be a low molecular weight acid with a good ED_{50} to several various strains of infectious bacteria, including *Escherichia coli, Klebsiella pneumoniae, Pseudomonas aeruginosa,* and *Staphylococcus aureus*, marking it as an effective broad-spectrum antibiotic.

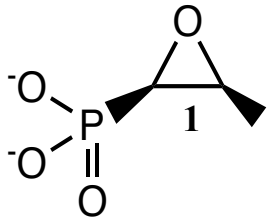

It was discovered that fosfomycin acts as a suicide inhibitor of the enzyme UDP-N-acetylglucosamine enolpyruvoyl transferase (MurA) in both Gram-positive and Gram-negative bacteria. MurA catalyzes the first committed step in bacterial cell wall biosynthesis. Fosfomycin inhibits this enzyme by forming a covalent adduct at the C-2 position to a catalytically required active site cysteine, C115 (*E. coli* numbering)(Figure 8).[28,29] Also of note, the substrate UDP-N-acetylglucosamine (UDP-GlcNAc) is necessary for fosfomycin to inhibit MurA. It is believed that this is due to UDP-GlcNAc causing a large conformational change in the enzyme opening C115 to attack.

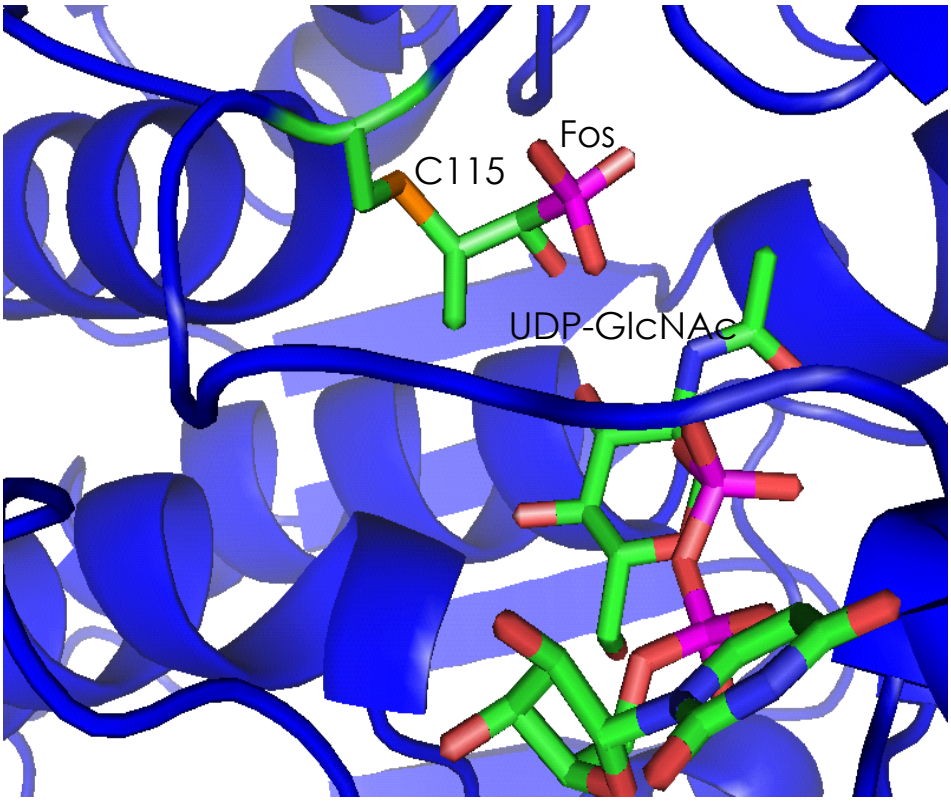

Figure 8: Crystal structure of MurA with fosfomycin covalently adducted to C115. Also shown is UDP-GlcNAc, required to implement the structural rearrangement that exposes C115. Made using PDB 1UAE.

Bacterial resistance to fosfomycin was noted early on via mutations in the uptake pathways necessary for the drug to enter the cells.[28] Fosfomycin enters the bacterium via either the glycerophosphate (glpT) or hexose phosphate transport systems (uhp). The glpT transport system is the primary system of flux for the antibiotic with the uhp system only becoming active in the presence of an inducer, such as glucose-6-phosphate. Bacteria that develop mutations in these uptake pathways are resistant to fosfomycin since the antibiotic cannot reach its target in the cytoplasm of the cell. Resistance has also been reported via an altered target enzyme. This enzyme, in *M. tuberculosis*, has a C114D mutation that allows the enzyme to remain active while also becoming resistant to fosfomycin.[30]

Another main source of bacterial resistance to fosfomycin is enzymatic in nature. Enzymatic fosfomycin resistance was first isolated from a multi-drug resistant plasmid, pOU900, isolated from a clinical infection of *Serratia marcescens*.[31] The fosfomycin resistance determinant was isolated and named Tn*2921*. It was later found that this determinant does not affect transport of fosfomycin into the cells, but was a novel enzymatic entity that modifies the antibiotic via the addition of the tri-peptide glutathione (GSH)(Figure 9).[32-36] This enzyme is a metalloenzyme that requires Mn^{2+} for activity and is activated 100-fold by the presence of K^{+}.[37,38]

Interestingly, the final product of the Tn*2921* enzyme, FosA, is a covalent adduct of fosfomycin and GSH with the covalent bond formed at the C-1 position of fosfomycin.[39] The crystal structure of the related, genomically encoded, FosA from *Pseudomonas aeruginosa* (60% sequence identity to the plasmid encoded, Tn*2921* FosA) gave insight into the mechanism by which this reaction occurs.[40] Fosfomycin coordinates directly to the Mn^{2+} ion at both the phosphonate moiety and the oxirane oxygen. The K^{+} is not directly involved in catalysis, but it is 4.4 Å from the nearest phosphonate oxygen, so it may help orient fosfomycin in the active site for attack at the C-1 position.

Over the last several years BLAST searches against protein data banks have revealed several more genomically encoded FosA enzymes as well as two other classes of fosfomycin resistance enzyme, the FosB and FosX classes (Figure 10). The FosB enzymes have about 30% sequence identity to the FosA enzymes but have slightly different function.[41] The FosB enzymes are found in Gram-positive bacteria, which do not biosynthesize glutathione. As such they may utilize either free L-cysteine or the newly described bacillathiol as a thiol substrate, Figure 9.[42] The FosB enzymes are not

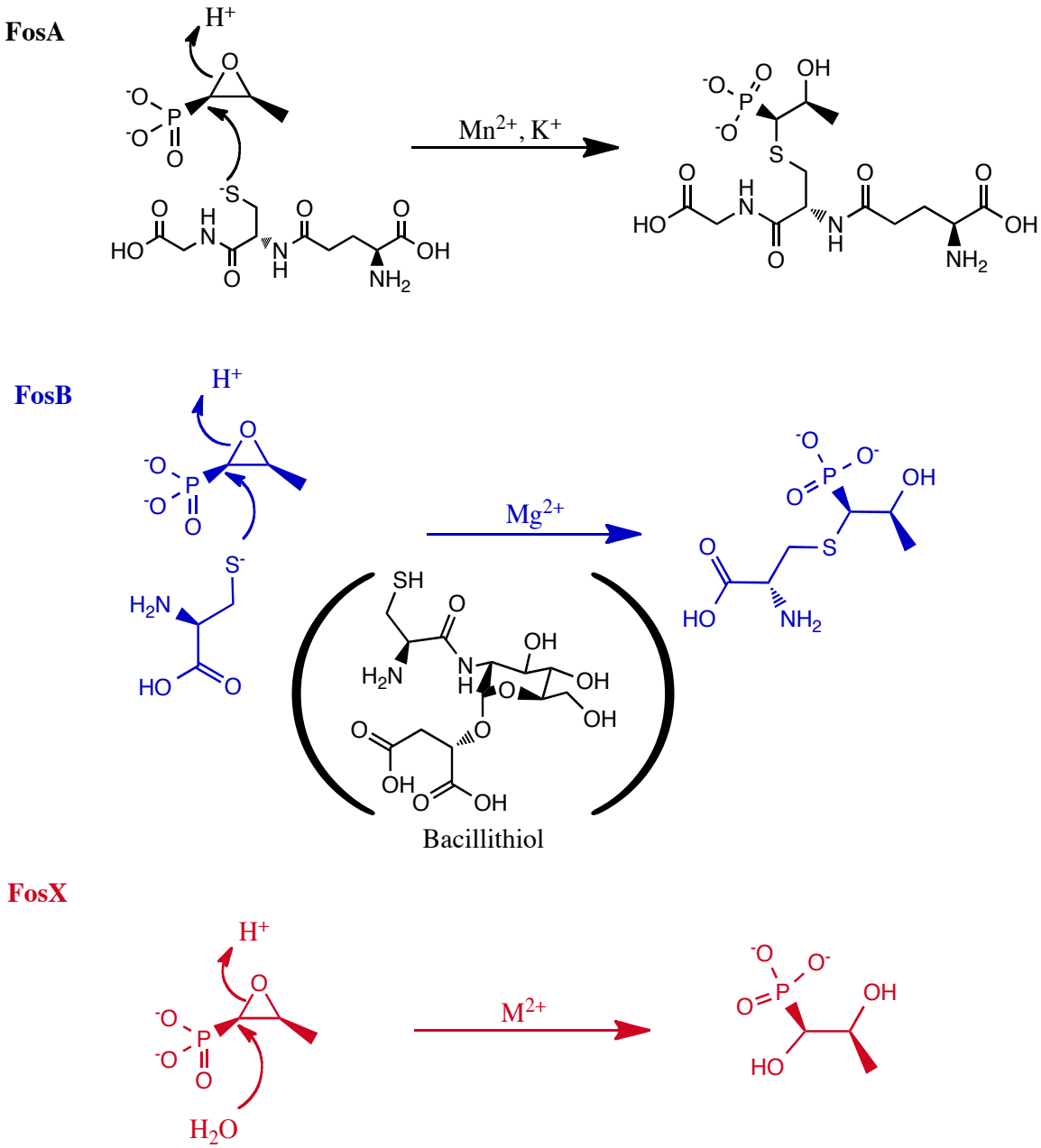

Figure 9: Mechanism of the FosA, FosB, and FosX enzymes.

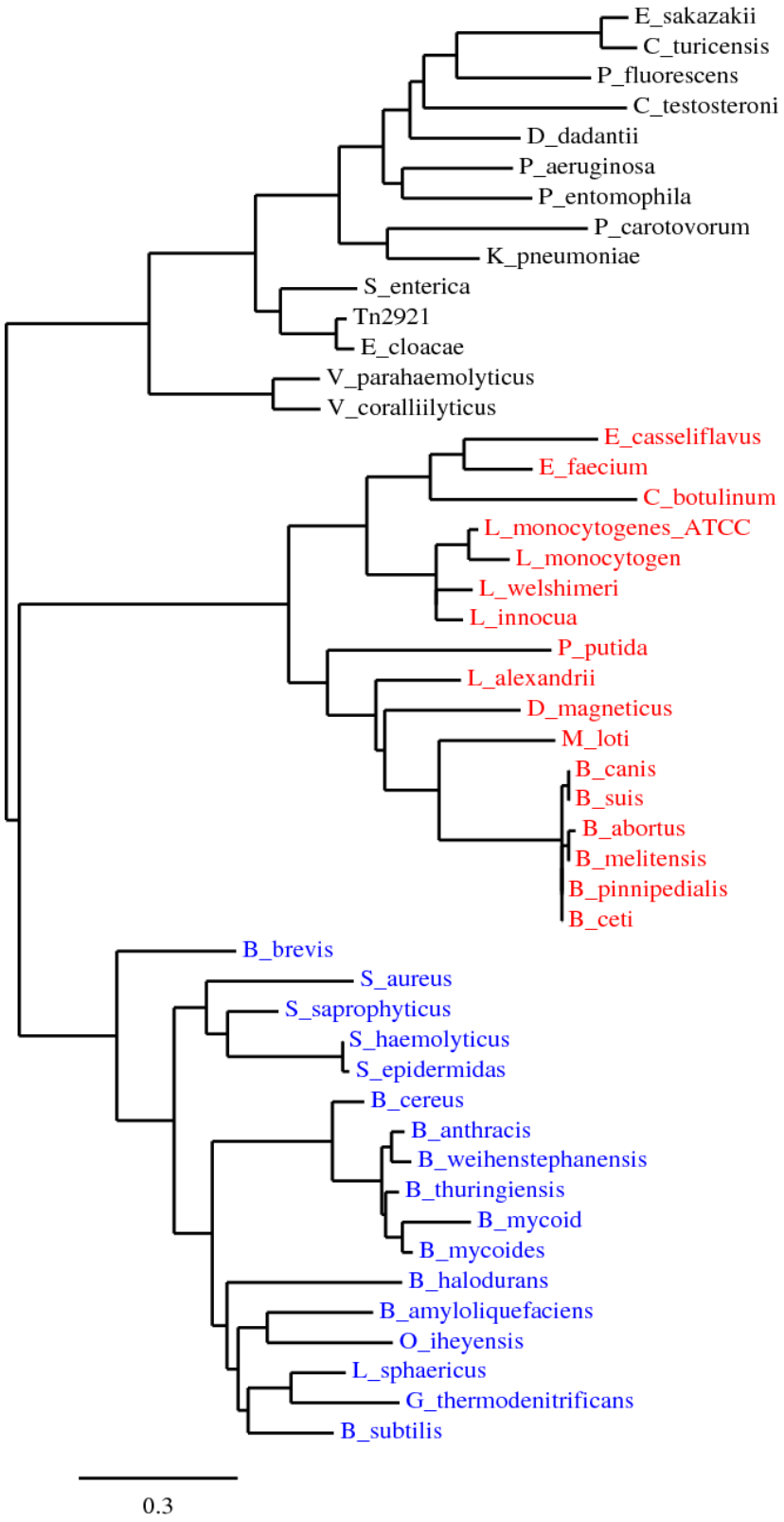

Figure 10: Phylogram of the Fosfomycin Resistance Enzymes. The FosA enzymes are in black, the FosB enzymes are in blue, and the FosX enzymes are in red.

activated by monovalent cations, but do retain the necessity of a divalent metal cation, most often Mg^{2+} is preferred. No structure has been elucidated for these enzymes, but they are expected to be very similar to FosA based on sequence identity.

The FosX enzymes are a rather different class of Fos. These enzymes also require a divalent metal cation; often Mn^{2+} is preferred, although Cu^{2+} can also work in many cases and is preferred in at least one. These enzymes are also not activated by monovalent cations, similar to the FosB enzymes. The major difference in these enzymes is that they do not use a thiol substrate for addition to the antibiotic but add water to the C-1 position of fosfomycin, hydrolyzing it to a 1,2-vicinal diol (Figure 9).[43,44] There is also a broad range of activity within this class of enzyme in that some transfer exemplary resistance to *E. coli* when introduced on a plasmid vector, and some transfer almost no resistance at all. This class of enzymes, therefore, may give deeper insights into the nature of enzyme structure/function relationships and offer a unique opportunity to study how these enzymes may have evolved.

Enzyme Evolution

In 1999 O'Brien and Herschlag wrote a review detailing the myriad ways in which enzymes that were catalytically promiscuous could be easily used in adaptive evolution for the formation of new enzymes with new primary functions.[45] The Fos enzymes provide an intriguing possibility to study the mechanism by which this may occur. The primary example for this is the FosX enzyme from *Mesorhizobium loti*.

The *M. loti* FosX is a very poor resistance enzyme with a $k_{cat} = 0.15\ s^{-1}$ and a minimum inhibitory constant (MIC) when transformed into *E. coli* on a plasmid vector of

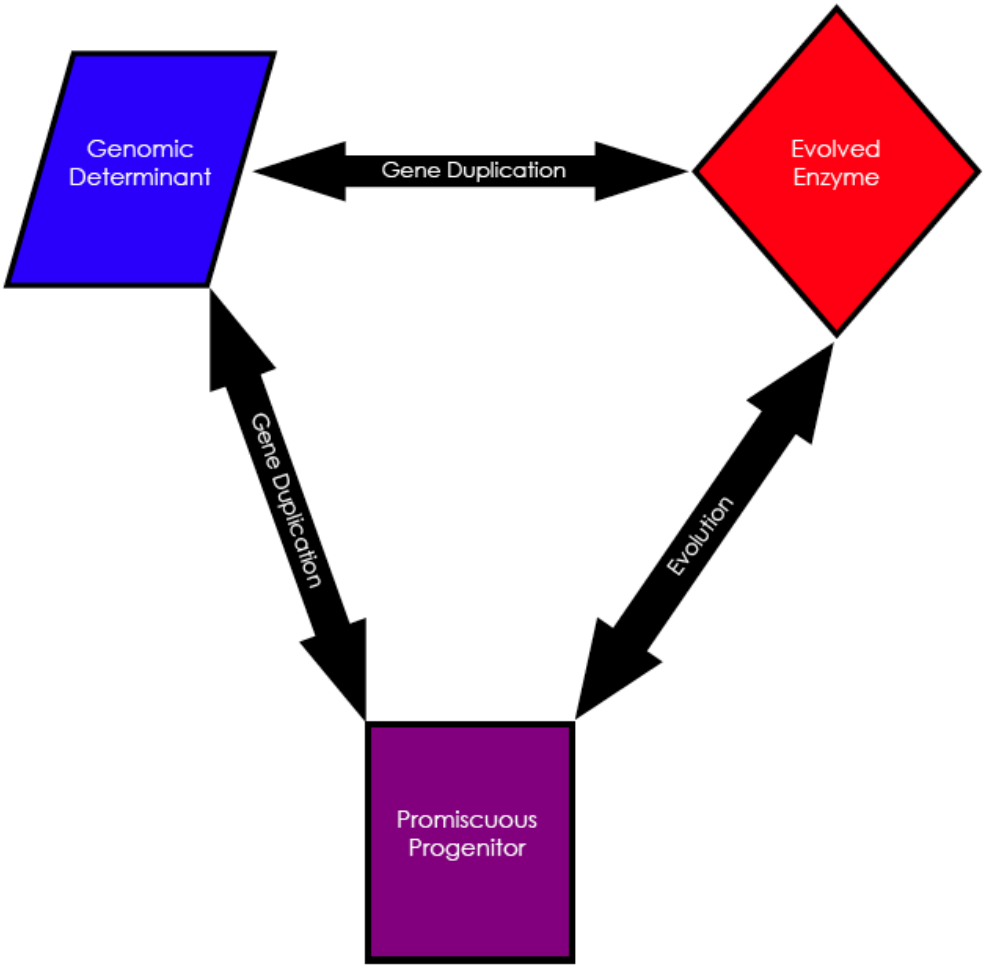

Figure 11: Development of new enzyme activities. An evolved enzyme, for phosphonate metabolism for instance, can be developed from a promiscuous progenitor or from the mutation of another genetically determined enzyme following a gene duplication event. These evolved enzymes are incorporated into the genetic material of the bacterium, or they can be further mutated to become a promiscuous progenitor for other metabolic functions, like fosfomycin resistance. This could also happen in reverse, which is why the circular depiction above is used.

< 50 μg/mL on fosfomycin/LB-agar plates (compared to a k_{cat} = 180 s^{-1} and MIC > 20 mg/mL for the FosA from *P. aeruginosa*). The *M. loti* FosX can, unlike any other Fos enzyme studied to date, catalyze both the FosX and FosA reactions, though both poorly. This leads one to wonder if this enzyme is truly a fosfomycin resistance enzyme, which it is most likely not.

The *M. loti* FosX is located in the *phn* operon, an operon containing several genes responsible for the metabolism of phosphonate compounds (Figure 12). Not much is known about this operon or the functions of the various genes of which it is composed. It is for that reason that the actual function of the *M. loti* FosX is not known, but it is doubtful that it is primarily a resistance mechanism. It is possible, however, that this enzyme may be an evolutionary precursor to both the actual FosA and FosX enzymes. The FosA enzyme is a GSH transferase, but it is structurally and mechanistically different from any of the canonical cytosolic GSH-transferases. It has been previously posited that FosA may actually have evolved from a member of the Vicinal Oxygen Chelate (VOC) Superfamily, of which it is a member along with the extradiol dioxygenases, glyoxalase I, and others.[46] It is possible that its more direct evolutionary precursor is something like the *M. loti* FosX, however, and that the FosX in turn evolved from another VOC family member.

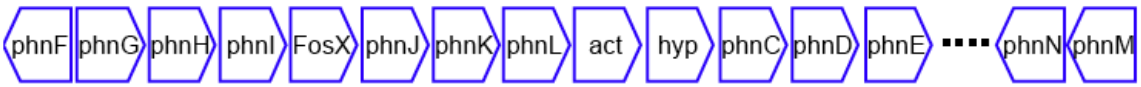

Figure 12: *phn* operon in *M. loti*

Much work has been done in recent years on trying to predict the future evolution of antibiotic resistance and also using what we do know about the evolution of related enzymes to create new functionality.[11,47,48] A thorough understanding of the evolution of the Fos enzymes may aid in the future prediction of how resistance to this antibiotic might spread and become a model system for the study of other resistant mechanisms. Many of the tools devised over the last several years in protein engineering will also be of

aid in exploring how the Fos enzymes might have evolved from a catalytically promiscuous, although not very active, precursor.

Drug Discovery

Many drug discovery efforts begin in one of three places – substrate analogs (often a result of rational screening), natural products, or high-throughput screening (HTS). Early attempts at finding inhibitors for the FosA enzymes focused on the first of these three. Several small phosphonates were screened for inhibitory capacity and one, phosphonoformate, proved to be an excellent transition-state analog inhibitor (Figure 13).[49] Phosphonoformate was not a specific inhibitor, however, as it showed toxicity to *E. coli* in an *in vitro* LB/agar plate assay. No other small phosphonates were found to be good enough inhibitors to pursue further.

There have been published examples of inhibitors found for the MurA enzyme which look nothing like fosfomycin.[18] One of the most effective ways to explore new chemical space for drug discovery is high-throughput screening (HTS). HTS works on a principle of creating assays so that each well of a 96-, 384-, or 1536-well plate acts as a micro test tube (Figure 14). These microplates enable one to run parallel assays to test several hundred to several thousand compounds at one time and quickly. HTS assays typically involve using either purified enzymes or whole cells and are capable of being run using minimum steps and time. An HTS assay typically can screen somewhere between 10,000 and 100,000 compounds a day and compound libraries can be anywhere from tens of thousands to millions of compounds.[50,51]

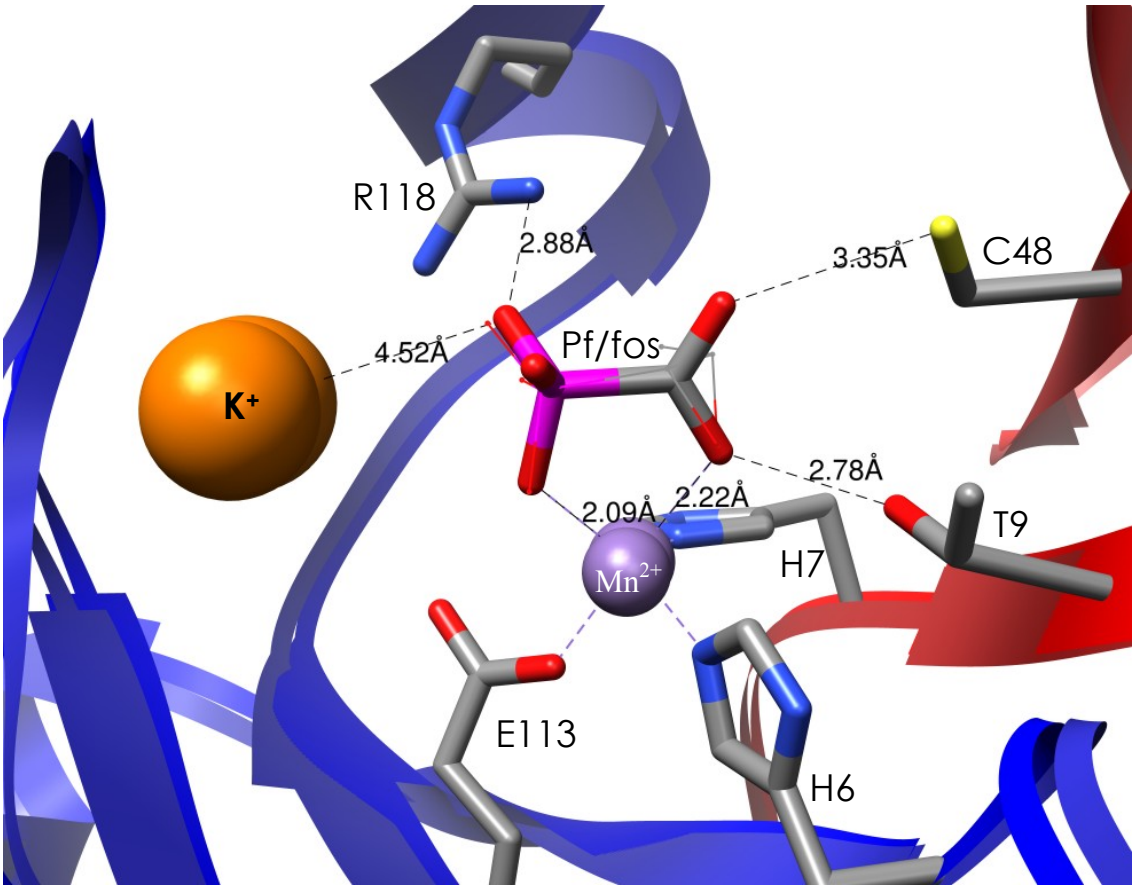

Figure 13: Phosphonoformate inhibits FosA by binding in the active site in the same place as fosfomycin. The Pf molecule is shown in stick form above with the fosfomycin shown in wire form in an overlay of two different Pa1129 FosA structures. Figure made using PDB 1LQP (fosfomycin) and 1NKI (phosphonoformate). References #42 and 51.

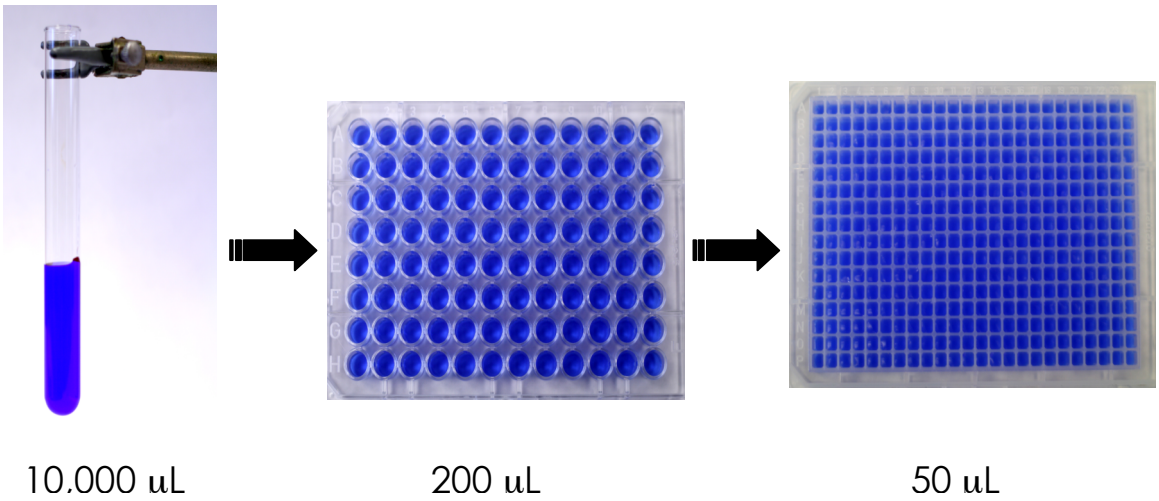

Figure 14: HTS theory – miniaturizing test tube experiments to run massively parallel reactions

HTS assays are primarily an exercise in probability and statistics. Given a large enough and diverse enough library, it becomes sufficiently probable that compounds of desired activity will be found. Statistically, a hit is defined as a compound that gives a signal greater than three standard deviations above the mean signal, a 99% confidence interval. HTS screens also need to be validated, automated, and reproducible.[52] Screening is only a first step in the larger process of drug discovery, but it can be an important way to find new chemical space to explore in the development of potent inhibitors of the fosfomycin resistance enzymes.

This Work

Fosfomycin is underutilized in the USA despite its broad spectrum activity. A recent meta-analysis of published clinical studies reported that fosfomycin was able to cure a number of infections in about 81% of cases, with improvement noted in another 3% of patients.[53] Still, despite the obvious health benefits of fosfomycin, it remains largely unused due to the nature of the antibiotic resistance mounted against it.

The work presented here attacks the problem of fosfomycin resistance from three fronts – uncovering the final mystery of how the substrate glutathione binds in the active site, exploring how these enzymes may have evolved, and developing HTS assays for the discovery of novel inhibitors that could provide therapeutic benefit.

The FosA and FosX enzymes have been mostly characterized in regards to their structure and function. The final piece to the puzzle was the nature of GSH binding to FosA. Due to the way that the enzyme packs in a crystal lattice, it is not possible to get crystals of FosA with GSH present. Crystals do not form in the presence of GSH and

soaking experiments break up the crystals. In order to solve this final piece of the puzzle, GSH was modeled into the active site of the FosA enzyme. Subsequent mutagenesis studies of the putative binding residues helped to confirm the model (and agreed with another published study which identified potential GSH binding residues).[54,55] This work helped to better characterize the nature of the structure/function relationships for FosA.

The final mechanistic work on FosA was also a valuable piece of knowledge in beginning to explore the evolution of the FosA enzymes from the catalytically promiscuous *M. loti* FosX. The primary differences between the two enzymes were identified and multiple point mutations were made in an attempt to increase FosA activity and to introduce GSH binding and K^+ activation. Similar transformations have been done by making point mutations and replacing movable loops in other enzyme families.[47] Attempts to do this resulted in enzymes with decreased function, so a new course was selected.

DNA shuffling techniques have existed for several years and can be used to create genes of mixed origin and new function.[48] Attempts to shuffle the DNA between the *P. aeruginosa* FosA and *M. loti* FosX have yielded some interesting results. The mutation of three amino acids in the *M. loti* FosX effectively kills the enzymes' FosX activity and greatly increases its FosA activity (from k_{cat} = 0.001 s^{-1} to 1.5 s^{-1}).[57] The DNA shuffling mutants, which are 90% identical to *M. loti* FosX on the DNA level, have these mutations as well as the wholesale incorporation of the FosA K^+-binding loop, as well as some other point mutations of unknown function.[56] These are the results of initial attempts, and may be the result of contaminated samples, but they do offer good insight into the small

number of changes that may need to be made to evolve an active FosA from a relatively inactive FosX.

The final project outlined here is a broad attempt to find new inhibitors and new chemical space to explore in the search for inhibitors to the Fos class of enzymes. The successful development of a FosA assay for the purified *P. aeruginosa* FosA should one-day aid in the development of potent inhibitors to this enzyme. The assay uses the thiol-specific fluorophore monobromobimane (mBBr) to screen for the presence of residual substrate glutathione. The whole assay takes only 1 hour to run to completion and is an extremely sensitive and effective assay. Validation runs on a small number of compounds, 4800 from the Vanderbilt Collection, have resulted in six verified hits, one that is a sub-micromolar inhibitor. Needless to say, the success of this assay in finding novel chemical entities in such a small number of compounds bodes well for the future screening of much larger compound libraries.

Also detailed here is the modification and development of a whole cell *E. coli* assay to test the bioactivity of compounds identified from the FosA HTS assay. This assay uses a slightly modified version of the one published by Sarker *et al.*[57] The bacterial growth indicator dye resazurin is reduced by live bacteria to resofurin. This change introduces not only a change in color, from dark blue to pink/red, but also a marked change in fluorescence. The ability to test for the bioactivity of inhibitors is key to the development of therapeutic agents. Developing strong enzymatic inhibitors that cannot cross the cell membrane and reach its target is useless and must be mitigated. Bioactivity assays will also enable the ability to test for the specificity of inhibition. One of the main problems with phosphonoformate was that it was not a specific inhibitor and

resulted in decreased growth in cells not stressed by antibiotic.[49] This assay will help tailor inhibitors to be bioactive, but specific as well.

The FosA HTS assay should be directly translatable to the FosB enzymes. The FosX enzymes, however, are a different story. Several attempts were made to develop a separate purified enzyme assay for the FosX enzymes, using purified FosX from *Listeria monocytogenes*, a potent resistance enzyme. All attempts to date have failed to develop a purified enzyme assay.

CHAPTER II

MATERIALS AND METHODS

Materials

FosA from *Pseudomonas aeruginosa* and FosX from both *Listeria monocytogenes* and *Mesorhizobium loti*, were purified as previously described.[58] $MnCl_2$ and phosphonoformate were obtained from Alfa Aesar (Ward Hill, MA). KCl, potassium phosphate (monobasic), ethylene diamine tetraacetic acid (EDTA), tris(hydroxymethyl)aminomethane (Tris), N-(2-hydroxyethyl)piperazine N'-(2-ethanesulfonic acid) free acid (HEPES), 3-(N-morpholino)-propanesulfonic acid (MOPS), tetramethylammonium hydroxide (TMA-OH), Luria broth (LB), fosfomycin (MP Biomedical, Solon, OH), resazurin (Acros Organics, Geel, Belgium), Acetonitrile (HPLC grade), and dimethyl sulfoxide (DMSO) were obtained from Fisher (Waltham, MA). Glutathione (reduced), isopropyl-β-D-thiogalactopyranoside (IPTG), dithiothreitol (DTT), and ampicillin were obtained from RPI (Mount Prospect, IL). Monobromobimane and thiazolyl blue tetrazolium bromide (MP Biomedical) were obtained from Sigma (St. Louis, MO). AccQ-Fluor Derivatizing Reagent (AQC) was purchased from Waters (Milford, MA). BL21 Gold (DE3) Competent *Escherichia coli* (Novagen – Madison, WI) and all restriction enzymes (New England Biolabs – Beverly, MA) were purchased from the Vanderbilt Molecular Biology Core (Nashville, TN). 96-well microplates (Whatman, Florham Park, NJ) and 384 well microplates (Greiner Bio-One, Monroe, NC) were obtained from VWR (West Chester, PA). Hydroxyapatite and Chelex 100 (Na^+) were obtained from Bio-Rad (Hercules, CA). DEAE Fast Flow resin

and the MonoQ 4.6/100 PE FPLC column were obtained from GE Healthcare and the Sephacryl S100 gel filtration column was from Pharmacia (now part of GE Healthcare, Piscataway, NJ).. Silicon oil, Al's Oil, and microbatch crystallography trays were obtained from Hampton Research (Aliso Viejo, CA).

Methods

GSH Docking and Energy Minimization

The manual docking and energy minimization of GSH in the active site of FosA was performed by Rachel Rigsby and Eric Dawson and is detailed in Rigsby *et al*.[55]

Generation of GSH Binding Mutants

Site-directed mutagenesis was performed on the *P. aeruginosa* FosA expression plasmid using the QuikChange site-directed mutagenesis kit (Stratagene, La Jolla, CA). Oligonucleotide primers (Invitrogen, Carlsbad, CA) were designed to change codon 34 from TGG to GCG (W34A) and CAC (W34H), codon 36 from CAG to AAC (Q36N), codon 39 from TAT to TTT (Y39F), codon 90 from AAG to GCG (K90A), codon 93 from CGC to GCG (R93A), and to insert CGC GTC GAG (RVE) between codons 93 (R) and 94 (S). All mutations were confirmed by DNA sequencing (Vanderbilt DNA Sequencing Core).

Expression and Purification of GSH Binding Mutants

Mutants were expressed and purified as described for native protein.[58] Briefly, for the mutants of *P. aeruginosa* FosA, bacteria were lysed by sonication on ice followed by centrifugation to pellet the cell debris. The lysate was dialyzed against 20 mM Tris (pH

7.5) with 1 mM DTT prior to loading onto a 2.8 x 18 cm DEAE-cellulose column equilibrated with the same buffer. Protein was eluted with a salt gradient [(20 to 500 mM NaCl in 20 mM Tris (pH 7.5)] at 4 °C. Fractions containing the enzyme were pooled and dialyzed against 20 mM KH_2PO_4 (pH 6.8) with 1 mM DTT. Protein was passed isocratically through a 2.8 x 6.5 cm hydroxyapatite column equilibrated with the same buffer. Fractions containing the enzyme were pooled and dialyzed against 20 mM TMA-HEPES (pH 8.0) containing 3 g. Chelex resin, 5 mM EDTA, and 1 mM DTT followed by dialysis against 20 mM TMA-HEPES (pH 8.0) with 1 mM DTT. Protein was then concentrated and passed isocratically through a 1.6 x 60 cm S100 gel filtration column. The protein was dialyzed in 20 mM HEPES (pH 8.0) with 1 mM DTT, concentrated, and stored at -80 °C.

Kinetic Analysis of Native and GSH Binding Mutants

The kinetic assay for native protein was followed as described to determine kinetic parameters for mutants.[58] Briefly, enzyme was incubated with the appropriate metal(s) prior to addition of thiol and fosfomycin (disodium or TMA salt). Reactions were quenched at a time such that less than 20% of the variable substrate was consumed and derivatized with a fluorescent reagent (AQC) prior to HPLC analysis. Data was fit to a non-linear Michaelis-Menten curve using GraphPad Prism © to calculate k_{cat}, K_M, and k_{cat}/K_M. For the K90A and R93A mutations, saturation with GSH was not possible for this analysis inasmuch as the maximum practical concentration of GSH in the assay is 100 mM. For these mutants a k_{cat}/K_M^{GSH} was calculated by fitting the linear portion of the curve with a straight line.[59]

Fluorescence Titration of P. aeruginosa FosA with GSH

Typically, a solution of 5 μM FosA in the presence of 50 μM $MnCl_2$ and 100 mM KCl was prepared in 20 mM TMA-MOPS (pH 8.0) that had been filtered through a 0.2 μm filter.

A solution of buffer containing $MnCl_2$ and KCl was prepared similarly. One micromolar enzyme was used for the Q36N, Y39F, S50A, K90A and R93A mutants. GSH was added to both solutions incrementally while monitoring the change in intrinsic protein fluorescence. Titration measurements were made in triplicate on a SPEX Fluorolog-3 spectrofluorimeter (Horiba Jobin-Yvon, Edison, NJ) in the constant wavelength mode. Solutions were excited at 275 nm (3 nm slit width), and emission measurements were taken at 340 nm (3 nm slit width) for most mutants. For the K90A and R93A mutants, excitation was at 295 nm (2 nm slit width) and emission was measured at 328 nm (4 nm slit width). This is due to the lower absorbance of GSH at 295 nm versus 275 nm and the need for much higher concentrations for these mutants. After correction for the inner filter effect of GSH the data were averaged and fit to a hyperbola to obtain a K_d.

Minimum Inhibitory Concentration (MIC) for GSH Binding Mutants

To test whether or not the mutations made in *P. aeruginosa* FosA affected the ability of the enzyme to confer resistance to the antibiotic, the mutant expression plasmids were transformed into *E. coli* and grown on LB plates containing different amounts of fosfomycin. Each plate contained between 0 and 20 mg/mL fosfomycin, 100 μg/mL ampicillin, and 10 μg/mL glucose-6-phosphate. Plates were divided into six sections to accommodate six different mutants. For each plate one section was native *P.*

aeruginosa FosA (positive control), another was *E. coli* transformed with empty vector (pET20, negative control), and the other four were various mutants. For each spot on the plate, 30 μL of suspension of bacteria (OD_{600} = 0.03) in LB/Amp media was added and spread onto the plate. Plates were incubated at 37 °C for 16 hours. Plates were visualized by spraying them with a solution of 0.5 mg/mL thiazolyl blue tetrazolium bromide.

Structural Overlay of P. aeruginosa FosA and M. loti FosX

The crystal structures for these enzymes have been solved, published, and are freely available via pdb.com.[40,43] A structural superposition of these enzymes, 1LQP and 1R9C, was done using the program Chimera (UCSF, San Francisco, CA).

Rational Mutagenesis of the M. loti FosX

All PCR reactions were made on the *M. loti* FosX enzyme already ligated into a pET-20 vector. The initial three mutations made, E44G, F46Y, and M57S, were made by Kerry Fillgrove, Ph.D.[57] All subsequent mutations were made in the background of this triple mutant. Several successive PCR experiments were run to make several different deletions and point mutations in the *M. loti* FosX Triple Mutant enzyme. Also, a PCR reaction was run to delete residues R99, V100, and E101 in the triple mutant background. Subsequently, the entire K^+- binding loop from the *P. aeruginosa* FosA was inserted into the *M. loti* FosX with successive point mutations. These mutations were R94W, P95K, P98R, R103D (by Lauren Beihoffer) as well as L89H, L91V, D92R, and M93E. Other deletion PCR reactions run in the *M. loti* FosX Triple Mutant K-loop background included the deletion of T36, E37, F39, S40, C41, and S42. The last point mutations

made were then S34W/H/Q/N, R43Q, and D27G or R85Q in either the S34Q or the S34N backgrounds.

Rational Mutant FosX Expression, Purification, and Activity

For each round of PCR the mutant DNA was isolated and sequenced. DNA with the desired sequence was then transformed into BL21 (Gold) DE3 *E. coli* and plated on LB/Amp plates. Single colonies were selected to inoculate a 200 mL liquid culture of LB medium with 100 μg/mL ampicillin. This culture was grown overnight at 37 ºC with shaking at 200 rpm. The OD_{600} of the culture was measured and a volume needed to make 2 L of LB/Amp with an OD_{600} = 0.02 was added to 2 L of LB/Amp in a fermentor and grown at 37 ºC with constant stirring and aeration. When the OD_{600} reached 0.6-0.8 800 μL of 1 M IPTG was added to induce protein expression. The culture was allowed to incubate for a further five hours.

The mutants were purified using the same method as that published for the *M. loti* FosX enzyme.[43,58] This is also the same method briefly discussed for the GSH Binding mutants. Activity was checked using the ^{31}P NMR assay.[58]

In-vitro DNA Shuffling

The *in-vitro* DNA shuffling experiments were performed by Matt Schaab and are detailed in the supporting information for Brown *et al*.[56]

Protein Expression and Purification for the DNA Shuffling Mutants

M. loti FosX (E44G/F46Y/M57S)

The triple mutant gene was constructed by procedures previously described for the E44G mutant.[43,44] The protein was expressed and purified following the procedures as described for the native *M. loti* FosX enzyme.[43]

DNA Shuffle Mutants S1.1, S1.2, S2.2 (S3.1)

Selected plasmids (specifically S1.1, 1.2, and 2.2) obtained from the DNA shuffling experiments were used to transform *E. coli* BL21 (DE3) cells via heat shock and spread onto LB plates containing 100 μg/mL ampicillin and incubated overnight at 37 °C. Single colonies from these plates were used for expression of the proteins as indicated below.

The S1.1 and S2.2 proteins were expressed and purified as follows. Single colonies were used to inoculate 100 mL of LB containing 100 μg/mL ampicillin. The culture was grown overnight at 37 °C with shaking at 225 rpm. Six 1 L portions of LB containing 100 μg/mL ampicillin were each inoculated with 10 mL of the starter culture. The cultures were grown at 37 °C with shaking at 250 rpm until the OD_{600} reached 0.8. Protein expression was induced by the addition of 100 mg IPTG. The temperature was lowered to 15 °C and cultures were incubated for 20 hr at 150 rpm. The cells were harvested by centrifugation and the cell paste was frozen and stored at -80 °C.

The cell paste was later thawed and suspended in 100 mL of 50 mM HEPES, pH 7.5, with 50 mM NaCl, 1 mM EDTA and 1 mM DTT. The cells were lysed via 4 cycles of sonication at 70% maximum output with 3 min on and 3 min off with gentle stirring on ice. The cell debris was removed by centrifugation. 1% (w/v) streptomycin sulfate was

added to the supernatant and stirred for 1 hr at 4 °C. Precipitated material was removed by centrifugation and the supernatant was dialyzed overnight against 4 L of 50 mM HEPES, pH 7.5, with 50 mM NaCl, 1 mM EDTA, and 1 mM DTT. The dialyzed protein was then loaded on a 2.8 x 18 cm DEAE column that had been equilibrated with the same buffer. The column was washed with 250 mL of buffer and then eluted with a 50 to 400 mM gradient of NaCl in the same buffer. The fractions containing the enzyme were identified by checking the A_{280} and by SDS-PAGE, pooled and dialyzed against 4 L of 30 mM KH_2PO_4, pH 7.5, with 1 mM DTT. The protein was concentrated to ~10 mL and loaded onto a 2.8 x 6.5 cm hydroxyapatite column that had been equilibrated with the phosphate buffer. The protein was eluted with an isocratic gradient of the same buffer. Fractions containing the enzyme were pooled and dialyzed against 4 L of 50 mM HEPES, 50 mM NaCl, 1 mM EDTA, and 1 mM DTT. The protein was concentrated to ~4 mL and further purified by gel filtration chromatography on a 1.6 x 60 cm Sephacryl S-100 HR column. The purity of the final protein preparation was estimated to be ≥ 98% by SDS-PAGE, using 15% Tris-HCl gels. The protein was dialyzed over night in 20 mM TMA-HEPES, pH 7.5 with 5 mM EDTA, 3 g. Chelex resin, and 1 mM DTT, followed by another round of dialysis in the same buffer minus the EDTA and Chelex resin. The protein was stored at -80 °C.

The S1.2 protein was expressed and purified as follows. Freshly transformed cells were streaked on LB agar plates containing 100 µg/mL ampicillin and the plates were incubated overnight at 37 °C. A single colony was used to inoculate 200 mL LB containing 100 µg/mL ampicillin. The culture was incubated overnight at 23 °C with shaking at 200 rpm. Four 15 mL aliquots of the culture was used to inoculate four 1 L

portions of LB containing 100 µg/mL ampicillin. The four 1 L cultures were incubated at 37 °C with shaking at 250 rpm. When the OD_{600} reached 0.6 to 0.8, 400µL of 1 M IPTG was added to each 1 L culture (final [IPTG] = 0.4 mM). The temperature was dropped to 15 °C and the shaking to 200 rpm and the cultures were incubated overnight. The cells were harvested by centrifugation and the cell pellets were suspended in 20 mM Tris, pH 7.5, and lysed by sonication in 4 x 3 min cycles with 3 min between cycles. The lysed cells were centrifuged and the lysate was dialyzed overnight against 20 mM Tris, pH 7.5, with 1 mM DTT.

The protein was purified by applying the dialyzed extract to a DEAE column that had been equilibrated with 20 mM Tris, pH 7.5. The column was eluted with a 0-0.4 M gradient of NaCl in the same buffer. The enzyme was detected by checking the fractions A_{280} and running SDS-PAGE on selected fractions. The pooled fractions containing the enzyme were then dialyzed against 20 mM KH_2PO_4, pH 6.8, with 1 mM DTT and 3 g. Chelex resin. The protein was concentrated to ~10 mL and applied to a hydroxyapatite column that was equilibrated with 20 mM KH_2PO_4, pH 6.8. The protein was eluted with an isocratic gradient of the same buffer. The fractions containing the enzyme were dialyzed overnight against 20 mM Tris, pH 8.0, with 1 mM DTT, 5 mM EDTA and 3 g. Chelex resin. The protein was concentrated to 2-3 mL and 0.5 mL aliquots were applied to a MonoQ 4.6/100 PE FPLC column equilibrated with 20 mM Tris, pH 8.0, and eluted with a 0 – 0.5 M gradient of NaCl in the same buffer. The protein eluted as the main peak at approximately 0.2 M NaCl. The protein was dialyzed overnight against 20 mM TMA-HEPES, pH 7.5, with 1 mM DTT, 5 mM EDTA, and 3 g. Chelex resin and again for 8 hr against a change of the same de-metallating buffer. The final dialysis was done

overnight against 20 mM TMA-HEPES, pH 7.5, with 1 mM DTT. The protein was concentrated to ~5 mL and stored at -80 °C.

Minimum Inhibitory Concentration (MIC) Assays for DNA Shuffling Mutants

Selected plasmids and the *M loti* triple mutant were used to transform *E. coli* BL21 (DE3) cells, which were then plated onto LB agar containing 100 μg/mL ampicillin. The plates were incubated overnight at 37 °C. A single colony was then used to inoculate 3.5 mL LB containing 100 μg/mL ampicillin. The liquid cultures were grown at 37 °C until the OD_{600} reached 0.6. The culture was then diluted to OD_{600} = 0.03 and 30 μL was then plated onto LB agar plates containing 100 μg/mL ampicillin, 10 μg/mL glucose-6-phosphate, and a variable concentration (0 to 1.0 mg/mL) of fosfomycin. The plates were incubated at 37 °C overnight.

Steady-State Kinetics for DNA Shuffling Mutants

Reactions were followed with the HPLC-based assay previously reported.[37,58] All reactions were run at 25 °C in 20 mM TMA-HEPES, pH8.0, containing 50 μM $MnCl_2$ and 100 mM KCl. Temperature was maintained using a water bath. Enzyme concentrations were 0.5 μM for reactions with triple mutant, *M. loti* FosX(E44G/F46Y/M57S), 0.3 to 0.4 μM S1.1 and 0.05 to 0.2 μM S1.2. Reactions were carried out with either a fixed concentration of [GSH] = 20 mM and a variable concentration of 0.05 to 50 mM fosfomycin or a fixed concentration of [fosfomycin] = 10 mM and a variable concentration of 0.2 to 100 mM GSH.

For reactions where fosfomycin was the variable substrate, reactions were initiated by addition of 20 μL of fosfomycin to 80 μL of a solution of enzyme, Mn^{2+}, K^{+},

and GSH (E•Mn•K•GSH) using the concentrations listed above. The reactions were incubated for 3 min and quenched with the addition of 200 μL of 5% trichloroacetic acid with vortex mixing for 10 s. The pH was returned to neutral by the addition of 100 μL of 50 mM NaOH and 100 μL of 1.0 mM valine was added as an internal standard. For reactions where GSH was the variable substrate 20 μL of GSH was added to 60 μL of a E•Mn•K solution and the reaction was initiated with the addition of a solution of 20 μL of fosfomycin. The reaction mixture was quenched after 3 min as described above.

The quenched reaction mixtures were derivatized with the AccQ-Fluor reagent kit from Waters (Milford, MA) following the manufacture's instructions. A 5 μL aliquot of the quenched reaction mixture was added to 80 μL of the supplied borate buffer followed by 15 μL of the AccQ-Fluor reagent. The mixture was heated at 55 °C for 10 min and then diluted with 400 μL of HPLC Buffer (140 mM sodium acetate, 12.5 mM triethylamine, pH 5 with phosphoric acid). A 20 μL aliquot of the derivatized solution was injected on a Beckman Ultrasphere C18 analytical column. Samples were eluted with HPLC Buffer and a linear gradient of 0 to 30% CH_3CN at a flow rate of 1.0 mL/min The concentration of the product was determined by the ratio of the peak area of the product eluting at 9.1 min to the peak area of the internal standard valine eluting at 14.5 min using a standard curve. Each reaction was done in triplicate and the data were fit with GraphPad Prism to a hyperbola (in the case of saturation kinetics) or a linear function where saturation was not observed. The triple mutant and the S1.1 and S1.2 mutants could not be saturated with GSH so that the k_{cat}/K_M^{GSH} for these proteins were determined from the linear dependence of the initial velocity on [GSH].[59]

^{31}P NMR for Shuffling Mutants

The ^{31}P NMR analysis was done using 5 μM enzyme, 50 μM Mn^{2+}, 100 mM K^{+}, 30 mM fosfomycin, and 100 mM GSH. One milliliter reactions were set up at 25 ºC and allowed to run for anywhere from 5 to 240 minutes. At designated time points, 300 μL of the reaction solution was removed and placed in a new tube containing 50 μL of chloroform ($CHCl_3$) and vortexed for 30 s. The organic layer was removed and discarded and the solution was demetallated using a small quantity of Chelex resin (Bio-Rad, Hercules, CA). The solution with Chelex was shaken for two hours and centrifuged. The solution was removed from the resin and put in a standard NMR tube. The resin was washed with 300 μL of D_2O and added to the sample. Data was collected using the auto-sampler on a Bruker 500 MHz NMR with an 11.7 Tesla Oxford magnet controlled by a Bruker DRX-500 Console with a 5 mm Z-gradient QXI probe using a ^{31}P proton decoupled pulse program. Substrate fosfomycin can be identified at δ11 ppm with the diol product at δ16 ppm and the GSH bound adduct at δ18 ppm. A v_{max} can be estimated from the relative peak heights of the substrate and product.

DNA Shuffle Mutant 2.2 Purification and Crystallography

DNA shuffle mutant 2.2 was purified using the same procedure as that for DNAs1.1 above.

Purified enzyme was used in several matrix screens to try to grow crystals. Success was achieved finally using an enzyme solution containing 10 mg/mL DNAs2.2, 2 mM Mn^{2+}, 100 mM K^{+}, and 20 mM fosfomycin and mixing that 1:1 with a solution of 20% PEG-3350, 100 mM NH_4Cl, and 0.4% 1,3-Propanediol in microbatch trays under Al's Oil. Crystals generally grew in 2-3 days. Data was collected with a Bruker

Microstar microfocus rotating-anode X-ray generator with a Proteum PT135 CCD detector, with kappa goniometers and a Bruker Kryo-Flex cryostat. Data was collected at 100 ºK using a solution of the crystal buffer with 20 % ethylene glycol as a cryoprotectant. Images were processed using HKL-2000. Phaser was used for the molecular replacement phasing using PDB 1R9C (*M. loti* FosX). Refmac was then used to refine the Phaser output. ARP/wARP was used to remove model bias, followed by further refinement using refmac. The structure was further modified using Coot, followed by further rounds of refinement in Refmac.

Monobromobimane (mBBr) Activity Check

To test whether or not mBBr would be a useful compound to detect the presence of GSH in enzyme reactions, 2 mL test reactions were run in a fluorimeter. The reaction used 200 nM Pa1129 FosA, 50 μM Mn^{2+}, 100 mM K^{+}, 750 μM fosfomycin, and 500 μM GSH in 10 mM NaH_2PO_4, 135 mM NaCl, pH 7.5. Reactions were run with and without enzyme or GSH to check for the presence of fluorescence from the GSH-mBBr conjugation product. The reaction fluorescence was measured with λ_{ex} = 370 nm and λ_{em} = 480 nm.

FosA HTS Assay Development: CRC Curve

The FosA enzymatic assay was developed using purified enzyme and the known inhibitor phosphonoformate (Pf).[49] The assay was performed by adding 20 μL of a solution containing 500 nM FosA, 125 μM Mn^{2+}, 250 mM K^{+}, and 1.25 mM GSH in 10 mM NaH_2PO_4, 135 mM NaCl, pH 7.5 (HTS Buffer) to 20 μL of a solution of Pf of varying concentrations (3x serial dilution from 20.25 mM) in HTS Buffer with 0.25%

DMSO. Finally, 10 μL of 3.75 mM fosfomycin in HTS Buffer was added to initiate the reaction. The final concentrations in the reaction were 200 nM FosA, 50 μM Mn^{2+}, 100 mM K^{+}, 500 μM GSH, 0-8.1 mM Pf, 750 μM fosfomycin, and 0.1% DMSO. The reaction was allowed to run for 60 minutes at room temperature in a covered, black, 384-well, solid bottom microplate. After 60 minutes, 10 μL of 1.3 mg/mL monobromobimane (mBBr) in acetonitrile was added to give a final concentration of 216 μg/mL mBBr (800 mM). The plate was covered with a black lid and the reaction was allowed to proceed for 30 min at room temperature. The fluorescence was then read on a Spectramax® M5 microplate reader (Molecular Devices, Sunnyvale, CA) with λ_{ex} = 370 nm and λ_{em} = 480 nm in top-reading fluorescence mode, sensitivity 6. Results were fit to a sigmoidal curve to calculate and IC_{50} and IC_{80} for Pf in this assay using GraphPad Prism.

HTS Instrumentation and Validation, Assay ver. 1.0

To make sure that this assay would work with the instrumentation available in the Vanderbilt HTS Core, a modified version of the enzymatic assay was performed in the core lab. The E•Mn•K•GSH solution, a 20 μL addition, was added to the reaction plates using a Thermo-Electron Multi-Drop Combi (Waltham, MA). The Pf dilutions were made in a clear, 384-well polypropylene plate and 20 μL of Pf was added to the reaction plate using a Velocity 11 Bravo®, robotic liquid dispensing system (Santa Clara, CA). The fosfomycin and the mBBr, 10 μL additions, were also added using the Multi-Drop Combi. All final concentrations are the same as stated above. The plates are then read on a Spectramax M5 microplate reader with the same settings listed above. Plates were

run with varying times allowed for the enzymatic reaction before the addition of mBBr to optimize the time course for the assay while maintaining a good IC_{50} curve.

IC_{50} and IC_{80} Z' Calculations

The viability of an assay for HTS is determined by calculating a Z' value for the assay.[60] The Z' was calculated by setting up individual plates of IC_{50} or IC_{80} concentrations of Pf, 60 and 200 μM respectively, in a checkerboard format against a buffer control in 384-well plates. The assay was performed using the exact same reaction mechanism as before and the Z' value was calculated as published.

Initial Compound Screen

The assay was tested by screening a small portion of the Vanderbilt Collection of compounds. The compounds from the Vanderbilt Collection, 10 plates (3200 compounds), were transferred from their storage plates to clear, 384-well polypropylene microplates in columns 3-22 (75 nL using a Labcyte Echo® 555 sonic liquid dispensing system [Sunnyvale, CA]) and diluted with 30 μL of HTS Buffer. 20 μL of the E•Mn•K•GSH solution was added to a black, 384-well polystyrene microplate using the Multi-Drop Combi (Note: It is important to keep the enzyme solution on ice to preserve maximum functionality). Twenty microliters of the compound solutions were then transferred from the clear polypropylene plate to the black polystyrene plate using the Velocity 11 Bravo. Columns 1, 2, 23, and 24 are used to make checkerboards of IC_{50} concentrations of Pf, 60 μM, and a buffer control by adding 1 μL of either Pf or buffer. After the enzymatic reaction incubated at room temperature for 30 minutes, the plates were read on the Spectramax M5 *before* the addition of mBBr. Once mBBr was added,

and the reaction allowed to run 30 min, the plates were read again, and the difference was taken between the two reads (Figure 15a). Hits are identified as compounds with a greater than three standard deviation in signal strength above the average (taken from all wells in columns 3-22) on an individual plate.

Hit Confirmation

To verify the hits identified in the compound screen, the compounds were ordered from ChemBridge. New 10 mM stocks were made for each compound in pure, anhydrous DMSO. One hit compound, CB5838696, was no longer available from ChemBridge, but four closely related structural analogs were available and they were used in the confirmation screen (CB5844324, CB5848410, CB5846450, and CB5838937). All 104 compounds identified as hits were arranged on a clear, 384-well, low volume microplate and the assay was performed as before. In addition to the normal assay, assays were done with 3x concentrations of test compounds and, also, in the absence of glutathione.

HTS Assay Version 2

This assay was done by adding 40 μL of a E•Mn•K•GSH solution (250 nM enzyme, 62.5 μM Mn^{2+}, 125 mM K^{+}, 625 μM GSH) to a black, 384-well polypropylene microplate and then immediate addition of the library compounds, 50 nL, to the same plate using the Echo 555. One μM Pf was then added manually to columns 1, 2, 23, and 24 in a checkerboard format against DMSO. The plate was incubated at room temp. for 10 min followed by the addition of 10 μL of fosfomycin with the Combi to start the reaction. The rest of the assay, post addition of fosfomycin, was run in the same manner

as the previous version of the assay except that the mBBr was dissolved in methanol instead of acetonitrile for better chemical stability in the microplates (Figure 15b). In addition, instead of picking hits on a per-plate basis, a population based hit picking scheme was used. All results were normalized to a % max signal of the positive control for each plate and then the average and standard deviation was calculated for all compounds screened (3200 total). Hits were identified as compounds with a % max signal greater than three standard deviations above the mean.

Hit Confirmation, Version 2

Hits from the second version of the assay were verified by ordering new compounds from the supplier and making new 100 mM or 50 mM stocks, depending on

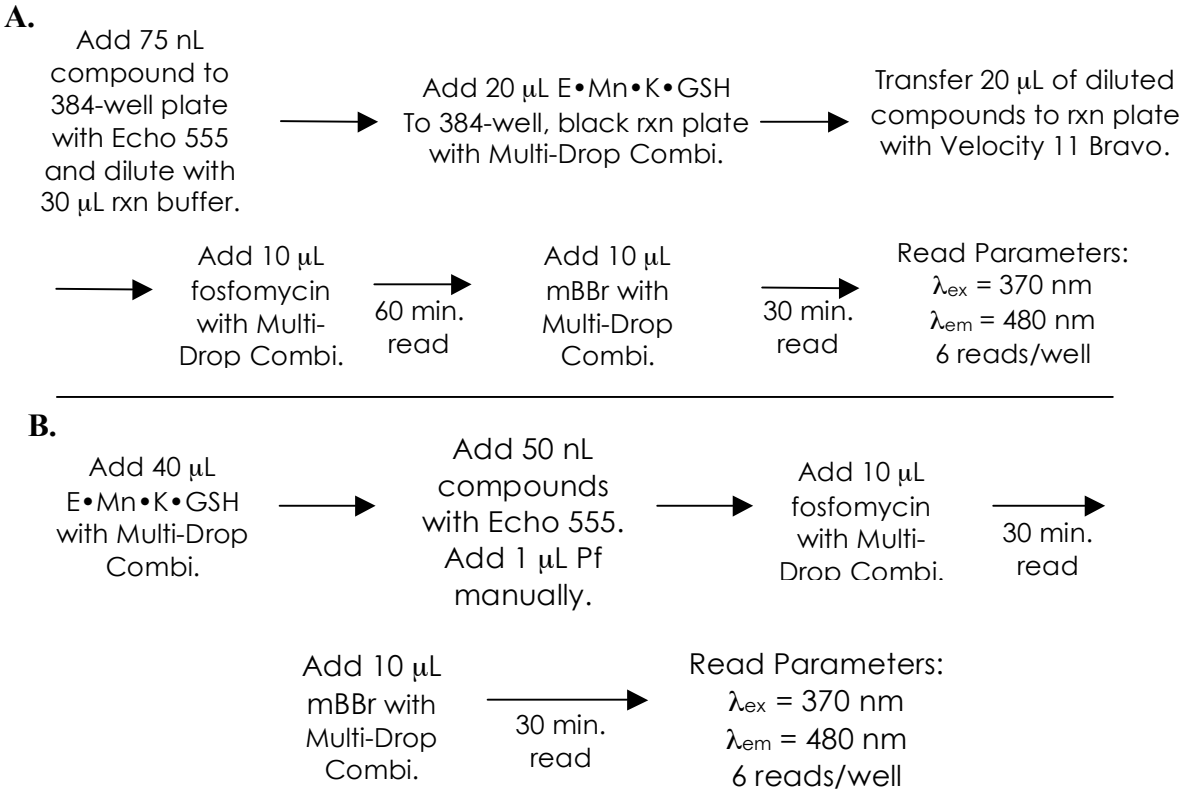

Figure 15: A) Workflow for assay version 1. B) Workflow for assay version 2. Version 3 is run the same way as version 2 but with the Zn standard added using the Echo 555.

solubility. CRC profiles were then created of the hits to confirm activity. See CRC profile method below.

Compound Screen, Assay Version 3

The positive standard used was a 5 mM $ZnCl_2$ solution in DMSO. Fifty nanoliters of this solution was added to the reaction plates with the Echo 555 immediately prior to the addition of the library compounds. All other steps proceed in the same manner as in assay version 2.

CRC Profile for Confirmed Hits

CRC curves of the confirmed hits were created by making 50 or 100 mM stock solutions of the compounds in DMSO, depending on solubility, and using the same assay procedure as the screen. A 3x dilution of each compound was made in quadruplicate in a clear, 384-well microplate. The assay was run as before and the data was fit to a sigmoidal curve using GraphPad Prism.

Compound Binding Titrations, K_d

Compound binding constants, K_d, were calculated by titrating compounds into a solution of 1 μM enzyme, 50 μM Mn^{2+}, 100 mM K^+, in 20 mM TMA MOPS, pH 7.5, and monitoring the changes in intrinsic protein fluorescence with λ_{ex} = 275 nm and λ_{em} =330 nm. Fluorescence titrations were done in a FluorLog-3 spectrofluorimter by Horiba Jobin-Yvon (Edison, NJ). Data was fit to a hyperbolic function to calculate the K_d after correction for the inner filter effect of the compounds.[61]

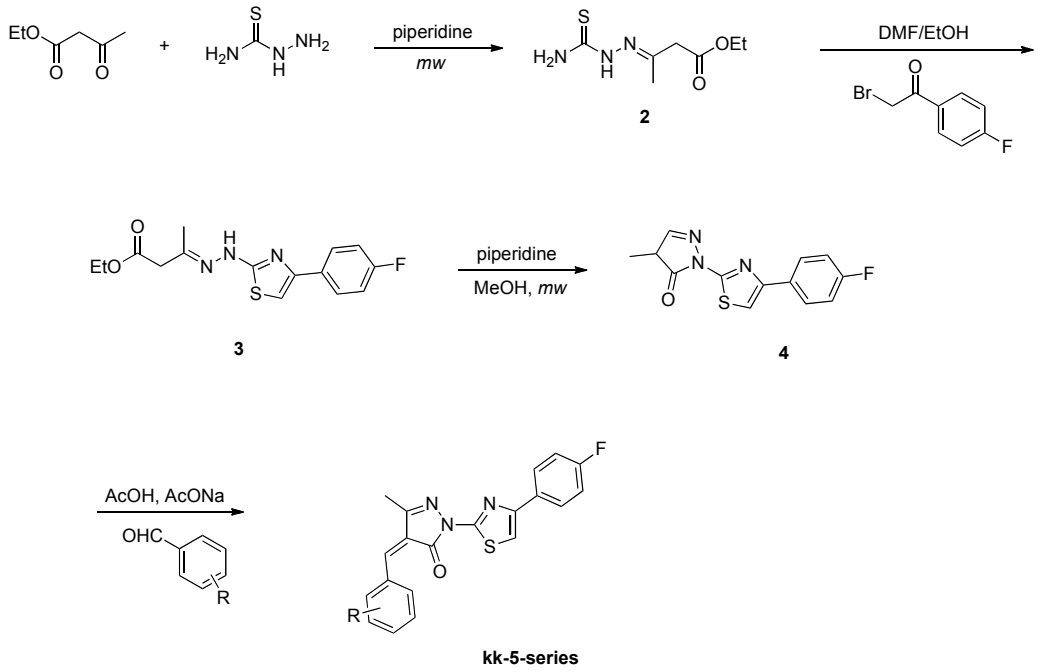

Figure 16: Synthetic Scheme for the synthesis of the various derivatives of CB 5838696, numbered kk-5-series by the Vanderbilt Chemical Synthesis Core. The derivatives were made by substituting the appropriate benzaldehyde in the final synthetic step.

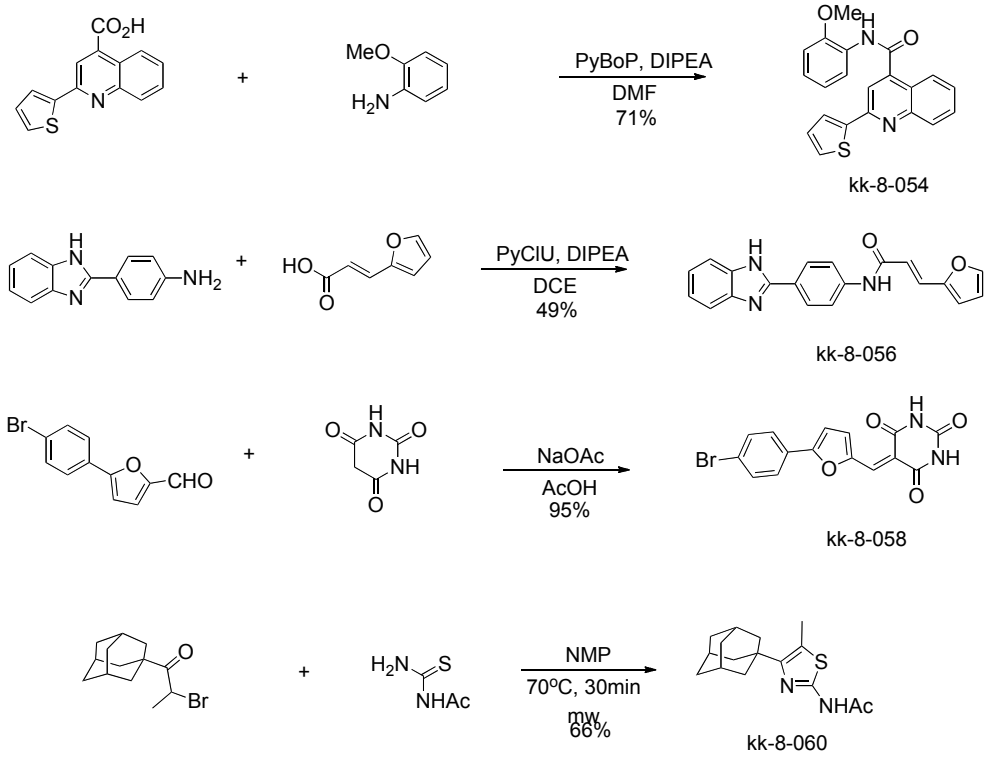

Figure 17: Synthetic schemes for all four members of the kk-8-series of compounds, all made in one step reactions.

Compound Synthesis and Activity

All compound synthesis was done by Dr. Kwangho Kim in the Vanderbilt Chemical Synthesis Core.

Synthesis of (E)-ethyl 3-(2-carbamothioylhydrazono)butanoate

A suspension of ethyl acetoacetate (1.0 mL, 7.91 mmol), thiosemicarbazide 0.72 g, 7.91 mmol), and piperidine (0.1 ml) in methanol (10 mL) was irradiated at 120 ºC for 15 min by microwave. The solvent was evaporated *in vacuo* and solid product **2** (1.21 g, 75 %) was obtained by flash column chromatography on silica gel (hexane/ethyl acetate, 2/1 v/v). ^{1}H NMR (DMSO, 400 MHz) δ (ppm) 10.29 (br s, 1H), 8.12 (br s, 1H), 7.58 (br s, 7.58), 4.09 (q, *J* = 7.2 Hz, 2H), 3.30 (s, 2H), 1.94 (s, 3H), 1.18 (t, *J* = 7.2 Hz, 3H); LCMS, single peak, 1.86 min, m/z, 204.1 (M+1).

Synthesis of (E)-ethyl 3-(2-(4-(4-fluorophenyl)thiazol-2-yl)hydrazono)butanoate

To a solution of (E)-ethyl 3-(2-carbamothioylhydrazono)butanoate **2** (1.21 g, 5.95 mmol) in ethanol/DMF (5 mL/5 mL) was added 2-bromo-1-(4-fluorophenyl)ethanone (1.29 g, 5.95 mmol) at room temperature. The reaction mixture was stirred for 2 h at room temperature. The precipitated product was filtered and washed with hexane (3 x 10 mL) to provide white solid product **3** (1.41 g, 74%). ^{1}H NMR ($CDCl_3$, 400 MHz) δ (ppm) 7.74-7.70 (m, 2H), 7.18 (t, *J* = 8.4 Hz, 2H), 6.68 (s, 1H), 4.20 (q, *J* = 7.2 Hz, 2H), 3.42 (s, 2H), 2.29 (s, 3H), 1.29 (t, *J* = 7.2 Hz, 3H); LCMS, single peak, 3.36 min, m/z, 322.8 (M+1).

Synthesis of 1-(4-(4-fluorophenyl)thiazol-2-yl)-4-methyl-1H-pyrazol-5(4H)-one

A suspension of (E)-ethyl 3-(2-(4-(4-fluorophenyl)thiazol-2-yl)hydrazono)butanoate **3** (1.41 g, 4.39 mmol) and piperidine (0.1 mL) in methanol

(7mL) was irradiated at 100 ºC for 15 min by microwave. The solvent was evaporated *in vacuo* affording crude solid that was purified by flash column chromatography on silica gel (MeOH/CH_2Cl_2 = 1/10) to provide **4** (1.08 g, 90 %) ^{1}H NMR ($CDCl_3$, 400 MHz) δ (ppm) 7.95-7.85 (m, 1H), 7.80-7.75 (m, 1H), 7.19-7.05 (m, 3H), 3.53 (s, 2H), 2.30 (s, 3H); LCMS, single peak, 2.92 min, ``m/z, 276.8 (M+1).

Synthesis of kk-5-series Final Products

A mixture of 1-(4-(4-fluorophenyl)thiazol-2-yl)-4-methyl-1H-pyrazol-5(4H)-one **4** (100 mg, 0.36 mmol), 4-hydroxybenzaldehyde (54 mg, 0.36 mmol) and anhydrous sodium acetate (36 mg, 0.44 mmol) were suspended in acetic acid (4 mL) and irradiated at 120 ºC for 15 min by microwave. The reaction mixture was filtered and the filtrate was poured on crushed ice. The solid product kk-5-033 (R = *para*-OH)(Figure 16), (54 %) obtained, was crystallized from ethanol. Compounds kk-5-095-2, kk-5-095-5, kk-5-141-1, and kk-5-141-2 were also synthesized by the similar method using appropriate benzaldehydes, Figure 16. ^{1}H NMR (DMSO, 400 MHz) δ (ppm) 8.54 (d, J = 8.4 Hz, 2H), 7.98-7.92 (m, 2H), 7.34 (s, 1H), 7.15 (s, 1H), 7.05 (t, J = 6.5 Hz, 2H), 6.72 (d, J = 9.2 Hz, 2H), 3.14 (s, 6H), 2.41 (s, 3H); LCMS, single peak, 3.74 min, m/z, 407.8 (M+1).

Synthesis of kk-8-054

To a solution of 2-methoxyaniline (0.11 mL, 0.94 mmol) in DMF (4 mL) was added diisopropylethylamine (0.41 mL, 2.34 mmol), 2-(thiophen-2-yl)quinoline-4-carboxylic acid (0.20 g, 0.78 mmol), and followed by PyBOP (0.45g, 0.86 mmol). The reaction mixture was stirred for 5 h at room temperature then solvent was removed *in vacuo* and white solid product (0.20 g, 71 %) was obtained by flash column chromatography on silica gel (hexane/ethyl acetate, 2/1 v/v)(Figure 17). ^{1}H NMR

($CDCl_3$, 400 MHz) δ (ppm) 8.62 (d, *J* = 7.6 Hz, 1H), 8.36 (s, 1H), 8.24 (d, *J* = 8.0 Hz, 1H), 8.15 (d, *J* = 8.4 Hz, 1H), 7.97 (s, 1H), 7.78-7.73 (m, 2H), 7.56 (t, *J* = 8.0 Hz, 1H), 7.51 (d, *J* = 4.8 Hz, 1H), 7.20-7.15 (m, 2H), 7.09 (t, *J* = 7.6 Hz, 1H), 6.95 (d, *J* = 8.0 Hz, 1H), 3.87 (s, 3H); LCMS, single peak, 1.49 min, m/z, 361.2 (M+1).

Synthesis of kk-8-056

A mixture of 5-(4-bromophenyl)furan-2-carbaldehyde (200 mg, 0.80 mmol), barbituric acid (102 mg, 0.80 mmol) and anhydrous sodium acetate (79 mg, 0.96 mmol) were suspended in acetic acid (2.7 mL) and irradiated at 120 ºC for 15 min by microwave. The reaction mixture was poured on crushed ice and filtered to provide orange solid product (274 mg, 95 %)(Figure 17). ^{1}H NMR (DMSO, 400 MHz) δ (ppm) 8.52 (d, *J* = 4.0 Hz, 1H), 8.09 (s, 1H), 7.90 (d, *J* = 8.4 Hz, 2H), 7.73 (d, *J* = 8.4 Hz, 2H), 7.49 (d, *J* = 4.0 Hz, 1H); LCMS, single peak, 1.37 min, m/z, 362.7 (M+1).

Synthesis of kk-8-058

To a solution of 4-(1H-benzo[d]imidazol-2-yl)aniline (100 mg, 0.48 mmol) in dichloroethane (4.5 mL) was added diisopropylethylamine (0.25 mL, 1.44 mmol), (E)-3-(furan-2-yl)acrylic acid (79 mg, 0.67 mmol), and followed by PyClU (0.23g, 0.72 mmol). The reaction mixture was stirred for overnight at room temperature then solvent was removed *in vacuo* and yellow solid product (77 mg, 49 %) was obtained by flash column chromatography on silica gel (hexane/ethyl acetate, ½ v/v)(Figure 17). ^{1}H NMR (DMSO, 400 MHz) δ (ppm) 10.43 (s, 1H), 8.12 (d, *J* = 8.4 Hz, 2H), 7.85 (d, *J* = 8.8 Hz, 3H), 7.63 (d, *J* = 7.2 Hz, 1H), 7.49 (d, *J* = 7.2 Hz, 1H), 7.42 (d, *J* = 15.6 Hz, 1H), 7.17 (q, *J* = 6.0 Hz, 2H), 6.88 (d, *J* = 3.2 Hz, 1H), 6.69-6.61 (m, 2H); LCMS, single peak, 1.18 min, m/z, 330.7 (M+1).

Synthesis of kk-8-060

A suspension of 1-(adamantan-1-yl)-2-bromopropan-1-one (200 mg, 0.74 mmol) and acethyl thiourea (262 mg, 2.22 mmol) in NMP was irradiated at 70 ºC for 30 min by microwave. The cooled solution was diluted with water. The product was filtered, washed with methanol and dried *in vacuo* to afford a white solid product (142 mg, 66 %) (Figure 17). ^{1}H NMR (CDCl3, 400 MHz) δ (ppm) 2.45 (s, 3H), 2.19 (s, 3H), 2.03 (bs, 9H), 1.75 (bs, 6H); LCMS, single peak, 1.49 min, m/z, 291.7 (M+1).

Zn Analysis by Neutron Activation

Five ChemBridge compounds, 5839909, 5992599, 6106988, 5847158, and 7433453 were sent to Elemental Analysis, Inc. (Lexington, KY) to be tested for zinc concentration. Elemental Analysis elected to use Neutron Activation Analysis. This technique uses radiation to form a radioactive nucleus in the sample. The identity of an element, like zinc, can then be determined based on the element's specific decay. The amount of zinc present in the sample can be calculated based on the intensity of the gamma ray emission.[62]

Zn Inhibition HPLC Assay

This uses the same conditions as the HTS assay. The final concentrations used were 200 nM Pa1129 FosA, 50 μM Mn^{2+}, 100 mM K^{+}, 500 μM GSH, 750 μM fosfomycin, and 0.1% DMSO in HTS Buffer (10 mM NaH_2PO_4, 135 mM NaCl, pH 7.5) with a final reaction volume of 100 μL. The reaction was allowed to run at room temperature for 30 min and then quenched by the addition of 200 μL of 5% TCA with vortexing. The pH was re-adjusted to neutral with 100 μL of 800 mM NaOH with

vortexing. An internal standard, 100 μL of 1 mM valine, was then added. A portion of the reaction, 15 μL, was then added to 70 μL borate buffer and then derivatized using 15 μL of the AccQ-Fluor Reagent from Waters. The sample was then diluted with 400 μL of HPLC buffer (140 mM sodium acetate, 12.5 mM triethylamine, pH 5 with phosphoric acid). The diluted reaction mixture was then applied to a 4.5 cm x 25 cm ultrasphere reverse phase column (Beckman-Coulter) and eluted with a 0-30% acetonitrile gradient. The concentration of product in the reaction was determined based on the ratio of the product peak to the internal standard, valine.

NMR Analysis of ChemBridge and kk-5-series of Compounds

Compounds CB 5848410, CB 5846450, kk-5-095-1, kk-5-095-3 (kk-5-141-1), kk-5-095-4 (kk-5-141-2), and kk-5-095-5 were analyzed by ^{1}H, COSY, HSQC and HMBC NMR in d_6-DMSO. Data was collected on a 600 MHz Bruker NMR with a 14.1 Tesla Bruker magnet controlled by a Bruker AV-II console with a 5 mm Z-gradient TCI Cryo-probe. Data was analyzed using TopSpin™ by Bruker.

Resazurin Bioactivity Assay

E. coli BL21 Gold (DE3) cells were transformed with either FosA in a pET-20b vector or empty pET vector. Single colonies were used to inoculate 5 mL LB/Amp cultures and grown at 37 °C with shaking. The OD_{600} was measured in a spectrophotometer and appropriate dilutions were made before using the cultures in reaction plates.

To test the viability of this assay, checkerboards were set up in clear, 96-well, microplates (Whatman, Florham Park, NJ). For the reaction, 120 μL of LB/Amp/G6P

was added to the plate (130 μL for empty vector pET-20 plates). To this was added 10 μL each of 1.5 M fosfomycin (FosA only), 15 mM resazurin, and live cells in LB/Amp with an OD_{600} = 0.3. A checkerboard pattern was set-up in each plate using either sterile water or antibiotic (50 mg/mL kanamycin for FosA and 1.5 M fosfomycin for pET-20). The final concentrations in each well were 100 μg/mL ampicillin, 500 μM glucose-6-phosphate (G6P), 100 mM fosfomycin, 1 mM resazurin, 3 mg/mL kanamycin (5.4 mM), and the final cell density was OD_{600} = 0.02, or 5 x 10^6 colony forming units per milliliter (cfu/mL). Growth was monitored both colormetrically and spectrofluorometrically. Plates were covered with a clear plate sealer (SealPlate®, Excel Scientific, Wrightwood, CA) and grown at 37 °C with shaking overnight. Fluorescence was measured in a Spectramax M5 microplate reader in top reading fluorescence mode, sensitivity 6, with λ_{ex} = 530 nm and λ_{em} = 590 nm. Z' values were calculated as before.

Cell viability with validated hit compounds from the FosA assay was done by adding compounds, in a 2x serial dilution, to plates with either FosA or empty vector pET-20 transformed cell lines. This assay was a slightly modified version of the one used by Sarker, *et al.*[57] For each plate, row A was used as a sterility control – no bacterial cells added. Row B was used as a negative control – cells are added but no potentially cytotoxic compounds are included. Rows C-F were used for the compound serial dilutions. Row G was used for a Pf dilution control. Row H was used for a 2x serial dilution of kanamycin as a positive control. Volumes used were as previously stated. Fluorescence readings were taken every two hours for twelve hours and again at 24 hours.

Attempts to Create a FosX HTS Assay

Several attempts were made to develop a HTS assay using the purified *L. monocytogenes* FosX. Protein was purified as published.[44]

Assay using 3-(dansylamino)phenyl boronic acid (DAPBA).

Test reactions were run using 150 μM DAPBA dissolved in either methanol or ethanol (Figure 18). Five different buffer systems were tested: 20 mM TMA HEPES, pH 8, 10 mM NaH_2PO_4 with 135 mM NaCl, pH 7.5, 20 mM Tris, pH 7.5, and 20 mM KH_2PO_4, pH 6.8, and 25 mM TMA MOPS, pH 7.5. Molar equivalents of purified fos-diol was used to check for signal difference between solutions with and without product. Data was collected using a FluorLog-3 spectrofluorimter with λ_{ex} = 337 nm and scanning the emission spectra from 450-600 nm.

Assay using 8-quinoline boronic acid (8-QBA).

A similar test was done using 8-QBA, which should give a concentration dependent signal (Figure 18).[63] Reactions were run using molar equivalents of 8-QBA and purified fos-diol from 500 μM to 20 mM in 100 mM KH_2PO_4, pH 7.5. The 8-QBA was dissolved in pure methanol and dilutions were made so that the final MeOH concentration was 25% in all reactions. Reactions were run on the FluorLog-3 spectrofluorimeter with λ_{ex} = 314 nm and scanning emission wavelengths from 330-530 nm.

Adrenaline Based FosX Activity Assay

This assay measured the amount of fos-diol indirectly and was a modified version of the one published by Wahler and Reymond and was run in clear 96-well plates (Figure 19).[64,65] The reaction was done by adding 10 μL of fosfomycin and 10 μL of inhibitor

solution to 160 μL of E•Mn to give final concentrations of 500 nM *L. monocytogenes* FosX, 100 μM Mn^{2+}, 1.5 mM fosfomycin, and 0-10 mM Pf. The reaction was allowed to run for one hour and then 10 μL of $NaIO_4$ was added to give a final concentration of 750 μM $NaIO_4$ and the oxidation reaction was allowed to run for another hour. At the end of that hour 10 μL of adrenaline was added to give a final concentration of 1.5 mM and the plates were allowed to stand at room temperature for 30 minutes. The A_{490nm} was recorded using a Spectramax M5 microplate reader.

Gallocyanine Based FosX Assay

The gallocyanine assay is run in exactly the same manner as the adrenaline assay; only the final signal is read spectrofluorometrically instead of spectrophotometrically, making it more sensitive (Figure 20). Since this assay is more sensitive than the adrenaline based absorbance assay, the final concentration of fosfomycin was dropped to 500 μM, and the final $NaIO_4$ and gallocyanine concentrations were dropped to 300 μM. The concentrations of enzyme and metal remained the same as did the reaction times. Plates were read on a Spectramax M5 microplate reader with λ_{ex} = 370 nm and λ_{em} = 600 nm. Phosphonoformate was used to develop both the adrenaline and gallocyanine assays. Other potential inhibitors were also tried. These include other small phosphonates like Ethylphosphonic acid (EPA), Phosphonoacetic acid (PAA), 2-Carboxyethylphosphonic acid (CEPA), ethyldiethoxyphosphinyl formate, Tris(trimethylsilyl) phosphite, ethoxycarbonyl phosphate (ECP), and acetyl phosphonate, metal chelators such as adenosine mono-, di-, and triphosphate (AMP, ADP, ATP), EDTA, EGTA, ADA, citrate, HEDTA, BAPTA, oxalate, as well as inactive metals like zinc.

PHOME FosX Kinetics Assay

PHOME can be used in HTS formats for the discovery of inhibitors to mammalian soluble epoxide hydrolases.[66] To test this reaction in relation to the *L. monocytogenes* FosX, 1 μM of enzyme was incubated in black 96-well microplates (Whatman) with 50 μM Mn^{2+} and a 2x serial dilution of PHOME (50 μM max). Fluorescence measurements were taken every 10 minutes for two hours with λ_{ex} = 316 nm and λ_{em} = 460 nm on a Spectramax M5 microplate reader. One half of the 96-well plate contained enzyme and the other half did not to act as a control since this reaction can occur spontaneously. For each concentration of PHOME, the enzymatically-catalyzed signal was determined by subtracting fluorescence values from the negative control from the enzymatic reaction. The data in counts per second (cps) was converted to product concentration using a standard curve, plotted vs. time, and fit to a linear line of best fit. The slope of that line gave a rate of reaction for each starting PHOME concentration. A plot of [PHOME] vs. Rate (mM/min) was fit to a Michaelis-Menton curve to obtain a k_{cat} and K_M for the reaction.

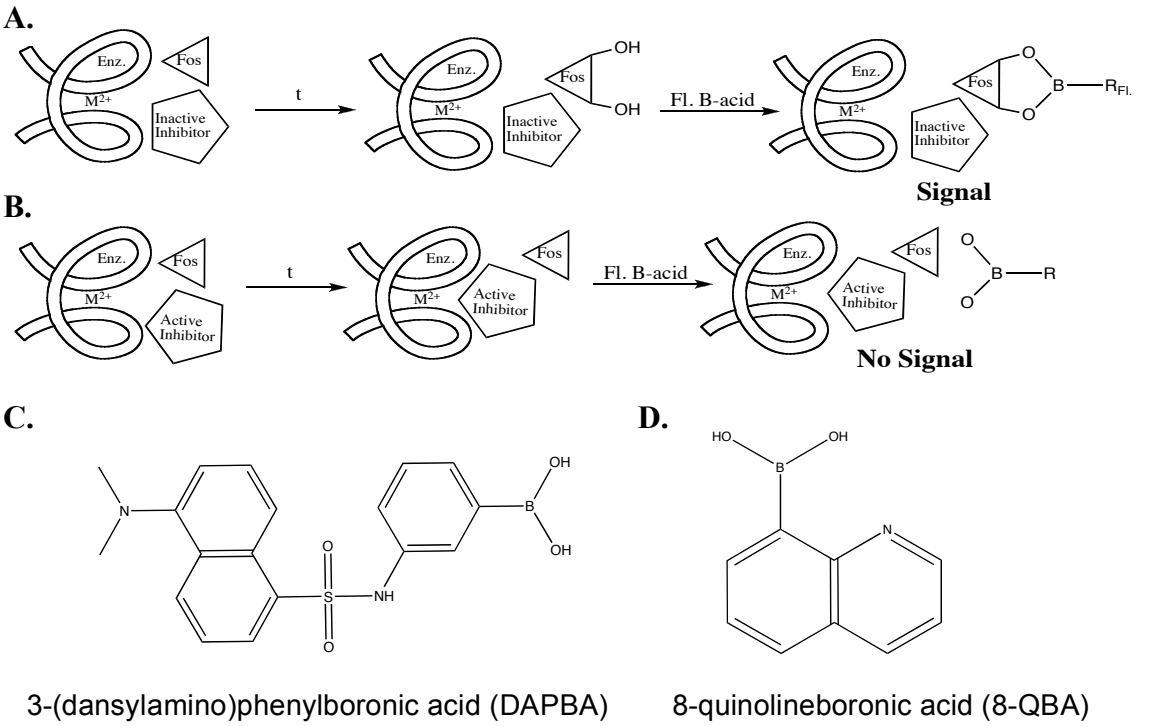

Figure 18: A-B) Theory behind the potential fluorescent boronic acid assay. C) Structure of DAPBA. D) Structure of 8-QBA.

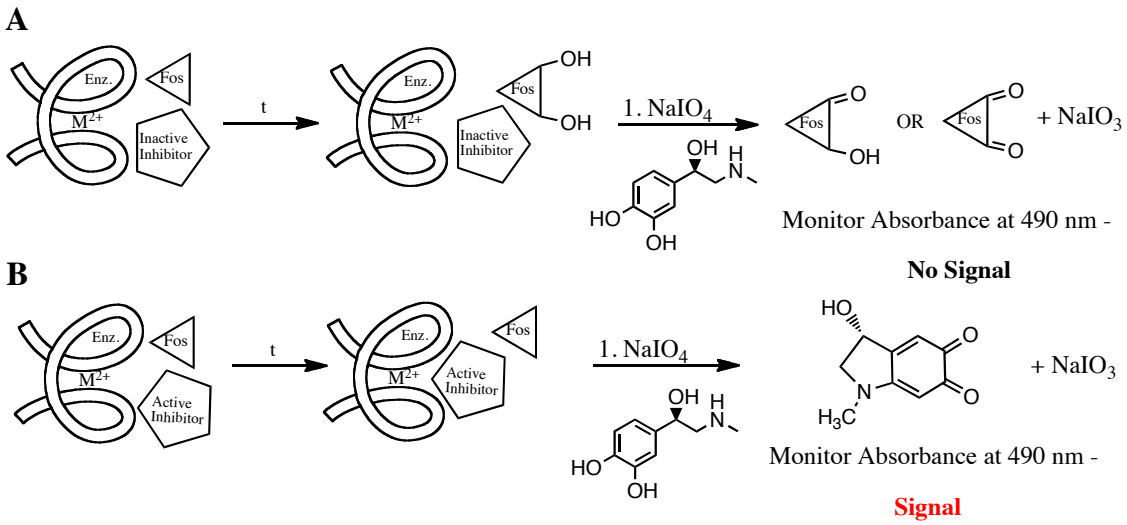

Figure 19: Adrenaline based assay. A) With no inhibitor present all of the periodate will be used up oxidizing the fos-diol product. The addition of adrenaline will result in no change in absorbance. B) With an inhibitor present, the periodate will not react with anything until the addition of the adrenaline for form adrenochrome. The production of adrenochrome can be monitored at 490 nm.

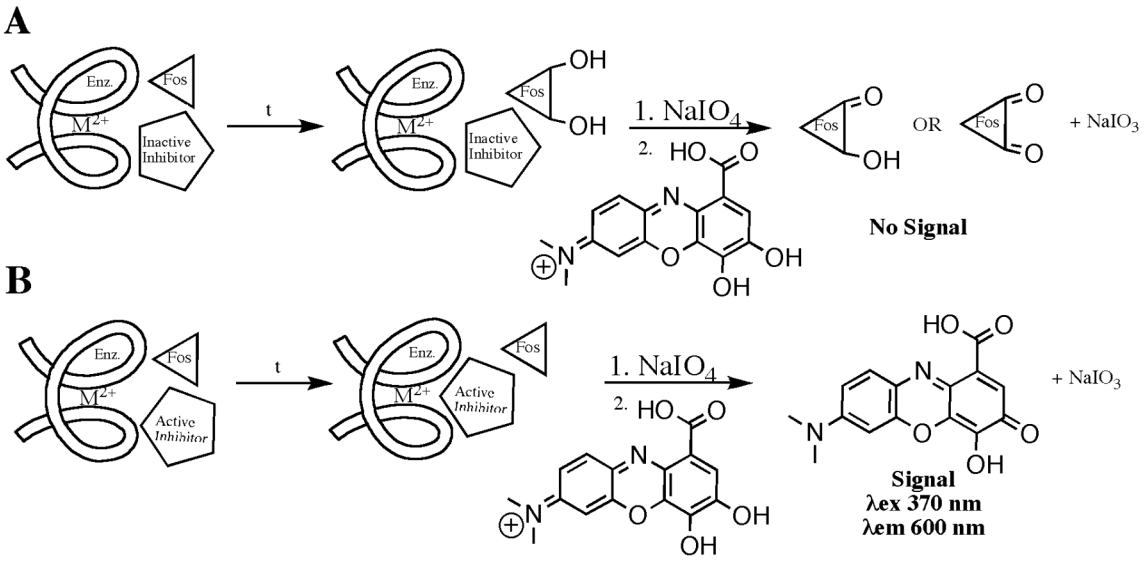

Figure 20: Gallocyanine based assy. This assay works the same as the adrenaline-based assay, Figure 59, but with a fluorescent reporter. The production of oxidized gallocyanine can be measured with λ_{ex} = 370 nm and λ_{em} = 600 nm.

CHAPTER III

GLUTATHIONE BINDING IN *P. aeruginosa* FOSA AND THE ROLE OF THE K^+-BINDING LOOP

Results

GSH Docking and Minimization

A putative GSH binding site was first identified by manual docking of GSH onto the *P. aeruginosa* FosA enzyme. This was followed by energy minimization of the docked complex.[55] Based on this model, amino acids within hydrogen bonding or electrostatic interactions to GSH include W34, Q36, Y39, S50, K90, and R93. Other residues within van der Waals contact distance include C48, Y62, H64, Q91, R119, and Y128. The distance from the GSH thiol group to the C1 position of fosfomycin is 3.48 Å. The details can be seen in Figures 21 and 22.

Kinetic Analysis of Native and Mutant Enzymes

The GSH molecule is normally activated for nucleophilic attack by ionization using assistance from an active site tyrosine or serine in canonical GSH transferases.[67] There were two early candidates to perform this ionization reaction, Y39 and S50. The model showed the hydroxyl group of Y39 3.45 Å from the GSH thiol group, indicating that it would be the more likely residue to perform this function. Indeed, the S50A mutation showed very little effect on catalysis but a large effect on the K_d^{GSH} indicating that it is most likely involved in GSH binding, but not activation. The conservative Y39F mutation showed a 13-fold reduction in k_{cat} and a 50-fold decrease in k_{cat}/K_M^{GSH} (Figure

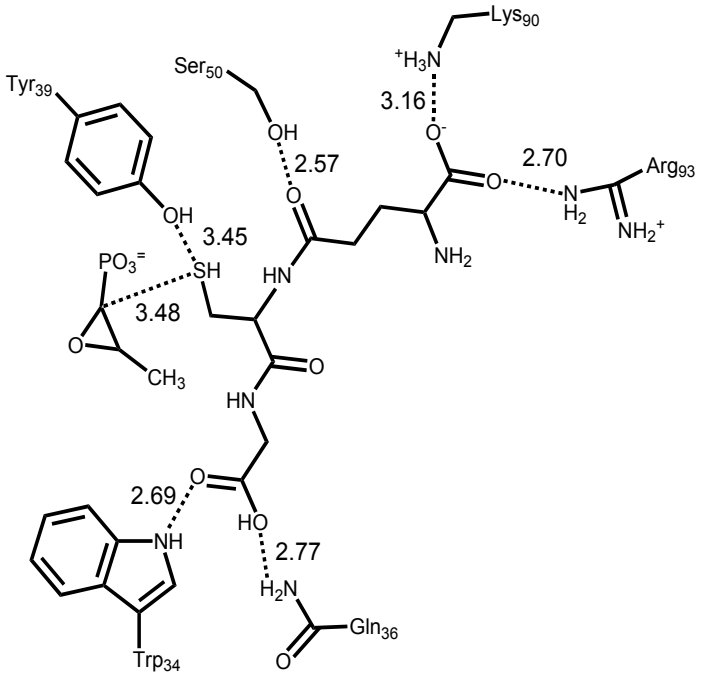

Figure 21: FosA residues that bind directly to GSH.

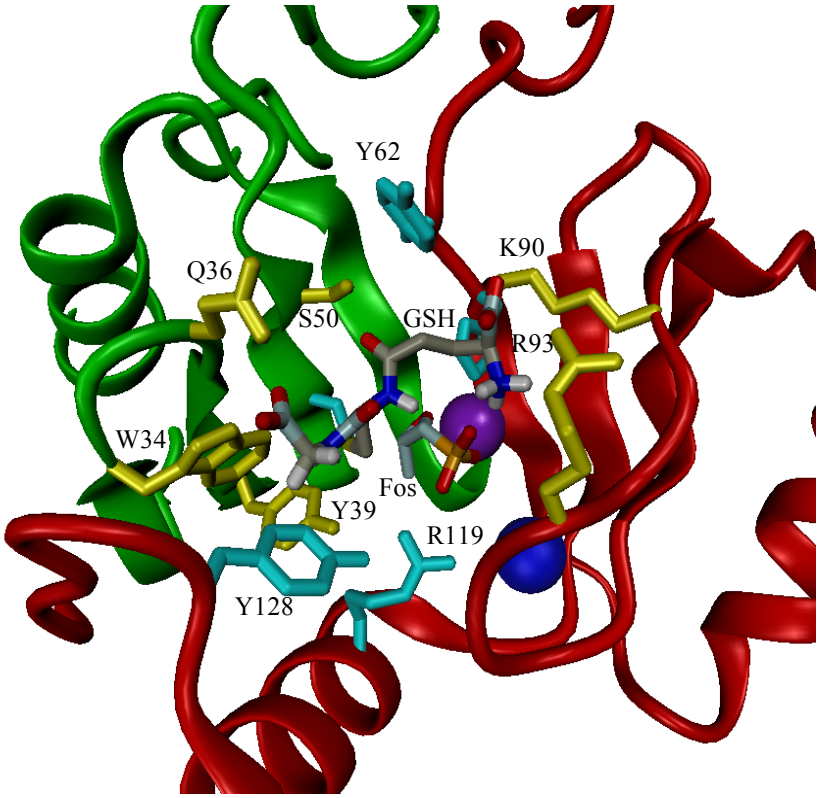

Figure 22: Ribbon diagram showing GSH bound in FosA. Primary sphere residues are shown in yellow. Second sphere residues are shown in cyan. Mn is in purple and K is in blue. Made by Eric Dawson.

23). This is a strong indication that Y39 is involved in the ionization of GSH to form the thiolate anion required for activity.

The model also suggests that W34, Q36, K90, and R93 are also within either hydrogen bonding or electrostatic bonding distance to the terminal carboxylate oxygens of GSH. In fact, the mutation of each of these residues results in a significant loss of activity in the FosA mutant enzymes.

GSH Binding Titrations with FosA

The titration of FosA with GSH results in a change in the enzymes intrinsic protein fluorescence, which can be monitored as a function of [GSH] to determine an equilibrium disassociation constant, K_d^{GSH}. The *P. aeruginosa* FosA has a K_d^{GSH} similar to the structurally unrelated canonical GSH transferases, around 130 μM.[38] The putative GSH binding mutants, however, all show a greatly elevated K_d^{GSH} (Figure 24). The Q36N, Y39F, S50A, K90A, and R93A mutants show a 150-400 fold increase in their K_d^{GSH} as compared to the native FosA enzyme. No K_d^{GSH} could be calculated for the W34A mutant due to the instability of the enzyme.

Two residues, K90 and R93, reside at the base of the K^+-binding loop. The FosA enzymes are activated 100-fold by K^+ and other monovalent cations.[38] It is notable that the K90A and R93A mutants have similar kinetic profiles to the native FosA enzyme when tested in the absence of K^+. To test this further a K^+-binding mutant was created with a three amino acid insertion (RVE was inserted between R93 and S94, in the position where those residues are located in the *M. loti* FosX enzyme). The catalytic and binding properties of this insertion mutant were similar to both the K90A and R93A mutants as well as the native mutant in the absence of K^+.

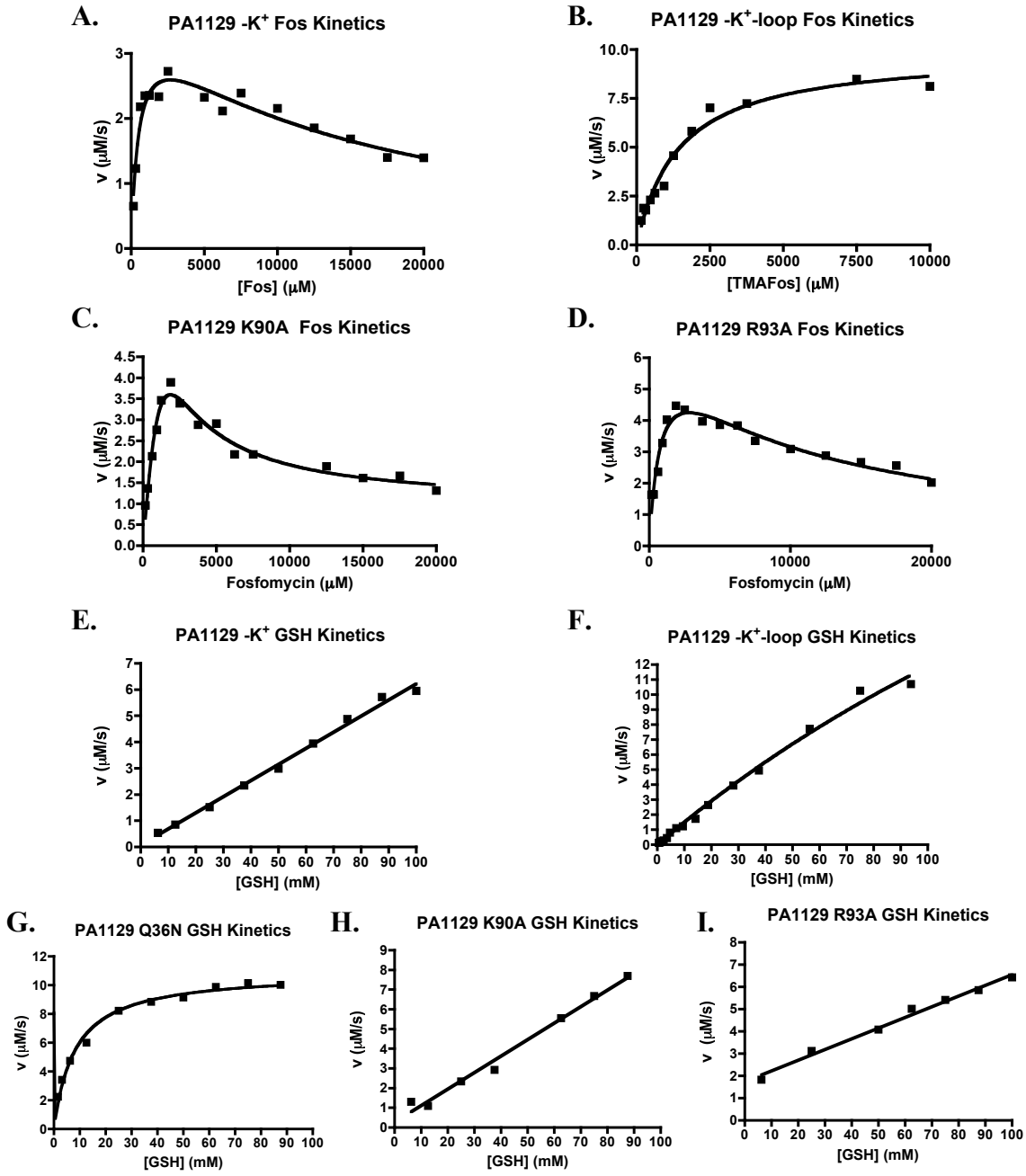

Figure 23: A-D) Fosfomycin kinetics curves. A, C, and D fit to partial substrate inhibition curves. B fit to Michaelis-Menten curve. E-I) GSH Kinetic curves. E, F, H, and I fit to linear regression curve to estimate k_{cat}/K_M directly. G fit to Michaelis-Menten curve.

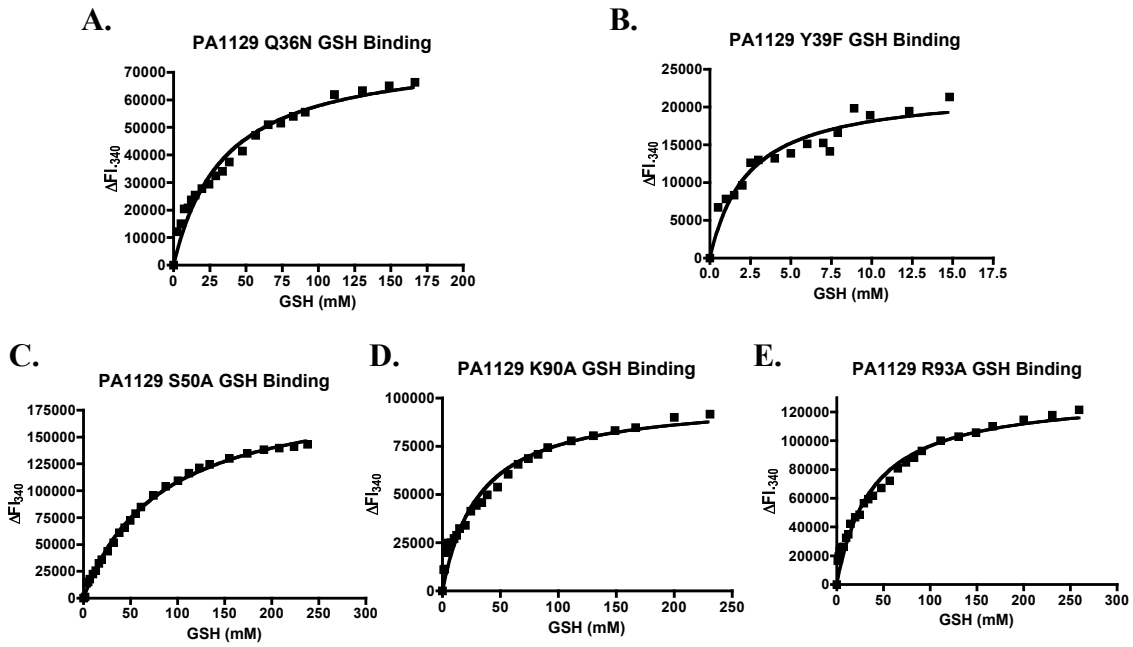

Figure 24: A-E) Changes in intrinsic protein fluorescence upon GSH binding for Pa1129 GSH binding mutants. All data were fit to one-site binding hyperbola in Prism.

Table 1: Summary of all kinetic data for Pa1129 GSH binding mutants.

Enzyme	k_{cat} (s^{-1})[b]	k_{cat}/K_M^{GSH} ($M^{-1}s^{-1}$)	K_d^{GSH}(mM)[a]	k_{cat}/K_M^{fos} ($M^{-1}s^{-1}$)[a]	MIC_{100}(mg/mL)[a]
$FosA^{PA}$	180 ± 6	(4.1 ± 0.8) x 10^4	.13 ± .03	(9.0 ± 1) x 10^5	>20
$FosA^{PA}$-K^+	~10	62 ± 2	39 ± 3	(1.4 ± 0.3) x 10^3	n.d.
$FosA^{PA}$-K-loop[c]	~14	26.6 ± 0.5	39 ± 2	(1.0 ± .2) x 10^4	2
W34A	32 ± 3	(2.0 ± 0.4) x 10^2	n.d.	(2.1 ± 0.5)x 10^4	<1
W34H	30 ± 4	(5.4 ± 1.1) x 10^3	.10 ± .02	(1.1 ± 0.3) x 10^4	>20
Q36N	109 ± 3	(1.4 ± 0.1) x 10^4	32 ± 3	n.d.	4
Y39F	14 ± 2	(8.7 ± 1.0) x 10^2	21 ± 1	(5 ± 3) x 10^5	1
S50A	134 ± 2	(6.2 ± 0.4) x 10^4	60± 3	(1.8 ± 0.9) x 10^6	2
K90A	~30	(3.4 ± 0.2) x 10^2	22 ± 3	(2.4 ± 0.9) x 10^4	2
R93A	~30	(1.9 ± 0.1) x 10^2	23 ± 3	(3 ± 1) x 10^4	2

The role of the W34 amino acid is more difficult to discern. The W34A mutant has a 30-fold decrease in the k_{cat}/K_M^{GSH}, consistent with a role in binding GSH, as predicted by the model. However, the protein precipitated at relatively low [GSH] in fluorescence titration experiments, which prohibited the calculation of a K_d^{GSH} for this mutant enzyme. Replacing the tryptophan with a histadine restores near native catalytic properties. The W34H mutant theoretically puts the imidazole NH group in a similar position as the original tryptophan. This mutant was stable and MIC results indicate that the imidazole is able to bind GSH effectively.

The S50A and Q36N mutants show quite different behavior from the other mutants. Both of these enzymes have a K_d^{GSH} similar to the other mutants, however they have near native k_{cat}/K_M^{GSH}. It is not known why this apparent paradox persists.

All of the single point mutations in the GSH binding site have a smaller effect on the catalytic efficiency of the enzyme with respect to fosfomycin (Table 1). This is consistent with the fact that all of these residues are thought to be involved in GSH binding, not in the recognition and binding of fosfomycin. The largest changes seen were for the K^+-binding loop mutant and the native mutant in the absence of K^+. This may suggest a larger role for K^+ in the activity of FosA.

Efficacy of FosA and Mutants in E. coli

The efficacy of the native FosA and mutant enzymes was tested by measuring how well they confer resistance to fosfomycin when transformed into *E. coli* (Figure 25). The native bacterium is very sensitive to fosfomycin with a $MIC_{100} < 0.025$ mg/mL on LB/agar/fos plates.[37] The native FosA enzyme can confer resistance to fosfomycin at greater than 20 mg/mL, which is the saturation limit of fosfomycin in agar plates. All of

the GSH-binding mutants show a significant decrease in their ability to confer resistance in *E. coli*. The largest changes were seen for the carboxylate oxygen binding residues, W34A, Y39F, K90A, R93A, and for the K^+-binding loop mutant. The W34A and Y39F mutants have an MIC less than 1 mg/mL while the K90A, R93A and K^+-binding loop mutants all have MIC values less than 2 mg/mL. The Q36N and S50A mutants show a greatly depressed MIC despite their enhanced kinetic abilities as compared to the other mutants. The W34H mutant has a native FosA like MIC.

There seems to be a loose correlation between the k_{cat}/K_M^{GSH} and the MIC values for the FosA mutants. Typically, mutants with a k_{cat}/K_M^{GSH} less than 10^3 have low MIC values while those with a k_{cat}/K_M^{GSH} greater than 10^3 have higher MIC values. Two of these mutants do not follow this correlation, however. The S50A and Q36N mutants have high k_{cat}/K_M^{GSH} values, but low MIC values. Both of these mutants also have high turnover numbers, but also have high K_d^{GSH}.

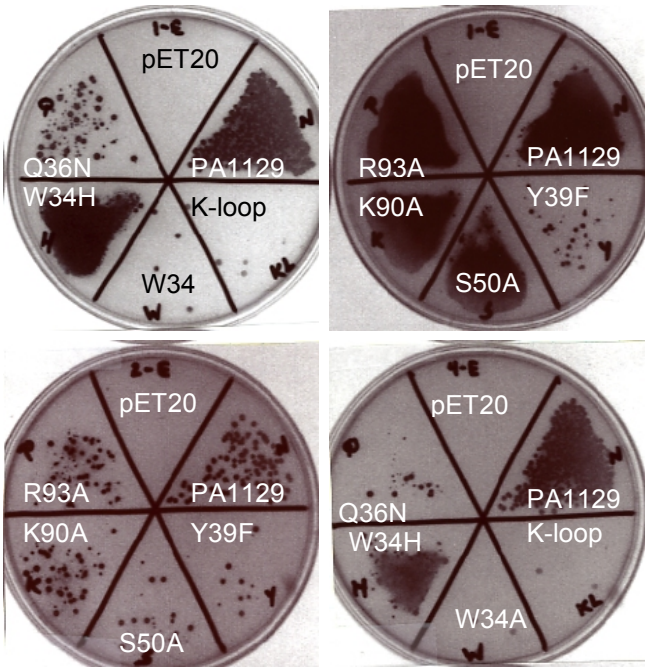

Figure 25: MIC plates for Pa1129 binding mutants. Plates were sprayed with thiazolyl blue before imaging to better visualize the bacterial growth.

Discussion

Model of the GSH-Binding Site

The GSH binding model suggests that there are six amino acids within hydrogen bonding or electrostatic interaction distance as well as another six amino acids within van der Waals contact. The model was tested experimentally by creating single point mutations of the putative binding residues and testing them for their kinetic profiles and substrate binding affinity, as well as their ability to confer resistance to fosfomycin when transformed into *E. coli*. Of the six amino acids tested, two, W34 and Y39, were designated as essential to function and one, K90, as "near-essential" by a saturation mutagenesis study published previously.[54] This is in keeping with the proposed role of these amino acids in the enzyme based on the model. The S50 and R93 amino acids were deemed non-essential, as they were able to tolerate several mutations at these positions. Q36 was not among the positions tested. It is also interesting to note that residues within van der Waals contact distance, H64 and R119, were deemed essential and C48 and Y128 were deemed "near-essential". This indicates that several of the residues indicated in the model are essential for enzyme function.

Activation of GSH

The *P. aeruginosa* FosA has several tyrosine residues in the active site that may facilitate in the ionization of GSH. The primary residue is Y39, whose hydroxyl group is 3.45 Å from the GSH sulfhydryl (Figure 26). Tyrosine 39 is also conserved in the FosB proteins which ionize L-cysteine, or possibly bacillathiol, for addition to fosfomycin.[41] Data from the canonical GSH transferases suggest that active site tyrosine residues can lower the pK_a of the GSH thiol group, aiding in the formation of the active thiolate

anion.[67] This interaction is usually assisted by hydrogen bonding interactions with other, secondary amino acids. Tyrosine 128 is in a position to form a hydrogen bond with Y39, according to the model. Tyrosine 128 was previously identified as a "near-essential" amino acid and is conserved in the FosA enzymes.[54] Other tyrosines that could contribute are Y62 and Y100. These two tyrosines are conserved among all members of the fosfomycin resistance protein family and play a role in fosfomycin binding.[49] There is no evidence that these residues participate in the binding or activation of GSH.

Relationship Between GSH and K^+ Binding

In the model of GSH binding in FosA, there are five other amino acids in hydrogen bonding or electrostatic interactions with GSH other than Y39. These five residues are W34, Q36, S50, K90, and R93. Serine 50 forms a hydrogen bond with the carbonyl at the γ-glutamate linkage to the cysteine of GSH. While the S50A mutant does show an elevated K_d^{GSH} consistent with its role in binding GSH, the mutation does not seem to effect the catalytic ability of the enzyme.

The other four amino acid contacts are responsible for bonding interactions with the two terminal carboxylates of GSH. Glutamine 36 does seem to bind GSH based on the catalytic profile of the Q36N mutant, showing an elevated K_d^{GSH}. The Q36N mutation, however, does not seem to effect catalysis, but does result in a loss of ability to confer resistance to fosfomycin. Tryptophan 34 seems to be structurally important to the enzyme as the W34A enzyme proved to be unstable in GSH titration experiments. The W34H mutant indicates that a hydrogen bond donor at this position is necessary for proper function, but that the donor does not necessarily have to be tryptophan.

The K90 and R93 amino acids are particularly interesting. These two residues reside at the base of the loop responsible for binding the monovalent K^+ ion (Figure 27). The model of GSH binding suggests that these two amino acids ion-pair with the terminal carboxylate of the γ-glutamate of GSH. The proximity of these residues to the K^+-binding loop may indicate a connection between K^+ and GSH binding. The mutation of either of these residues, the mutational disruption of the K^+-binding loop (RVE insertion), or the absence of K^+ in reactions with the native enzyme all lead to very similar decreases in K_d^{GSH}, k_{cat}/K_M^{GSH}, and in their ability to confer resistance to fosfomycin when transformed into *E. coli*. It has been known for some time that the addition of K^+ to FosA is necessary for maximum function, but the exact role of K^+ in the reaction has remained elusive.

The crystal structure of the *P. aeruginosa* FosA enzyme seems to indicate that the K^+ may aid in orienting fosfomycin in the active site of the enzyme.[40] This hypothesis was bolstered by the observation that in the crystal structure of the *Listeria monocytogenes* FosX with the diol product bound the product is bound in a 180º opposite orientation to the substrate bound in the *P. aeruginosa* FosA.[44] The results presented here indicate that the role of K^+ in FosA is more complex. It is probable, based on these results, that the binding of K^+ is also responsible for structuring the K^+-binding loop for the proper binding of GSH. The structuring of the K^+-binding loop is necessary for the proper orientation of K90 and R93 to bind GSH.

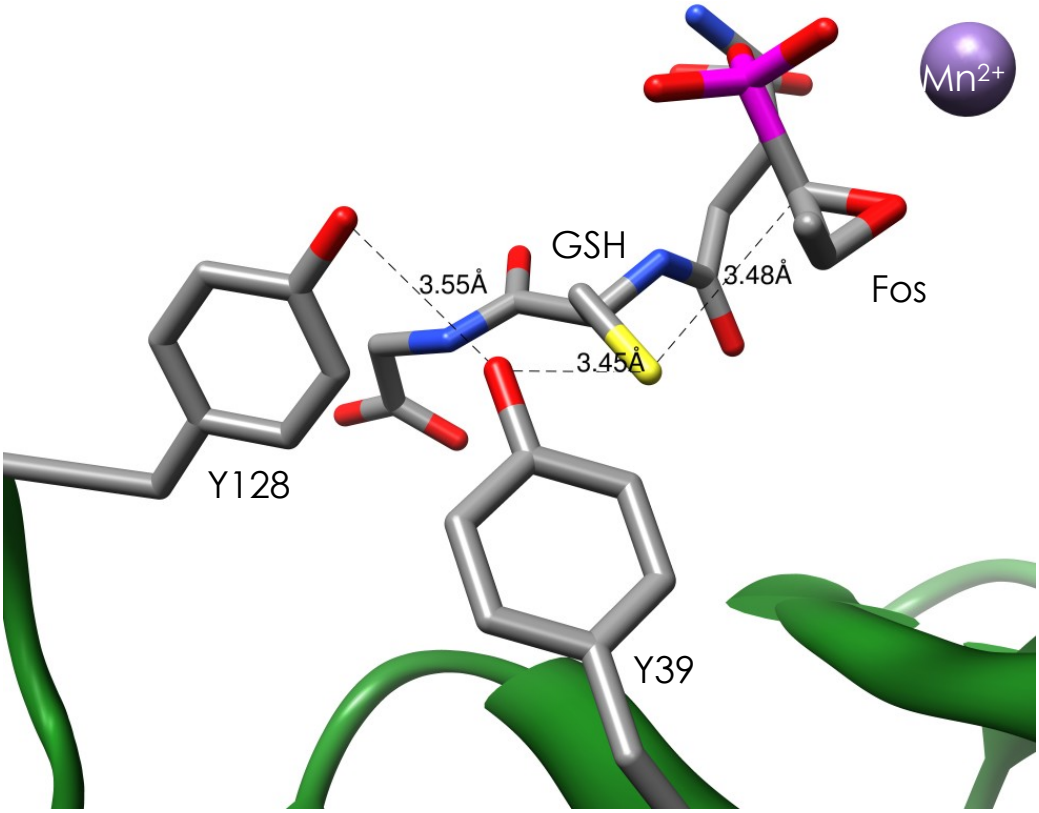

Figure 26: Activation of GSH by Y39 and Y128 with distances shown between the tyrosine hydroxyl groups, the GSH sulfhydryl, and the C1 position of fosfomycin.

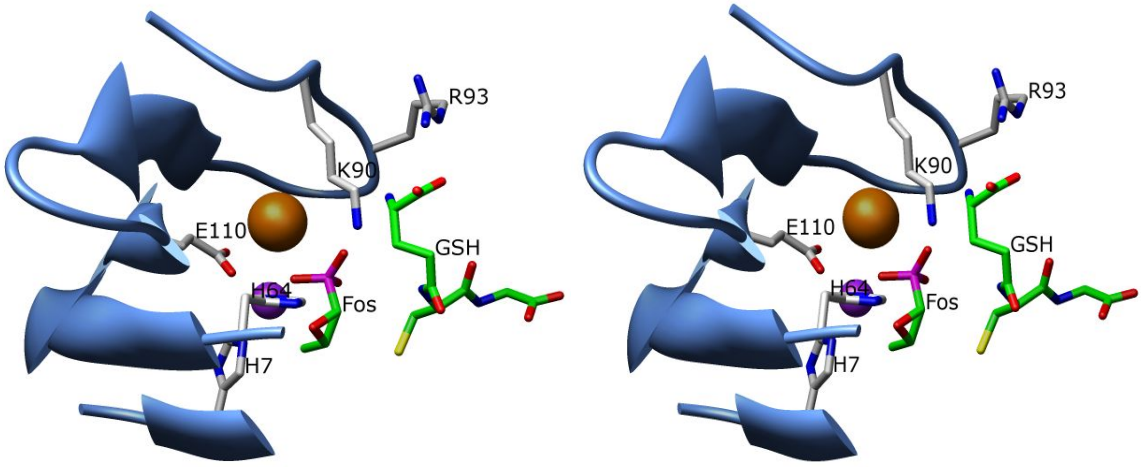

Figure 27: Stereo view of GSH bound in Pa1129 showing the relationship between K^+ binding and the position of K90 and R93. The K^+ ion is shown in orange.

CHAPTER IV

RATIONAL DESIGN AND DNA RECOMBINATION IN THE EVOLUTION OF A BETTER FOSA FROM THE *M. loti* FOSX

Results

Enzyme Structure Overlay

The initial step in analyzing the evolutionary structural changes that may have taken place between the FosX and FosA enzymes was to create a structure overlay of two of these enzymes. The most interesting FosX protein to use for this analysis was the one from *Mesorhizobium loti*. The *P. aeruginosa* FosA and the *M. loti* FosX overlay very well with a mean RMSD = 0.9 Å (Figure 28).

Rational Mutagenesis of the M. loti FosX

Once the structural alignment was complete, a search for differences in the active sites of the enzymes showed three specific amino acids to target. These three amino acids in the FosX were E44, F46, and M57 (Figure 29). The corresponding amino acids in the *P. aeruginosa* FosA are a glycine, tyrosine, and serine. Kerry Fillgrove made the point mutations in the *M. loti* FosX to the corresponding FosA residues in an iterative fashion. Dr. Fillgrove discovered that the single mutation E44G was sufficient to completely abolish the hydrolase activity of the FosX. The subsequent mutations were successful in increasing the GSH-transferase activity of the FosX enzyme. The k_{cat} for the *M. loti* FosX GSH transferase activity went from 0.15 ± 0.02 s^{-1} for the native enzyme to 5.0 ± 0.2 s^{-1} for the E44G/F46Y/M57S triple mutant.

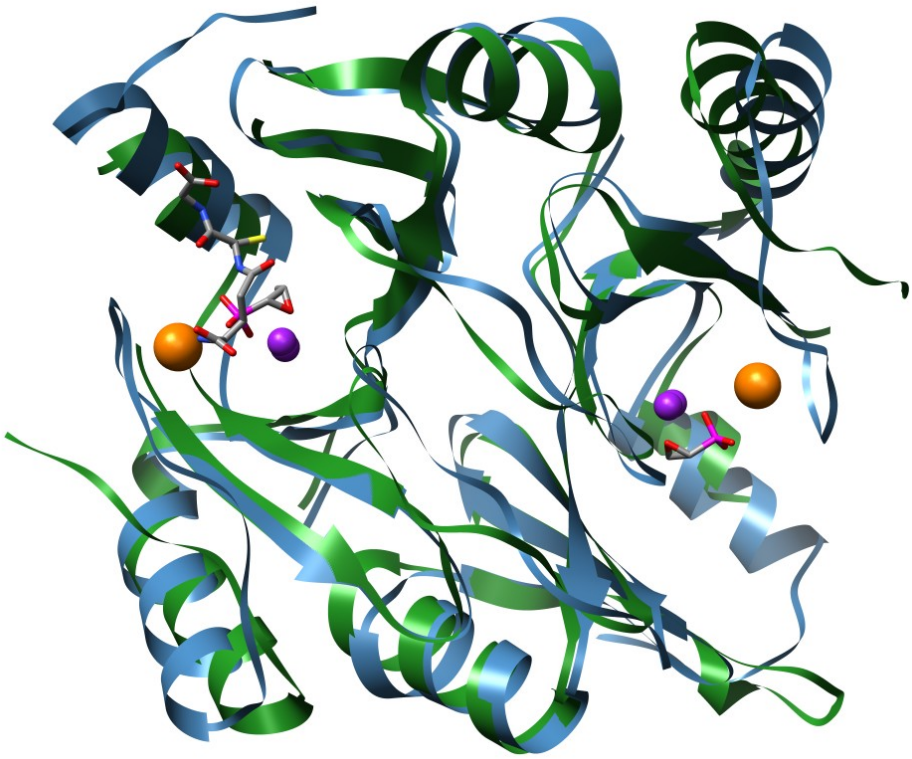

Figure 28: Ribbon diagram of an overlay of the *P. aeruginosa* FosA, blue, and the *M. loti* FosX, green. Mn is shown in purple, K in orange, and fosfomycin and GSH in stick form. Used FosA structure with GSH modeled in and PDB 1R9C for FosX.

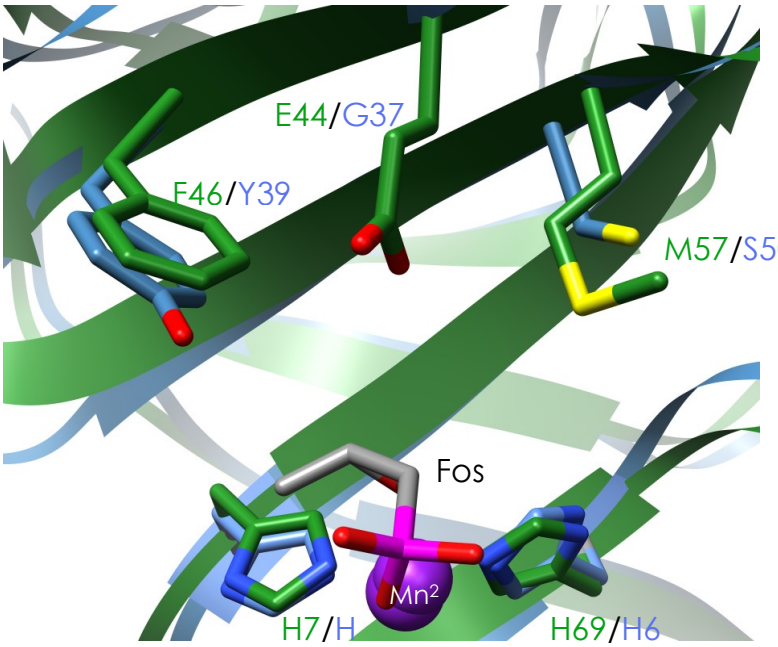

Figure 29: Active site overlay of the *P. aeruginosa* FosA, blue, and *M. loti* FosX, green, depicting the three amino acid differences between the two enzymes. GSH was removed to clarify the image.

Many additional mutations were made in this triple mutant background. These included the deletion of R99, V100, and E101, which shows up as an insertion in what is the K^+-binding loop in FosA in multiple sequence alignments (Figure 30). Additional K^+-binding loop mutants included L89H, L91V, D92R, M93E, R94W, P95K, P98R, and R103D. These mutations should have recapitulated the *P. aeruginosa* FosA K^+-binding loop in the *M. loti* FosX. Subsequently, residues T36, E37, F39, S40, C41, and S42 were deleted in a loop region that showed these residues to be an insertion when compared to the FosA enzymes in multiple sequence alignments (Figure 31). The final mutations made were S34W/H/Q/N and R43Q to attempt to introduce GSH binding residues and D27G or R85Q in either the S34Q or S34N backgrounds to break a salt bridge formed in the FosX enzymes (Figure 32). Unfortunately, every single mutation made after the initial triple mutation resulted in a decrease in activity. No subsequent mutagenesis was ever able to rescue activity.

	87																102
$FosA^{P.a.}$	R	E	W	K	Q	N	R	-	-	-	S	E	G	D	S	F	Y	F	L
$FosA^{T.n.}$	T	I	W	K	Q	N	K	-	-	-	S	E	G	A	S	F	Y	F	L
$FosX^{M.l.}$	D	M	R	P	P	R	P	R	V	E	G	E	G	R	S	I	Y	F	Y
$FosX^{L.m.}$	E	M	K	P	E	R	P	R	V	Q	G	E	G	R	S	I	Y	F	Y

Figure 30: Multiple sequence alignment of the FosA enzymes from *P. aeruginosa* and *Tn2921* with the FosX enzymes from *M. loti* and *L. monocytogenes*. Residues involved in GSH binding are colored red. Residues involved in K^+-ion binding are colored orange. A three amino acid insertion in the *M. loti* FosX K^+-binding loop is colored blue.

DNA Shuffling

Abandoning rational mutagenesis strategies, a DNA shuffling protocol was attempted., The DNA from two different Fos genes were shuffled and expressed in pET-20 vectors.[48] It is possible that at this point either an engineered mutant of $FosX^{ML}$ was

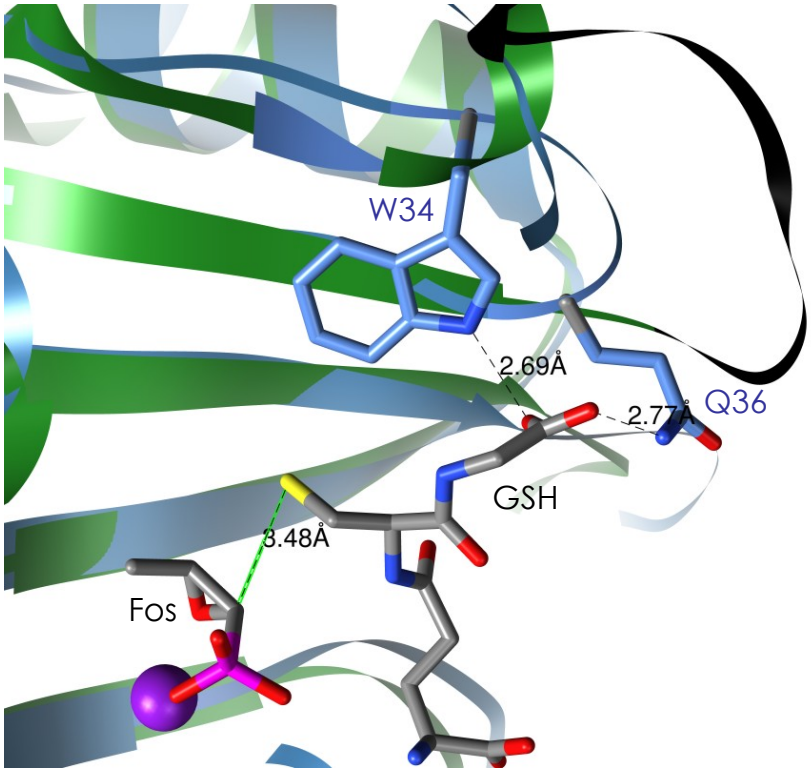

Figure 31: Ribbon diagram of an overlay of the *P. aeruginosa* FosA, blue, with the *M. loti* FosX, green, depicting one face of GSH binding. A seven amino acid insertion in FosX is shown in black at the top right.

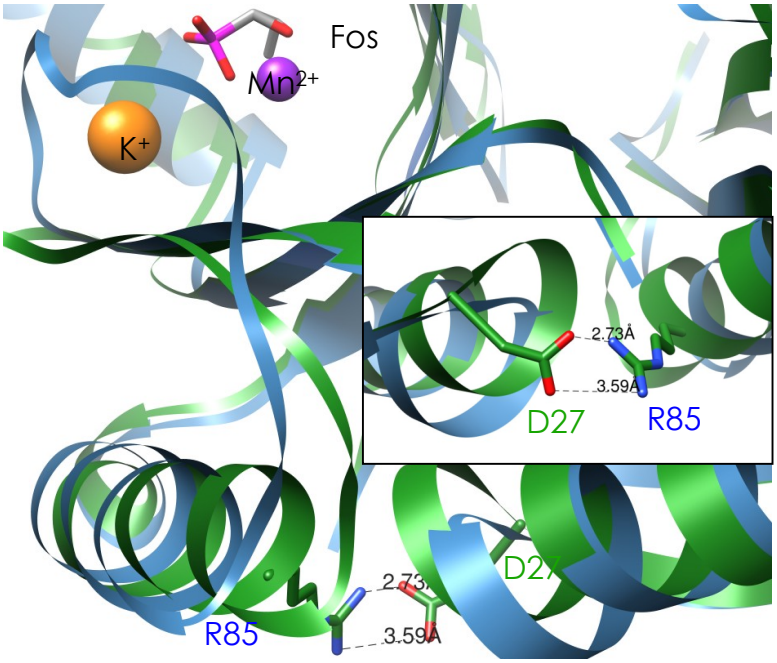

Figure 32: Two views of the FosX salt bridge formed between D27 and R85. The larger picture shows this from a similar vantage point as the overlay in Figure 26. Inset is a detail view of the interaction between D27 and R85 (180º view from larger picture).

used or, at least, contaminated the PCR reactions. The results of the three shuffling experiments resulted in the identification of six mutational variants (Table 2). One of these variants was identified 10 times while the other five were only identified one time each. The DNA analysis of these mutants showed that the most common variant has the same exact DNA sequence as an engineered mutant created by Lauren Beihoffer, with the exception of two single base mutations (Figure 33). These single base mutations are responsible for the E60K and A63V mutations seen in all of the six mutant variants.

All of the mutants identified to date have had some variant of the active site triple mutant created by Kerry Fillgrove (unpublished). Four of them have the exact same mutations, E44G/F46Y/M57S. One mutant has two of the same three but has an E44S mutation and one has only one of the same mutations with E44S and M57L mutations. All six variants have the E60K and A63V mutations. These are not the corresponding FosA residues but random mutants. Five of the six mutants have the $FosA^{PA}$ K^+-binding loop recapitulated. A sequence alignment of the mutant strains against $FosX^{ML}$ indicates the deletion of P96, G104, and R105 in this region, not the R99/V100/E101 deletion made in the rationally designed mutants. One mutant has an S99P mutation in the K^+-binding loop (using mutant numbering). A couple mutants also contained single point mutations that were not seen in any other variants. One mutant has a T123M mutant and one has a E126K mutant.

Despite the potentially contaminated shuffling, three of the mutational variants were chosen to measure their kinetics and inhibitory capacity. The three mutants chosen were shuffle mutants (DNAs) 1.1, 1.2 and 2.2. Of these three, DNAs1.1 and 1.2 showed

Table 2: DNA recombinant mutants isolated.

Gene Name	Triple Mutant Residues			Other Residues			K-loop Residues 94-103
1.1	E44S	F46Y	M57L	E60K	A63V		WKQNRSEGDS(ΔP96, G104, R105)
1.2	E44G	F46Y	M57S	E60K	A63V	T123M	WKQNRSEGDS(ΔP96, G104, R105)
2.2, 2.3, 2.4, 2.6, 2.7, 2.9, 2.10, 2.11, 3.1, 3.2	E44G	F46Y	M57S	E60K	A63V		WKQNRSEGDS(ΔP96, G104, R105)
2.8	E44G	F46Y	M57S	E60K	A63V		WKQNRPEGDS(ΔP96, G104, R105)
3.3	E44G	F46Y	M57S	E60K	A63V	E126K	WKQNRSEGDS(ΔP96, G104, R105)
3.4	E44S	F46Y	M57S	E60K	A63V		WKQNRSEGDS(ΔP96, G104, R105)

Figure 33: Alignment of DNA shuffle mutant 2.2 with an engineered *M. loti* FosX mutant containing the E44G/F46Y/M57S triple mutant as well as the RVE K^+-loop deletion and R94W/P95K/P96Q/R97N/P98R/G102S/R105D.

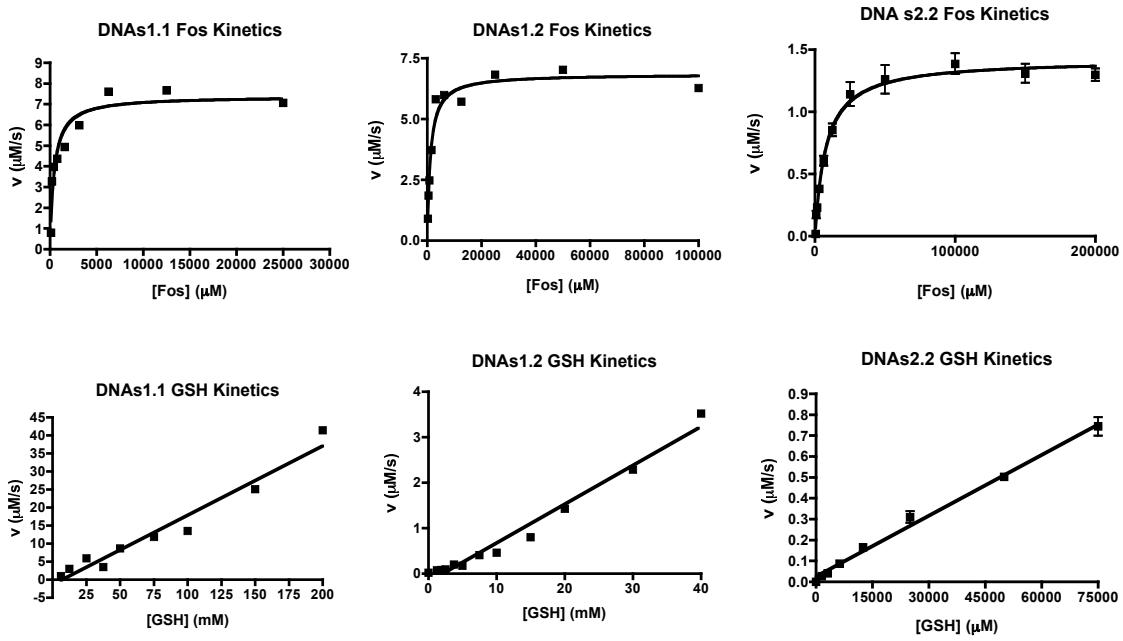

Figure 34: A-C) Fosfomycin kinetics for DNAs1.1, 1.2, and 2.2. D-F) GSH kinetics for DNAs1.1, 1.2, and 2.2.

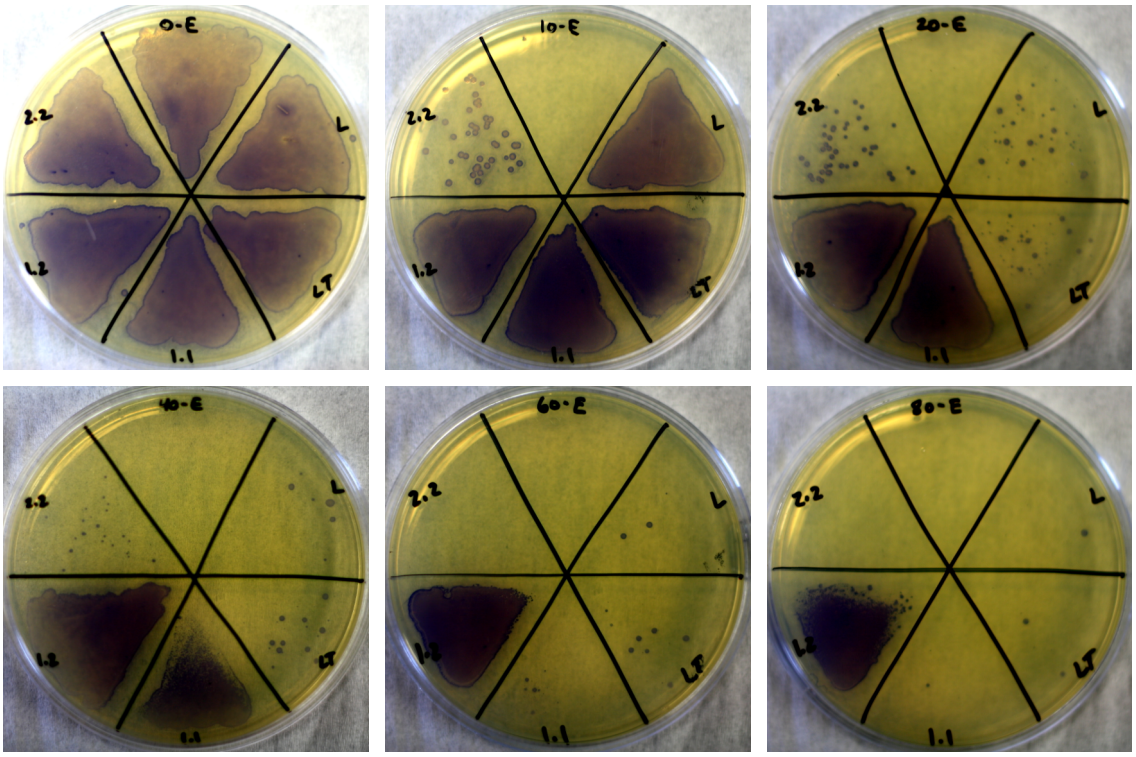

Figure 35: MIC plates for DNA shuffle mutants. The number before "E" on each plate is the [fos] (µg/mL). MIC values: for empty vector pET-20 (E), 10 µg/mL, for native *M. loti* FosX (L), 20 µg/mL, for the *M. loti* Triple mutant (LT), 20 µg/mL, for DNAs1.1 (1.1), 60 µg/mL, for DNAs1.2 (1.2), >80 µg/mL, for DNAs2.2 (2.2), 10 µg/mL.

improved kinetics over the native $FosX^{ML}$ and the triple mutant as well. DNAs2.2 did not. DNA 1.1 and 1.2 have a k_{cat}/K_M^{fos} of $5 \pm 1 \times 10^4$ and $1.2 \pm 0.2 \times 10^5$ $M^{-1}s^{-1}$ respectively. However, their k_{cat}/K_M^{GSH} was still very poor; only $6.4 \pm 0.5 \times 10^2$ and $4.3 \pm 0.2 \times 10^2$ $M^{-1}s^{-1}$ respectively. Both mutants did have a much better MIC than native $FosX^{ML}$ or the triple mutant; 60 μg/mL for DNAs1.1 and 120 μg/mL for DNAs1.2. Interestingly, despite only a few differences in amino acid sequence, DNAs2.2 had very poor kinetics (similar to native $FosX^{ML}$) and a worse MIC than even native *M. loti* FosX (Figures 34 and 35 and Table 3).

Structure of DNAs2.2

The DNA shuffle mutant 2.2 was crystallized in microbatch trays under Al's Oil (a 1:1 v/v mix of silicon oil and paraffin oil) by microseeding. The crystallization condition was a 1:1 mix of enzyme and buffer and crystals formed in 2-3 days. A structure was solved to 2.0 Å using the native $FosX^{ML}$ structure to solve the phasing using molecular replacement. The overall structure is very similar to the native $FosX^{ML}$, which is not unexpected since the two enzymes are 87% identical. The DNAs2.2 enzyme crystallized as a dimer in the asymmetric unit. Interestingly, no metal ions were seen in the active site of the enzyme despite being present in a two fold molar excess in the crystallization conditions. The only ligand apparent was a possible ammonium ion in one active site, but not the other.

The most interesting aspect of this structure is what should be the K^+-binding loop. In the DNAs2.2 mutant, this loop actually forms a β-strand and joins the β-sheet on the bottom half of the active site. This leaves the active site very open. It also kinks the c-terminal end of the loop 90º when compared to the K^+-binding loop in the $FosA^{PA}$

enzyme. The position of the E60K and A63V mutations is also interesting. These two residues are about 20 Å from the active site and oriented towards the outside of the enzyme so it is not apparent what their function might be. Still, these mutations are seen in all of the shuffle mutants.

Table 3: Summary of Kinetic Data and MIC values for DNA shuffling mutants.

Enzyme	k_{cat}/K_M^{fos} $M^{-1}s^{-1}$	k_{cat}/K_M^{GSH} $M^{-1}s^{-1}$	MIC (mg/mL)
Pa1129 FosA	$9.0 \pm 1.4 \times 10^5$	$4.1 \pm 0.8 \times 10^4$	>20
***M. loti* FosX**	$5.0 \pm 0.6 \times 10^2$	n.d.	0.02
KLF *loti* Trip.	$8 \pm 3 \times 10^3$	$4.9 \pm 0.2 \times 10^2$	0.02
Shuffle 1.1	$5 \pm 1 \times 10^4$	$6.4 \pm 0.5 \times 10^2$	0.06
Shuffle 1.2.3	$1.2 \pm 0.2 \times 10^5$	$4.3 \pm 0.2 \times 10^2$	0.16
Shuffle 2.2	9 ± 1	0.49 ± 0.03	0.01-0.02

Discussion

Enzyme Structure Overlay

The fosfomycin resistance enzymes are members of the VOC superfamily of enzymes, which include the extra-diol dioxygenases, bleomycin resistance protein, methylmalonyl-CoA epimerase, and glyoxalase 1. While all of these proteins vary in their reaction mechanism, they are all structurally very similar. All members of the VOC superfamily are homodimers that use a βαββββ motif to form a cup-shaped metal ion-binding site. Previous reviews of this superfamily have shown that despite their differences, the many members of this superfamily are basically super-imposable structurally.[46] It is therefore not surprising that two more functionally related enzymes, such as the *P. aeruginosa* FosA and the *M. loti* FosX, are structurally very similar.

Rational Mutagenesis of the M. loti FosX

The most interesting question in regards to the FosA/X enzymes is what small changes within their general structural scaffold leads to such a large disparity of function between the two enzymes. The work done on the functional analysis of several different mutants has helped to answer this question, in part.

There are only three different amino acids in and around the active site of the FosA and FosX enzymes. These three amino acids, E44, F46, and M57 in the *M. loti* FosX, were mutated to their FosA equivalents, glycine, tyrosine, and serine. It was found that the single E44G mutation was sufficient to completely abolish the FosX activity of the *M. loti* enzyme. The crystal structure of the *M. loti* FosX suggests that this residue is properly positioned to activate water for addition to the C1 position of the antibiotic.[43] The other two residues serve to increase the turnover of the FosA reaction catalyzed by

the *M. loti* enzyme. The F46Y mutation introduces the tyrosine residue responsible for ionizing GSH for addition to fosfomycin in the FosA enzyme and M57S introduces a putative GSH binding residue.[55] Also, the smaller serine residue opens up space for GSH binding. An overlay of the *M. loti* FosX with the *P. aeruginosa* FosA with GSH modeled in suggests that M57 would sterically hinder the binding of GSH.

This original triple mutation, made by Kerry Fillgrove, was the first step in engineering a better FosA enzyme from the *M. loti* FosX scaffold. This initial mutation was a good first step, increasing estimated k_{cat} 30 fold to a marginally respectable 5.0 s^{-1}. However, it was also shown that as more and more GSH is added to the reaction the turnover rate continues to increase, indicating that this enzyme is not saturating with respect to GSH. The next step in developing a better FosA activity was to engineer a better GSH binding site.

The first step in creating a better binding site was trying to create a K^+ binding loop. This may sound like a very roundabout method, but recall from Chapter 3 that two of the GSH binding residues, K90 and R93, are located on the K^+-binding loop. The loss of the enzymes ability to be activated by potassium, presumably by no longer binding it properly, as evidenced by the K^+-loop mutant made in the *P. aeruginosa* FosA, results in poor activity similar to the single point mutations of K90 and R93 to alanine. Introducing proper K^+-binding and activation in the *M. loti* FosX should result in proper GSH binding. Therefore, the subsequent introduction of the corresponding K90 and R93 residues from FosA should be able to be inserted into the FosX and create a GSH binding site.

A multiple sequence alignment of several FosA and FosX enzymes shows that there is a three amino acid insertion in the K^+-binding loop in the FosX enzymes. The first task in engineering a proper K^+-binding loop in FosX was to eliminate the three amino acid insertion. In the *M. loti* FosX, these residues were R99, V100, and E101. Unfortunately, the deletion of these residues in the triple mutant background not only did not introduce any K^+ activation, but actually demonstrated a decrease in turnover as compared to the active site triple mutant alone. We decided, therefore, to completely replace the FosX loop with the corresponding residues from the FosA enzyme so that the *M. loti* FosX would have the entire *P. aeruginosa* FosA K^+-binding loop reconstituted in the triple mutant background. These mutations did not lead to any increase in activity and remained less active than the triple mutant alone.

The other end of GSH, the glycine carboxylate, is bound to FosA by hydrogen bonding interactions with W34 and Q36. In the *P. aeruginosa* FosA these two residues protrude from a turn between two β2 and β3 of the first βαβββ motif. According to multiple sequence alignments, there is a seven amino acid insertion in this region in the FosX enzymes. The deletion of this insertion and the mutation of appropriate residues to the corresponding tryptophan and glutamine residues in the background of the triple mutation plus the K^+-binding loop results in an even further reduction in activity in the enzyme.

The deletion and mutation of these loops in the enzyme resulted in decreased functionality. For this reason the attempt to rationally design a better FosA enzyme from the *M. loti* FosX was abandoned. Instead a different approach was tried – DNA shuffling.

DNA Shuffling

In theory, DNA shuffling is able to take to similar genes and shuffle the genetic material to create a library of new genes with varying function.[48] This process works better the more similarity there is in the sequence as this aids in gene overlap. The *P. aeruginosa* FosA and *M. loti* FosX are only about 48% identical, severely limiting the potential number of overlaps possible. Still, from three different shuffling experiments six different mutant variants were isolated. However, subsequent analysis seemed to indicate that there was not much, if any, real overlap of any length of the two gene products. Subsequent analysis seems to indicate that either the FosX gene used was not the native FosX but an engineered mutant that had the triple mutant, the RVE deletion, as well as seven other point mutations in the K^+-loop region. It is possible that this gene was just contaminating the PCR reactions, but the exact nature of the contamination introduction is not known.

All of the mutants isolated to date are genetically identical to the engineered FosX enzyme with only a few single base pair mutations. These single mutations are responsible for the variation among the shuffle results. The DNA shuffling procedure is known to introduce random mutations in numbers similar to error prone PCR.[48] All of the mutants isolated had some version of the active site triple mutation. The variation seen among the mutants was due to single base mutations, which were a result of the shuffling procedure, not from an actual shuffling event. All of the mutants have the designed K^+-binding loop with the exception of one, which again has a single base mutation that changes a serine to a proline in the middle of the loop.

There are several new mutations that are introduced, but these are also the result of single base mutations. It is unclear why every single mutant isolated contains both the E60K and A63V mutations. These two residues are located about 20 Å from the active site of the enzyme and do not seem to add any function that can be tested kinetically. Still, their presence in every mutant does seem to suggest some selective advantage. The other two new mutations were only seen once each and both are near the C-terminus of the enzyme and wouldn't seem to be involved in the proper functioning of the enzyme.

Only three of the six mutants have been functionally characterized and two of the three show markedly increased activity as compared to the native *M. loti* FosX. The third mutant, DNAs2.2, however, is almost non-functional as an enzyme and has an even worse MIC than the native FosX. However, there are only a few amino acid differences between this mostly inactive mutant and the two more active mutants, DNAs1.1 and 1.2. DNAs1.1 and 2.2 only differ in the triple mutant residues with 2.2 having the same mutations as those originally created by Kerry Fillgrove and 1.1 having instead E44S and M57L mutations. The only difference between DNAs1.2 and 2.2 is the T123M mutation at the C-terminus. It is not clear at this time why these few mutations institute such a big difference in activity. Structural studies of these enzymes, however, could prove invaluable in discerning the nature of these relationships.

Structure of DNAs2.2

The crystal structure of DNAs2.2 is interesting (Figure 36). Overall, this structure aligns very well with the native FosX enzyme as well as the *P. aeruginosa* FosA. The one major structural difference, however, is a rather substantial one. In DNAs2.2 the K^+-binding loop actually forms a β-strand and joins the β-sheet surrounding the active site.

This opens up the active site, but it also prevents the binding of either K^+ or GSH. There is a small loop formed by three residues, but it is more of a β-turn instead of a loop. Even so, an overlay of DNAs2.2 and the *P. aeruginosa* FosA shows that this small turn is oriented 90º from the FosA K^+-binding loop (Figure 37).

What this structure really does is explain why our attempts to engineer a better FosA from the *M. loti* FosX were unsuccessful. The very first deletion event, that of the RVE residues from the K^+-binding loop, resulted in the proper shortening of that loop to form the β-strand seen in the crystal structure. Every mutation made from that point on only served to modify an already drastically changed loop. There is no way to introduce K^+-binding to this system and the GSH binding residues are not in the proper location.

This structure does not answer the question of why this enzyme is not active as compared to the DNAs1.1 and 1.2 mutants. In fact, the DNAs2.2 crystal structure did not have any density past T122, just missing out on the T123M mutation seen in DNAs1.2. Still, this region is not very close to the active site so an apparent benefit from this single mutation is not evident. Hopefully the structures of DNAs1.1 and 1.2 can be solved for better comparative analysis.

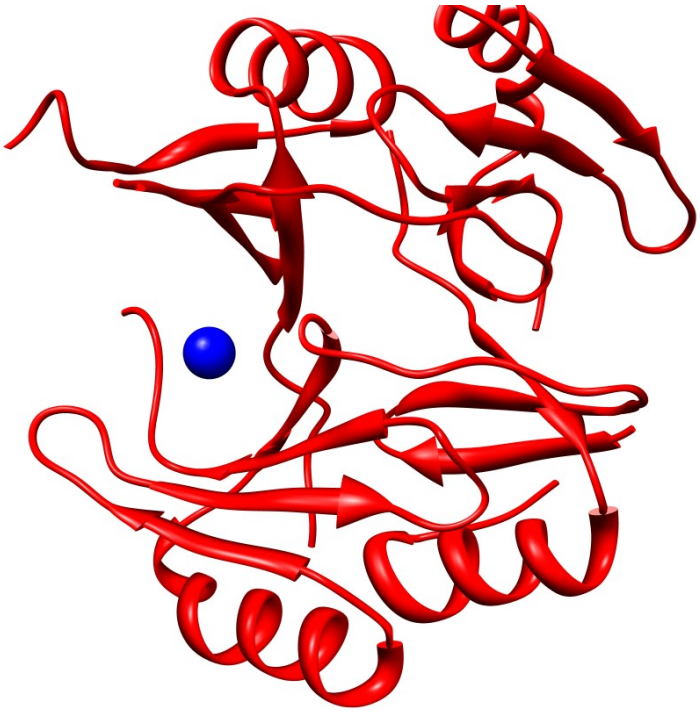

Figure 36: Ribbon diagram of DNAs2.2. The enzyme crystallized to 2.0 Å as a dimer in the asymmetrical subunit. Also shown above is ammonia from the crystal buffer, in blue.

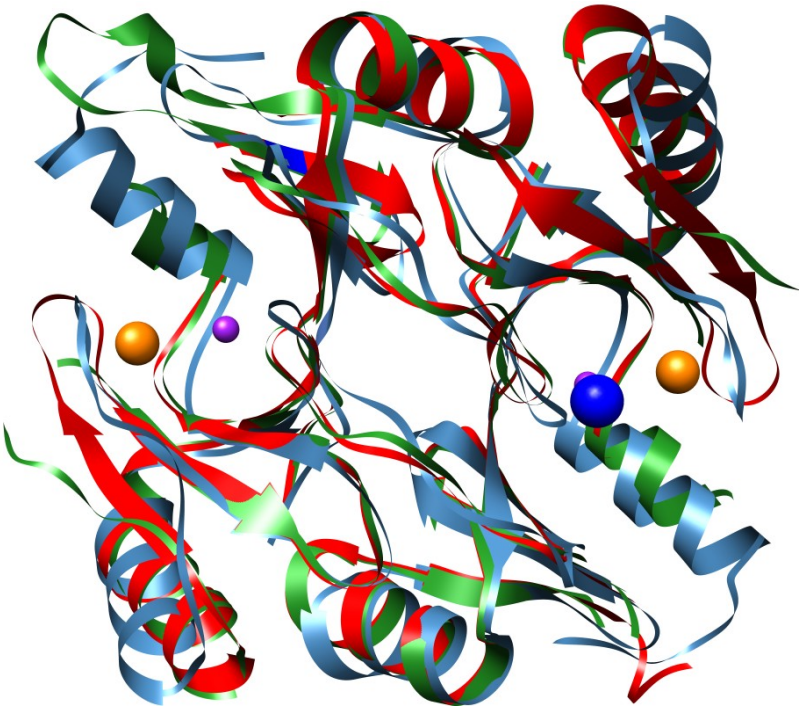

Figure 37: Ribbon diagram of an overlay of the *P. aeruginosa*, FosA in blue, *M. loti* FosX, in green, and DNA s2.2 in red. Mn^{2+} is shown in purple, K^{+} in orange, and the ammonium ion is shown in bright blue.

CHAPTER V

DEVELOPMENT OF HIGH-THROUGHPUT SCREENS FOR THE DISCOVERY OF BIOACTIVE INHIBITORS TO FOSA FROM *P. aeruginosa*

Results

Monobromobimane (mBBr) has been used for many years as a selective fluorescent tag for thiol compounds.[68-70] These applications were mostly focused on HPLC based discovery and separation of these compounds. In this project, a new spin was put on this old bit of technology.

To test the reaction of mBBr and GSH in a FosA reaction system, 2 mL reactions were run on a fluorimeter to check the mBBr signal in the reaction buffer system. The compound mBBr has very little intrinsic fluorescence, but the GS-mB product is highly fluorescent. The product fluorescence can be easily measured with λ_{ex} = 370 nm and λ_{em} = 480 nm (Figure 38). These first experiments showed that there was a definite difference in the fluorescence intensity between reactions with and without enzyme or GSH and indicated that this might be a viable method to use in creating an HTS assay (Figure 39).

Assay Development

The first two versions of this assay were developed using the known FosA inhibitor phosphonoformate, $K_i = 0.4 \pm 0.1$ μM.[49] As a known entity, phosphonoformate (Pf) was a good candidate from which to create an assay since it would make a good standard from which to proceed. The first step was to measure a concentration-response

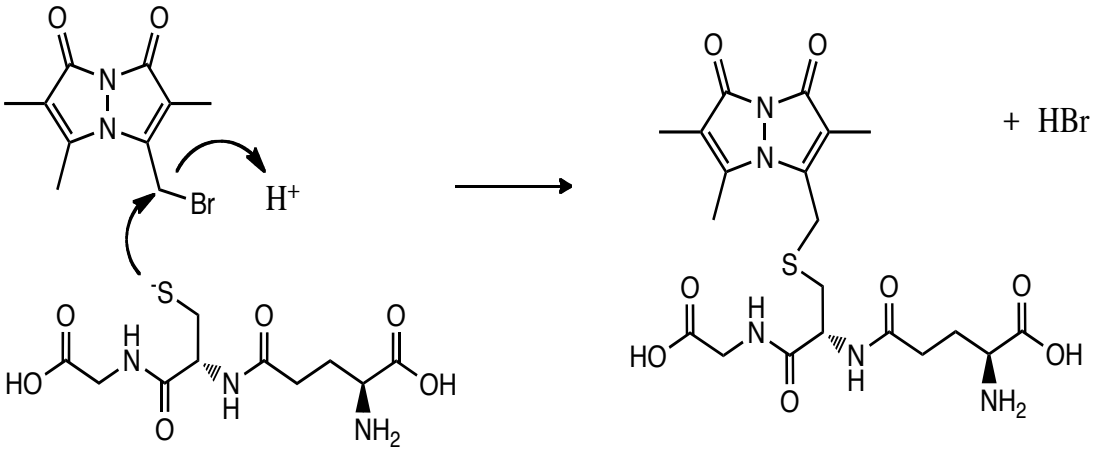

Figure 38: Reaction of GSH with mBBr to form the fluorescent covalent product.

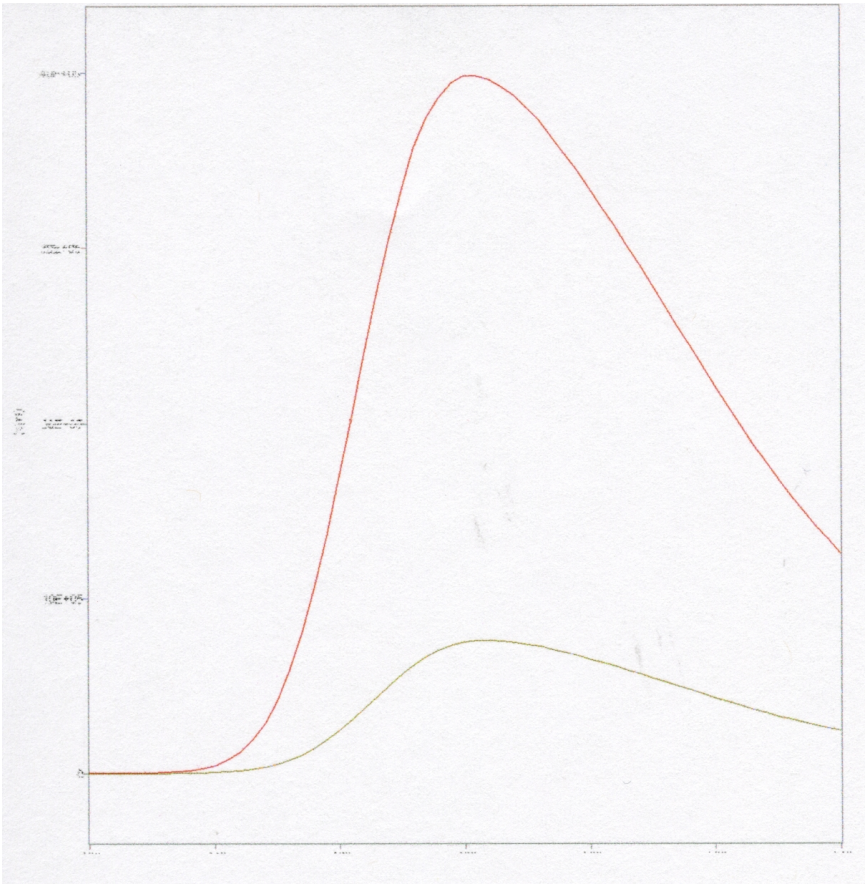

Figure 39: Initial test of mBBr reaction: 200 nM Pa1129, 50 μM Mn^{2+}, 100 mM K^{+}, 750 μM fosfomycin, 500 μM GSH, 60 min reaction time. Add 1 mM mBBr and let reaction run for 30 min. Red line adds 1 mM Pf to reaction mixture.

curve (CRC) for Pf in this assay system. A final concentration of 8 mM was selected as a starting point and a 3x serial dilution was made in the reaction buffer. The reactions were run in solid black 384-well microplates. This initial experiment showed that phosphonoformate did indeed inhibit FosA under these conditions. The data was averaged and fit to a sigmoidal dose-response curve using GraphPad Prism. An IC_{50} = 60 μM and an IC_{80} = 200 μM were calculated for Pf.

The assay was re-tooled after the first minor screen to increase efficacy. The Pf control IC_{50} for this second version of the assay was 19 μM and the IC_{80} was 72 μM (Figure 40). For reasons that will be discussed later, Pf was later replaced with a $ZnCl_2$ solution in DMSO. Zinc has an IC_{50} = 158 ± 4 nM in this assay and completely inhibits the reaction at a concentration of 5 μM (Figure 40). A zinc concentration of 5 μM was used to completely inhibit the reaction as the control in the screens.

Z' Calculations

The best way to establish whether or not an assay is valid for a HTS format is to calculate the Z' for that assay.[60] This was performed for Pf before running any unknown compounds to determine HTS viability of the assay. Full plate Z' values were calculated for both IC_{50} and IC_{80} concentrations of Pf by setting up a full plate checkerboard of Pf against a DMSO control. The Z' for each concentration of Pf was calculated to be 0.76 and 0.85, respectively. The Z' values using the second version of the assay for Pf were both calculated to be 0.78 (Figure 41). A Z' > 0.5 indicates that an assay is able to successfully discriminate between partially inhibited and uninhibited populations of enzyme and is viable for high-throughput screening.

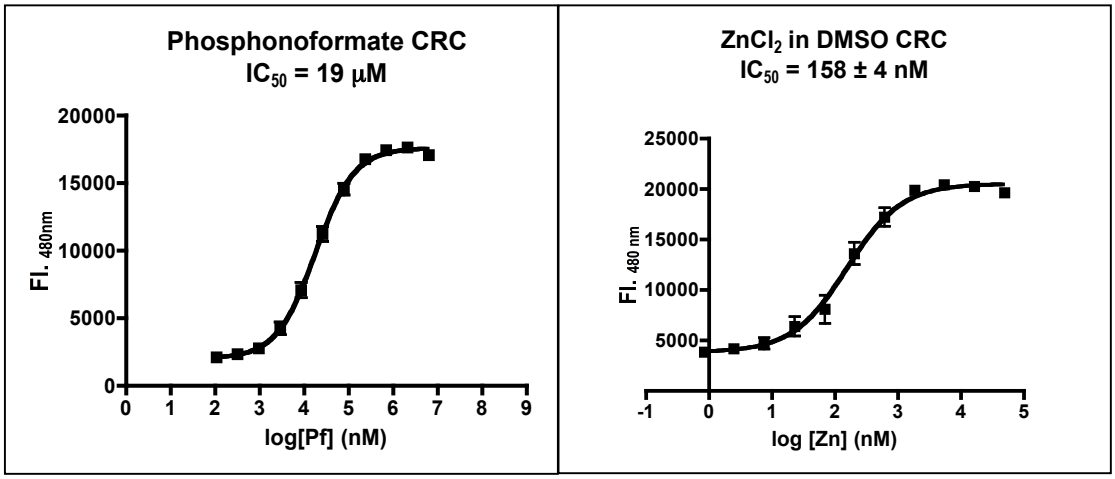

Figure 40: Concentration-Response Curves for phosphonoformate in the second version of the assay and for $ZnCl_2$ in the final version of the assay. All data in quadruplicate.

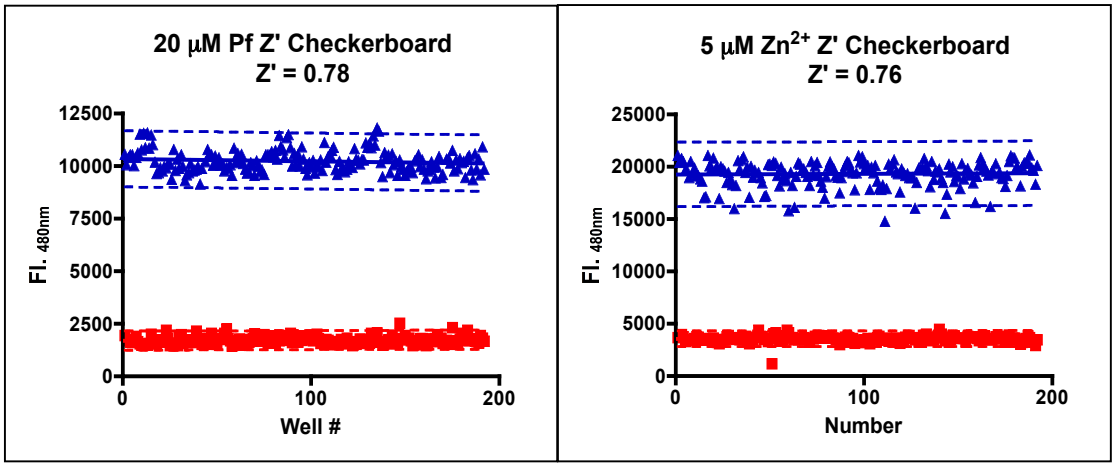

Figure 41: Full plate Z' calculations for phosphonoformate in the second version of the assay and for $ZnCl_2$ in the final version of the assay. The blue triangles are the positive control, either Pf or Zn, and the red squares are the negative controls, DMSO. The dotted lines indicate three standard deviations above and below the mean for each population.

A concentration of 5 μM Zn gives a Z' = 0.7 (Figure 41). All of these results indicate a viable HTS assay, which is adequately able to resolve inhibited and uninhibited reactions.

Compound Screens

A small screen (3200 compounds) was performed using the Pf standard assay to estimate an initial hit rate. Hits were defined as compounds that gave a signal greater than three standard deviations above the mean for all compounds tested on a single plate. The fluorescence reading of each plate was measured both before and after the addition of mBBr in order to eliminate any false positives that would result from the intrinsic fluorescence of the compounds being tested. Using this strategy, a total of 104 hits were identified, a hit rate of 3.25% (Figure 42).

When the same compound screen was repeated using the second version of the assay the method of picking hits was modified. Instead of picking hits on a per-plate basis, hits were picked based on the whole population of compounds screened on that day. The raw data was normalized to a % of the maximum value for the positive controls on each plate and then the percentages for all 3200 compounds were used to determine the average and standard deviation. Hits were identified as compounds that gave a % max signal greater than three standard deviations above the mean for all compounds screened. This reduced the number of hits from 104 to just two, a hit rate of 0.063% (Figure 43).

The third, and final, version of this screen changed the standard to $ZnCl_2$ in DMSO, but all other factors remained constant. In this final version of the assay four hits

Plate Number	1		2		3		4		5		6		7		8		9		10	
	Well	Fl.480	Well	Fl.480	Well	Fl.480	Well	Fl.480	Well	Fl.480	Well	Fl.480	Well	Fl.480	Well	Fl.480	Well	Fl.480	Well	Fl.480
	J4	1550	D4	1710	H19	1600	D6	1706	E4	-1872	D5	1632	D9	1342	D4	1528	D17	1212	D4	1572
	H5	1756	D8	1671	J20	1600	H8	1546	P20	5827	D6	1547	D17	1502	D6	1499	H3	993	D6	1323
	G8	2204	E15	-751	L8	1579	H14	1626			D8	1578	H3	1436	D10	1447	H5	1011	D8	1612
	P10	1661	H8	1758	O11	2032	L3	1708			D12	1747	H5	1482	D12	1715	H19	1039	D12	1527
	L12	1758	J19	1692	O13	1821	L11	2019			D16	1538	H9	1652	H8	1531	K3	1012	D16	1391
	P12	1672	K12	1967	P16	1705	L13	1658			H4	1806	H19	1482	H16	1337	K5	1047	D18	1511
	J18	1645	L5	1713			L15	1670			H10	1750	L10	1873	K4	1236	K7	1228	H4	1596
	L18	1648	L7	1667			L17	1738			I4	1527	L14	1702	K6	1366	K9	955	H6	1599
	P20	1650	O16	2106			L19	1612			L7	1760	L16	1426	K8	1208	K11	1052	H12	1479
	P22	1575	P13	1663			N15	-453			L11	1553	L18	1638	K16	1311	K13	1070	H14	1384
							O18	1502			L13	1926	L20	1914	L21	1854	K15	1030	H18	1445
							P3	1614			L15	1756	L22	1687			K17	977	H22	1525
							P17	1561			L17	1930					K19	955	K4	1365
							P21	1510			L21	1585					K21	1038	K10	1251

Category	3σ Below	Hits at 3σ	Hits at 3.5σ	Hits at 4σ	Hits at 5σ
Hits	3	104	68	35	8
Hit Rate	0.09%	3.3%	2.1%	1.1%	0.3%

Figure 42: Hits from the first compound screen. Hits were picked by identifying compounds with a greater than 3σ deviation above the mean for all compounds on a single plate. The multiple colors depicted above illustrate an attempt to create a hierarchy of inhibitory capacity among these compounds.

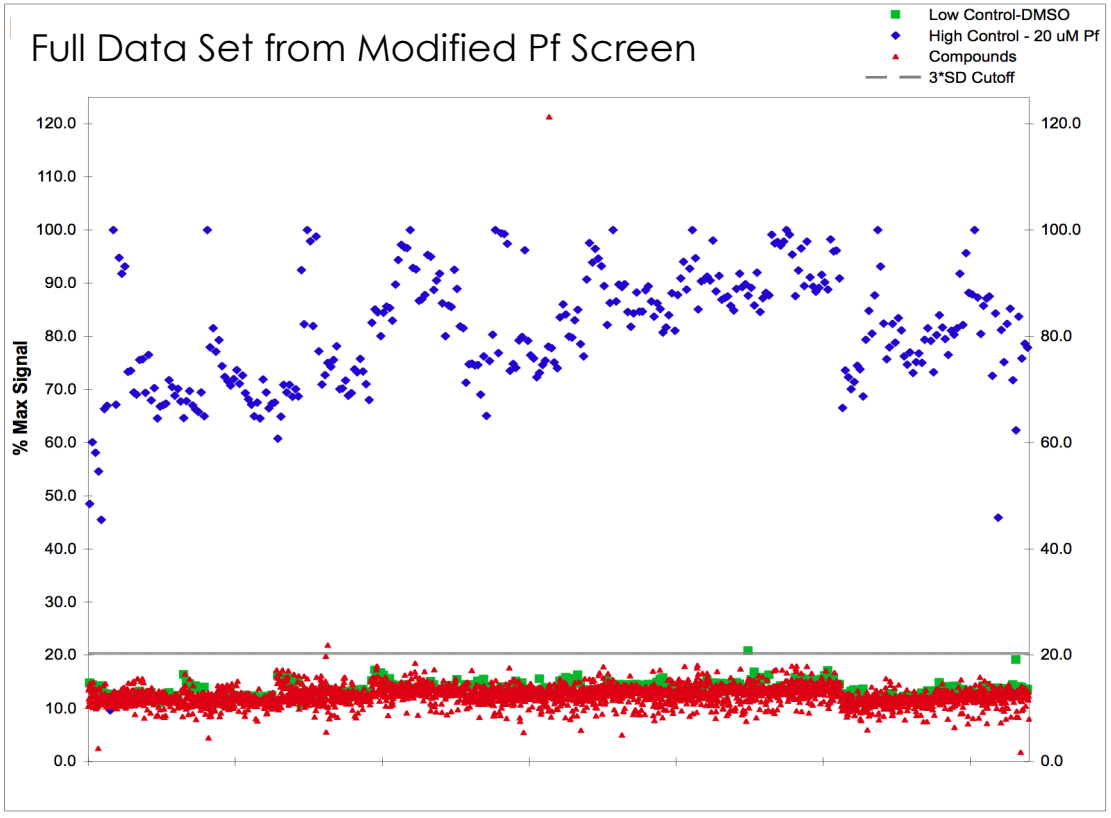

Figure 43: Full data set analysis from the second compound screen. The Z' for the controls over the whole data set was only 0.43. The compound average was 12.4 with a standard deviation of 2.6. The positive control, Pf, is in blue, the negative control, DMSO, is in green, the compounds are in red and the grey line designates the hit cutoff, here at 20.3. Hits are compounds above this cutoff line.

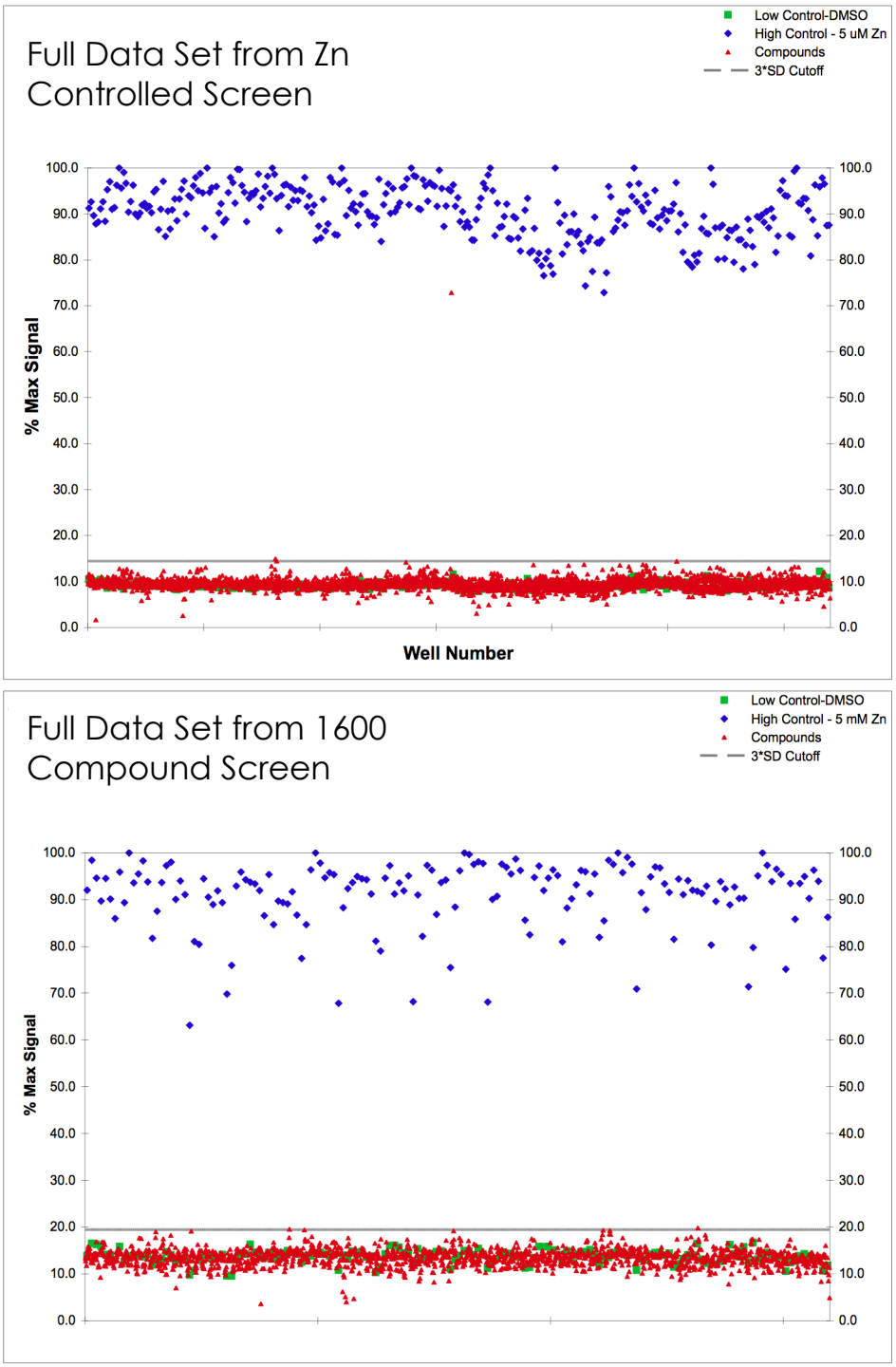

Figure 44: Full data set analysis for two zinc controlled assays. For the 3200 compound assay the control Z' was 0.77. The average for the compounds was 9.5 was a standard deviation of 1.7. The 3s cutoff was 14.4. For the 1600 compound screen the control Z' was 0.66. The compound average was 13.4 with a standard deviation of 2.0. The 3s cutoff was 19.4. The positive control, Pf, is in blue, the negative control, DMSO, is in green, the compounds are in red and the grey line designates the hit cutoff. Hits are compounds above this cutoff line.

were recorded, a hit rate of 0.125%. A subsequent assay of 1600 compounds netted five more hits, a rate of 0.3125% (Figure 44).

Hit Confirmation

The hits from the first version of the screen were confirmed by ordering new compounds from ChemBridge and making new 10 mM stocks in DMSO. The assay was repeated in the exact same manner. One compound, CB 5838696 was no longer available from ChemBridge so four structurally similar analogs were ordered for the confirmation experiments. These compounds, CB 5844324, 5848410, 5846450, and 5838937, were the only compounds to show any activity in the confirmation screen. This gives an effective confirmation rate of only 0.96%, only one compound out of 104.

The confirmation screen was also performed in the absence of GSH to make sure that the signal wasn't coming from any compound reaction with mBBr. No reaction was seen to indicate that this would be a problem with these compounds.

Since the second and third versions of the assay resulted in significantly fewer hits, the method of confirmation was changed to a CRC profile assay. The fewer number of compounds made this type of assay more viable. Both of the hits from the second version of the assay, CB 5838696 and CB 5155620, were confirmed in this manner. This gives a confirmation rate of 100%.

All four of the hits from the 3200 compound screen from the third version of the assay were confirmed. These hits were the same as for the second version of the assay as well as compounds CB 5155500 and CB 5841758. Of the five hits from the subsequent 1600 compound screen, only four could be screened in the confirmation assay. One compound ID could not be identified. Of the four that could be screened, two

compounds were confirmed as active. These were compounds CB 6106988 and CD 1597-0070. Compounds CD 1605-0089 and CD 6031-1896 were not confirmed. This gives confirmation rates of 100% for the 3200 compound screen and 50% for the 1600 compound screen, an overall confirmation rate of 75%.

CRC for Confirmed Hits

The derivatives of CB 5838696 were tested for their concentration-response profiles. All of the compounds were screened on a single plate to limit plate-to-plate variation. For the four derivatives of CB 5838696 tested, CB 5844324, 5848410, 5846450, and 5838937, IC_{50} values of 470 ± 10, 690 ± 10, 960 ± 20, and 1300 ± 200 nM were calculated. This is 20-60 times lower than the model inhibitor, phosphonoformate, which has an IC_{50} = 17.8 ± 0.1 μM. The other confirmed hits have much higher IC_{50} values. In order of efficacy: CB 5155500 = 15.1 ± 0.3 μM, CB 5847158 = 17.9 ± 0.4 μM, CD 1597-0070 = 28.8 ± 0.6 μM, and CB 6106988 = 74 ± 1 μM (Figure 45). An IC_{50} could not be calculated for CB 5155620 due to solubility issues.

Compound Synthesis and Activity

Compound CB 5838696 and its four analogs were independently synthesized by the Vanderbilt Chemical Synthesis Core (VCSC) as they became less commercially available. The synthetic methods were not available from ChemBridge, so it was not possible to follow the exact method. The method used can be found in Figure 16. The compounds from the VCSC were determined to be structurally identical to the ChemBridge compounds based on ^{1}H, COSY, HSQC, HMBC, and selective NOESY NMR, see Appendix. The kk-5-series of compounds showed no activity against FosA.

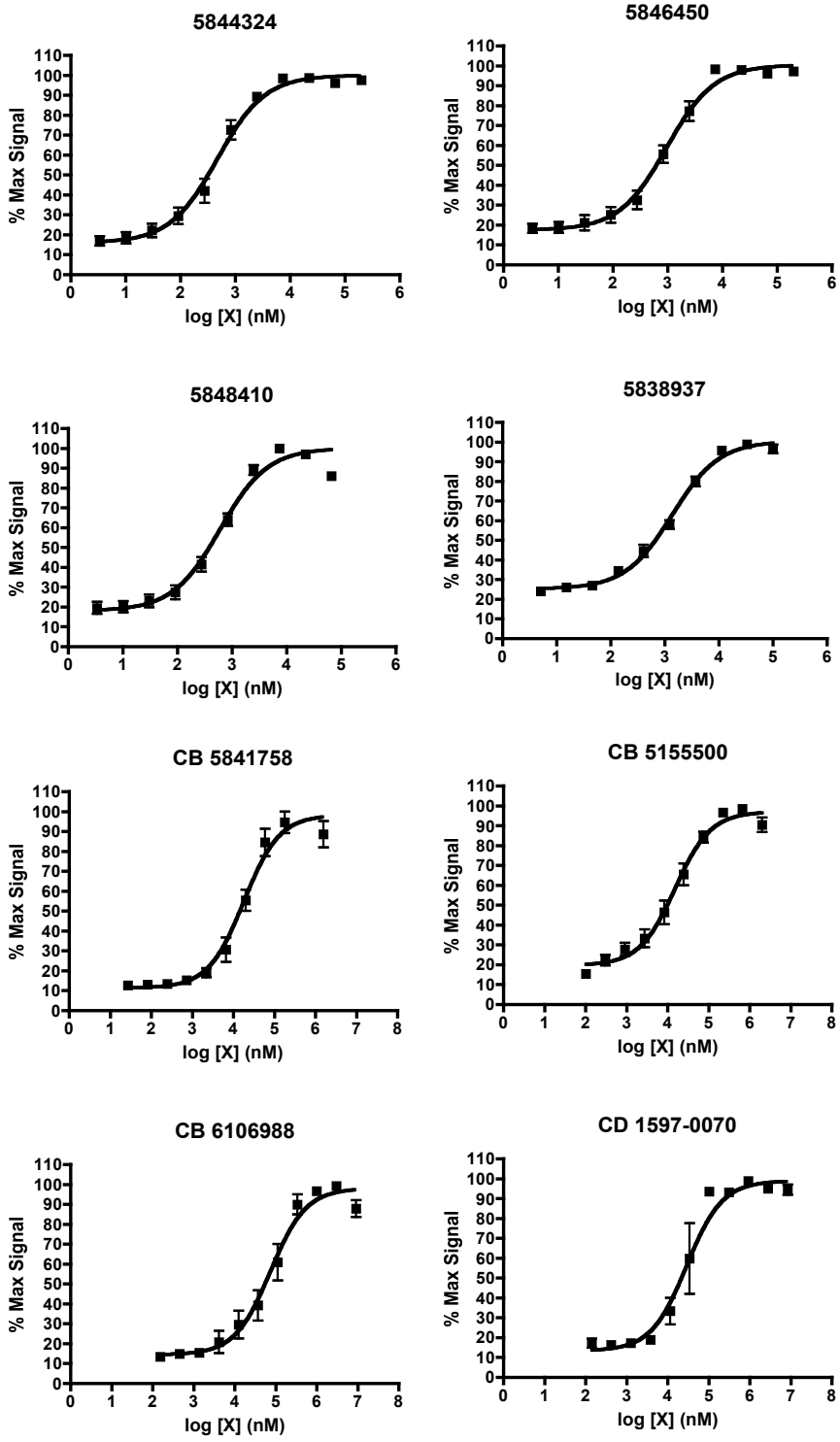

Figure 45: Concentration-Response Curves for hit compounds from the various screens.

The kk-8-series of compounds, however, showed comparable inhibition of FosA as their commercially purchased counterparts.

To check for potential impurities in various compounds, both the CB 5846450 and its corresponding VCSC compound were further purified by HPLC. Single peaks were seen in the HPLC traces for both compounds indicating the lack of any potential organic impurities. The HPLC purification did not change the activity of the kk-5-series compound; it was still inactive. However, the ChemBridge compound lost all activity after HPLC purification (Figure 46).

The only explanation for this loss of activity seems to be the presence of an inorganic impurity. The only synthetic information ChemBridge could supply was that their compounds were synthesized solvent free with $ZnCl_2$. The presence of high concentrations of zinc would not affect the NMR spectra or show up in the HPLC profile. It could, however, potentially inhibit the FosA metalloenzyme. Indeed, when stoichoimetric amounts of zinc are added to an HPLC purified ChemBridge compound, its inhibitory activity is restored (Figure 47).

The kk-8-series of compounds constitute the independent synthesis of four of the five other hits found via HTS screening. These compounds showed similar activity to their commercially purchased counterparts. The one compound not synthesized, CB 5155620, was not re-synthesized because an IC_{50} couldn't be calculated for this compound due to solubility issues.

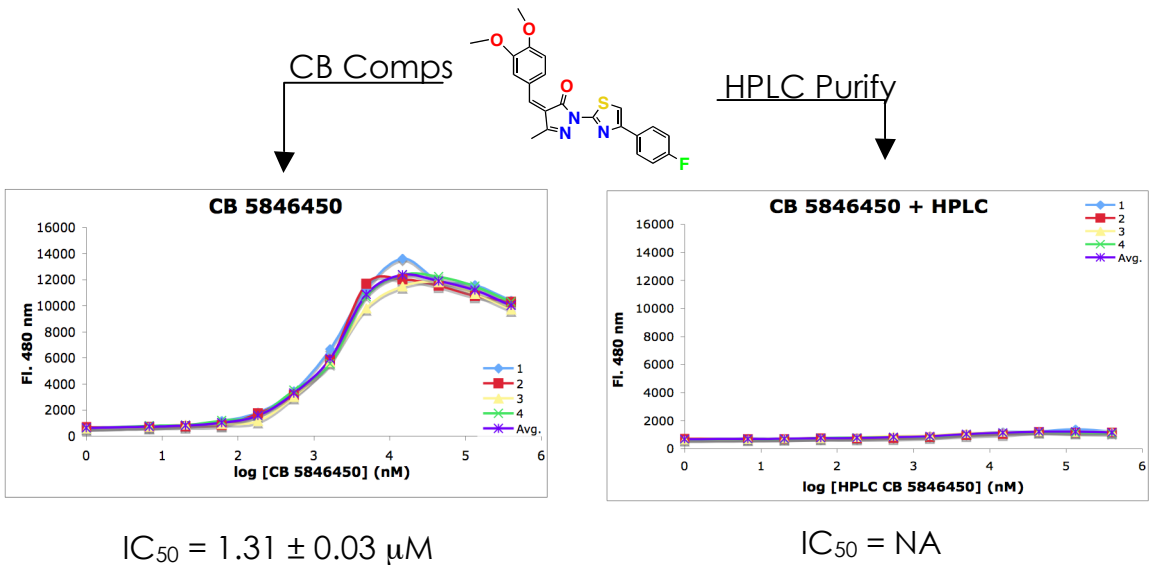

Figure 46: HPLC Purification of CB 5846450 results in a near total loss of inhibitory capacity. ChemBridge has only been able to divulge that the chemist they purchased these compounds from made them using a solvent free method with $ZnCl_2$. $ZnCl_2$ has been shown to inhibit $FosX^{L.m.}$ (IC_{50} = 3 μM, see Chapter 6).

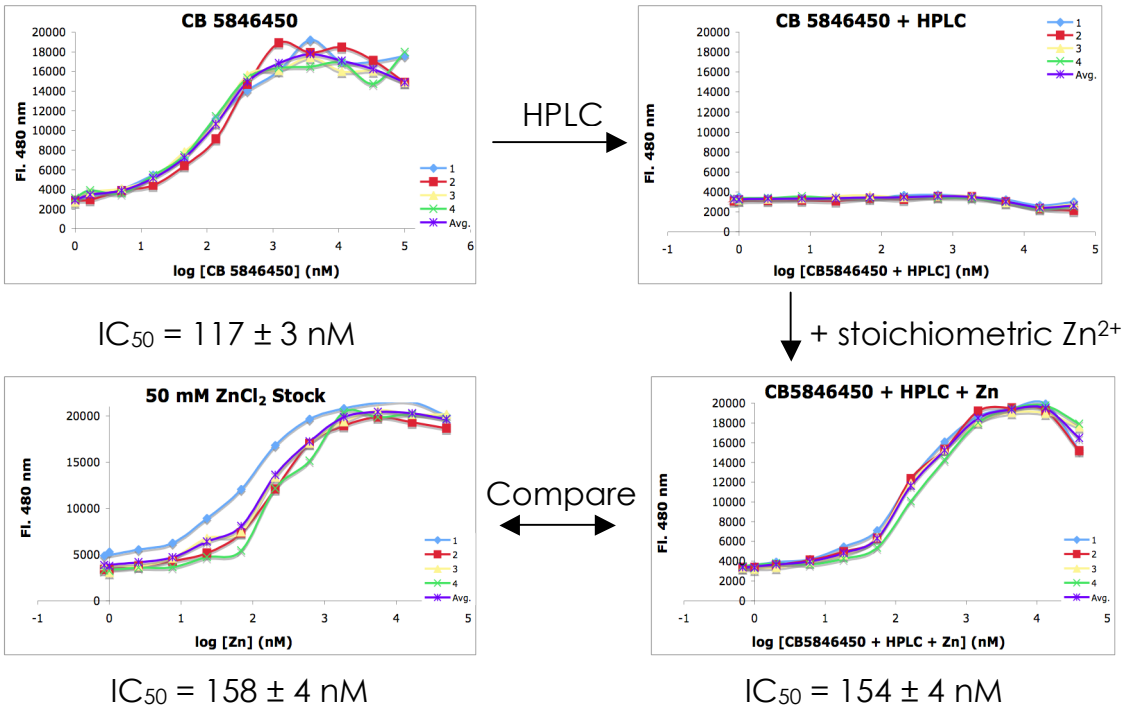

Figure 47: Single experiment demonstrating that Zn is most likely responsible for compound activity. HPLC purification renders the compound inactive but the addition of stoichiometric zinc restores activity in a manner similar to pure Zn^{2+}.

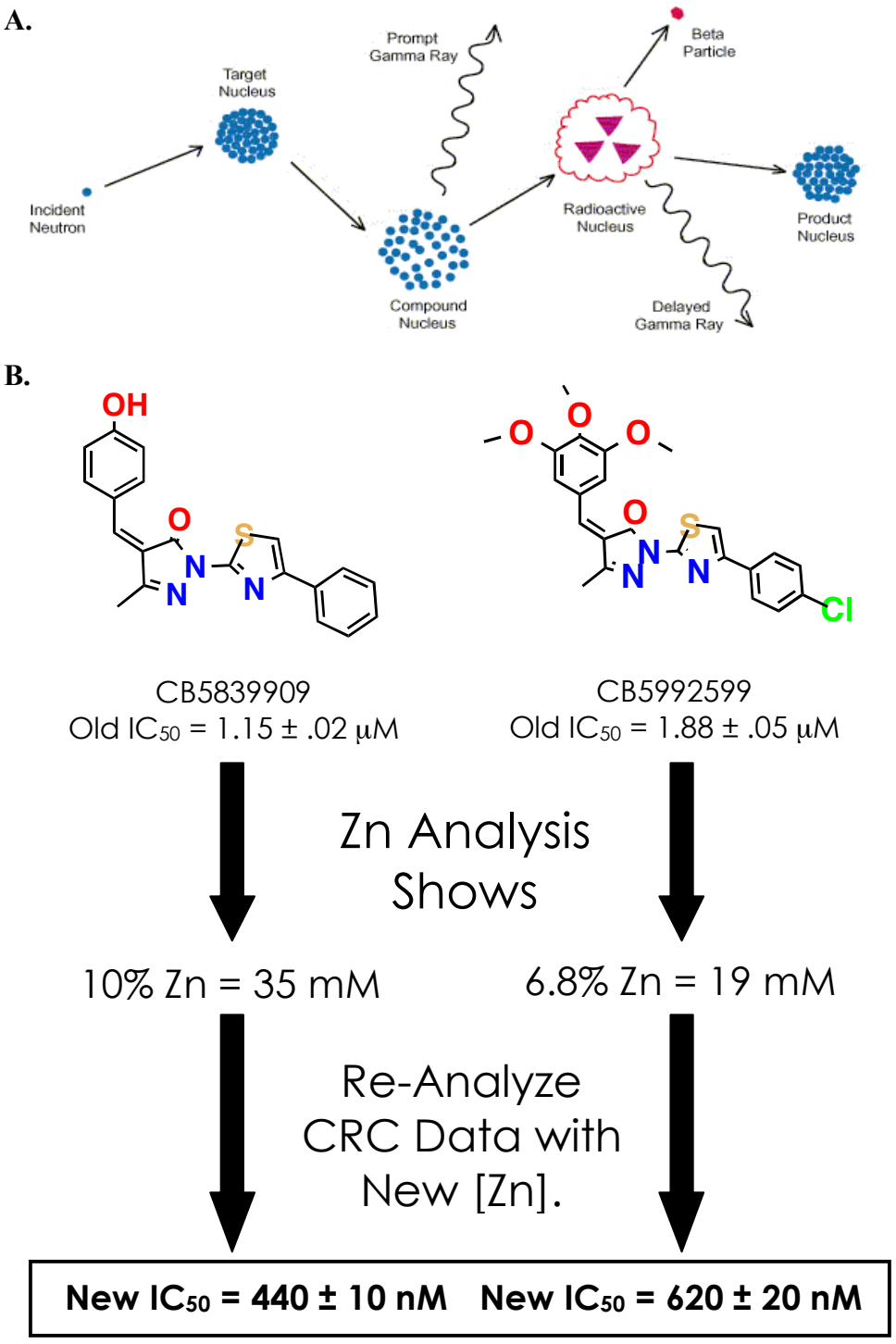

Figure 48: A) Cartoon depiction of the technique of NAA, taken from ref. 63. B) NAA analysis of compounds CB 5839909 and 5992599 showed heavy zinc contamination in the dry powder. Re-calculating the CRC for these compounds knowing the zinc concentrations gives IC_{50} values very similar to zinc alone.

Zn Analysis by Neutron Activation

None of the five ChemBridge compounds tested were available to send for zinc analysis; so two other analogs were purchased. These two compounds, CB 5839909 and CB 5992599, were sent to Elemental Analysis, Inc. in Lexington, KY for testing by Neutron Activation Analysis (NAA). NAA works by measuring the element specific radioactive decay of a target element. The emitted gamma rays are elementally specific in their half-life and energy. The amount of a target element in a sample can also be determined based on the intensity of the gamma ray emission. The amount of zinc present was determined to be 6.8 ± 0.4% and 10.0 ± 0.4% of the dry weight for compounds CB 5839909 and CB 5992599, respectively. Re-analyzing the CRC data for these two compounds using the known concentrations of zinc changes the IC_{50} for CB 5839909 from 1.15 ± 0.02 μM to 440 ± 10 nM and the IC_{50} for CB 5992599 from 1.88 ± 0.05 μM to 620 ± 20 nM (Figure 48). The IC_{50} for pure Zn is 158 ± 4 nM. No detectable zinc was seen for compounds CB 6106988, 5847158, and 7433453 (an active derivative of CB 5155500 and 5155620).

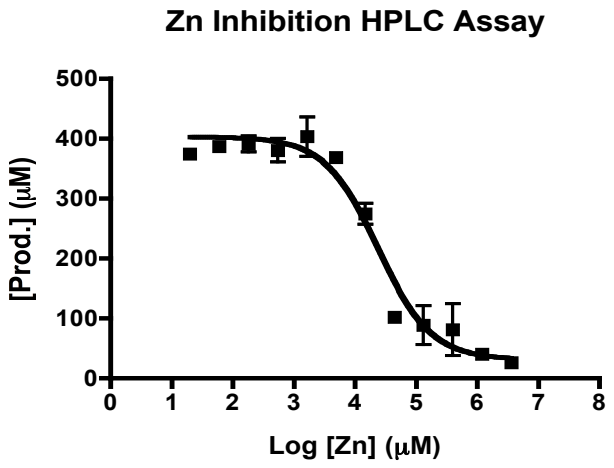

Figure 49: Concentration-Response Curve for Zn in the HPLC assay.

HPLC Assay

The same HPLC based assay system used for FosA kinetics can also be used for inhibitor analysis.[58] Using the exact same reaction conditions but with the kinetic assay quench and derivatization the amount of fos-GSH product can be measured directly. Using Zn as an inhibitor an $IC_{50} = 24 \pm 2$ μM can be measured directly (Figure 49).

Resazurin Bioactivity Assay

It is possible to grow liquid culture of *E. coli* in 96-well plates and monitor the growth of the cells using the color change dye Resazurin (Figure 50).[57] In checkerboard tests, using kanamycin as a positive control, Z' values of 0.75 can be achieved in as little as six hours, indicating a robust difference in the fluorescence of the dye between wells with and without growth. When stretched out to 24 hrs., Z' values of 0.85 are observed. The liquid cultures were grown using LB media with 100 μg/mL ampicillin and 500 μM glucose-6-phosphate (G6P). The FosA gene was expressed in a pET-20b vector with a leaky promoter. The vector contributes ampicillin resistance and the G6P aids in the uptake of fosfomycin by activating phosphate transport systems.[28] The plate set-up is a slightly modified version of the one used by Sarker *et al.* (Figure 51).[57] This set up makes possible the testing of several different serial dilutions of compounds in each plate.

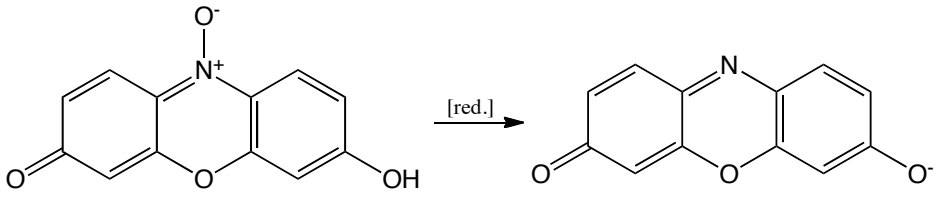

Resazurin Resofurin

Figure 50: Resazurin is reduced by living bacteria to resofurin. This imparts both a color change, from dark blue to bright pink, but also a fluorescent change that can be monitored with $\lambda_{ex} = 530$ nm and $\lambda_{em} = 590$ nm.

	1	2	3	4	5	6	7	8	9	10	11	12
A	Sterile Control											
B	Negative Control											
C	Compounds											
D												
E												
F												
G	Phosphonoformate											
H	Kanamycin											

Figure 51: 96-well plate set-up for the resazurin assay. The sterile control contains no bacteria and the negative control does have bacteria but no compounds.

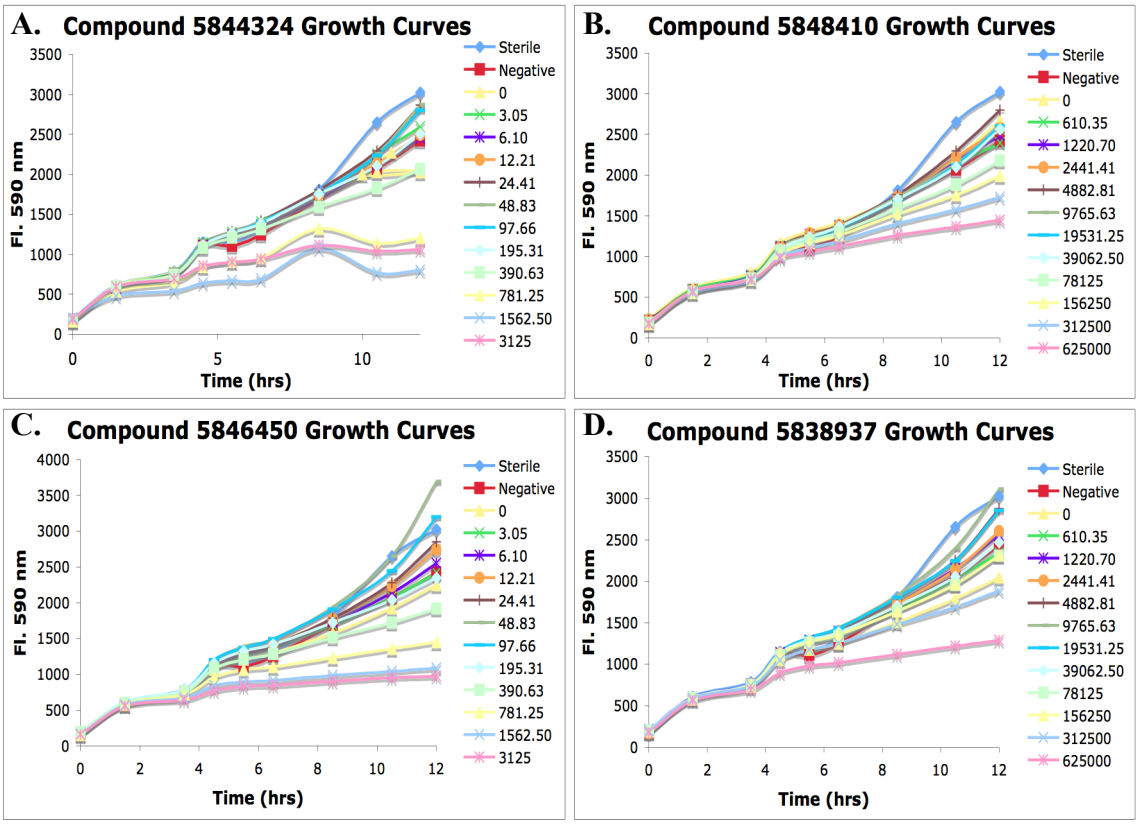

Figure 52: Resazurin growth curves for the four analogs of the hit compound CB 5838696 over a 12-hour period. The numbers in the legends of A and C are concentrations in micromolar while those in B and D are in nanomolar.

The four derivatives of CB 5838696 all have very low solubility in LB medium, about 50 μM. At higher concentrations, around 3 mM some growth slow down can be observed (Figure 52). At these concentrations, however, there is a lot of precipitate compound and it is very likely that the slight activity noted is most likely due to the heavy zinc contamination of the compounds.

When the confirmed hits from the Zn-controlled screens were tested for their bioactivity, four compounds were found to show a concentration-dependent effect on growth rates of *E. coli* transformed with the Pa1129 FosA (Figure 53). All four of these also showed effects on the growth rates of *E. coli* transformed with an empty pET-20 vector as well (Figure 54). Compounds CB 5155500, CB 6882791, and CB 7226895 demonstrate a decrease in growth at around 400 μM while compound kk-8-054 (same as CB 6106988) shows a decrease in growth at 100 μM. Millimolar concentrations of all four compounds are able to almost slow growth completely. The trends are not as easy to spot in the empty pET vector cells, but all four compounds do show a decrease in growth rates as well.

Several of the compounds tested are able to inhibit bacterial growth even after 24 hours of incubation at 37 ºC (Figure 55). Compound CB 7226895 does not completely inhibit the growth of transformed *E. coli*, either with or without FosA. Compounds CB 5155500, CB 6882791, and kk-8-054 all have the ability to deter the growth of *E. coli* transformed with the Pa1129 FosA. At concentrations of 780 μM, both CB 5155500 and CB 6882791 are able to inhibit the long-term growth of *E. coli* transformed with Pa1129 FosA (Figure 56). However, no long-term effect is seen in the growth of *E. coli* transformed with empty pET-20, except at very high, 6 mM, concentrations of CB

5155500. At a concentration of 195 µM, compound kk-8-054 demonstrates a long-term effect on the growth of *E. coli* with and without the FosA enzyme (Figure 56).

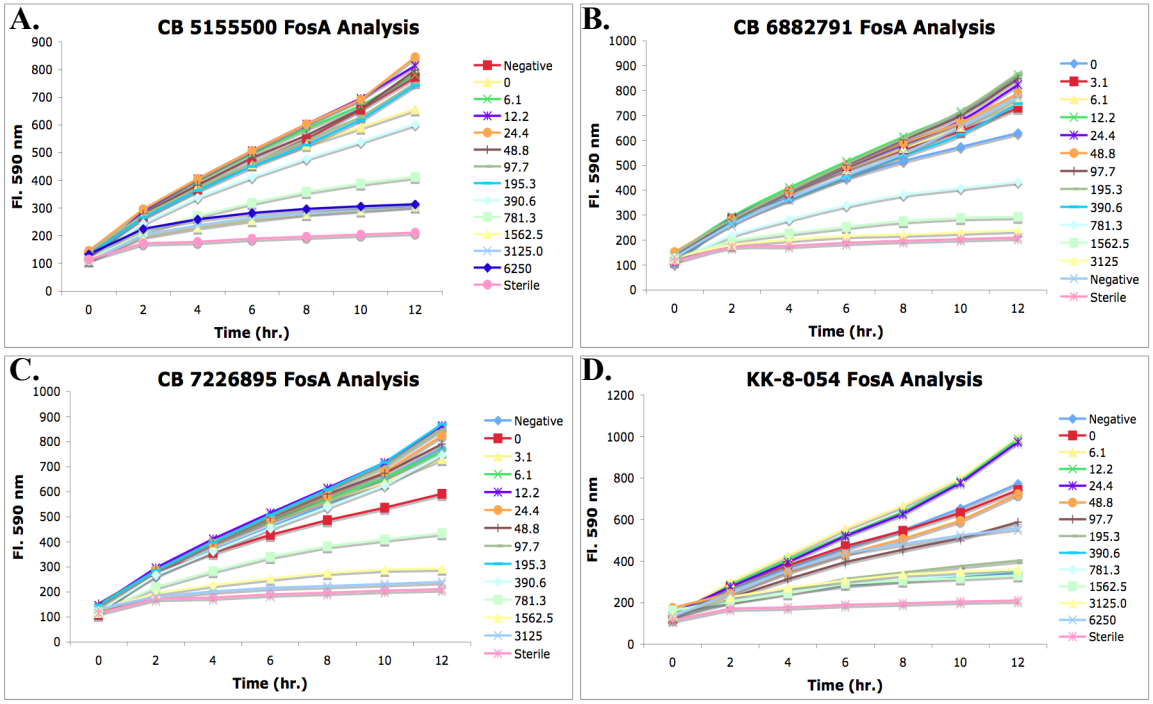

Figure 53: Growth curves for *E. coli* transformed with a pET-20 vector containing the Pa1129 FosA. The numbers in the legend for each chart is the concentration of inhibitor in micromolar. A) CB 5155500. B) CB 6882791. C) CB 7226895. D) KK-8-054.

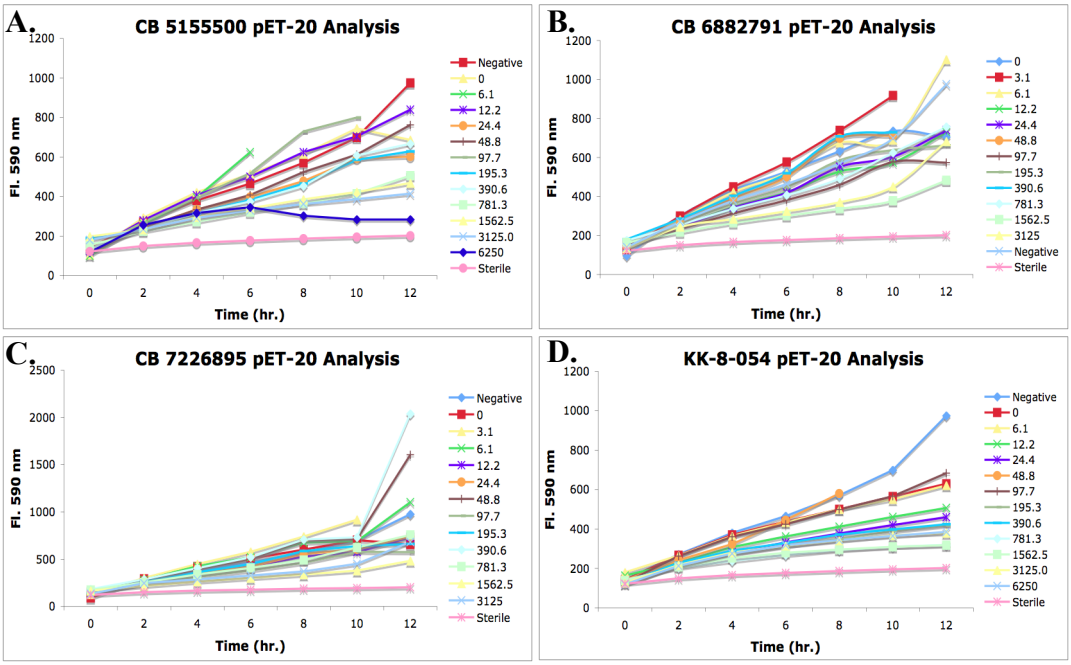

Figure 54: Growth curves for *E. coli* transformed with an empty pET-20 vector. The numbers in the legend for each chart is the concentration of inhibitor in micromolar. A) CB 5155500. B) CB 6882791. C) CB 7226895. D) KK-8-054.

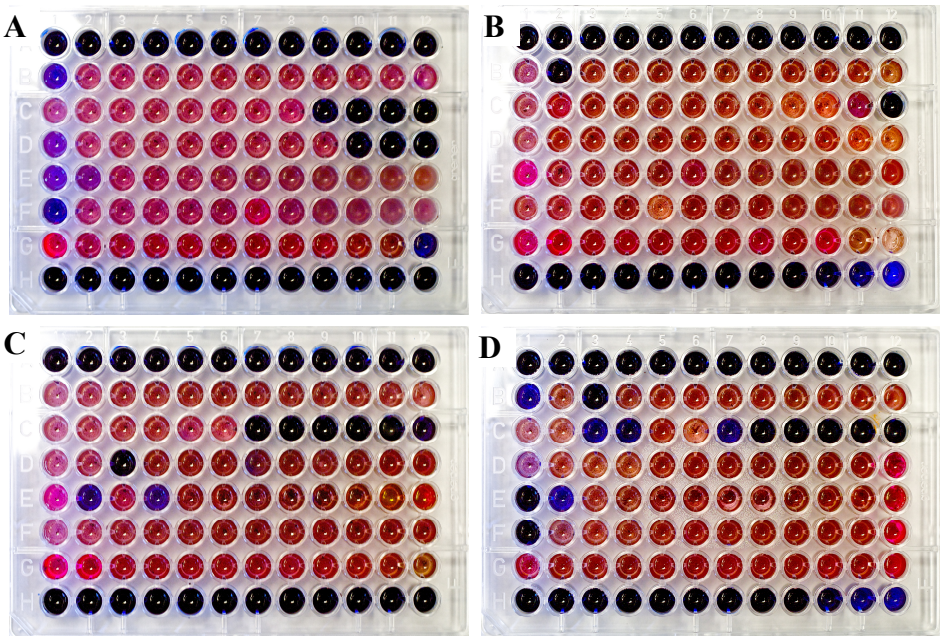

Figure 55: 96-well plates with E. coli grown over 24 hr. in the presence of resazurin. The dark blue wells are where no cell growth occurred. The red wells are where cell growth did occur. A) Cells with the Pa1129 FosA and compound CB 5155500, 6882791, 7226859, and 6107397 in rows C-F. B) Cells with empty pET-20 and compound CB 5155500, 6882791, 7226859, and 6107397 in rows C-F. C) Cells with the Pa1129 FosA and compound kk-8-054, kk-8-056, kk-8-058, and kk-8-060 in rows C-F. D) Cells with empty pET-20 and compound kk-8-054, kk-8-056, kk-8-058, and kk-8-060 in rows C-F.

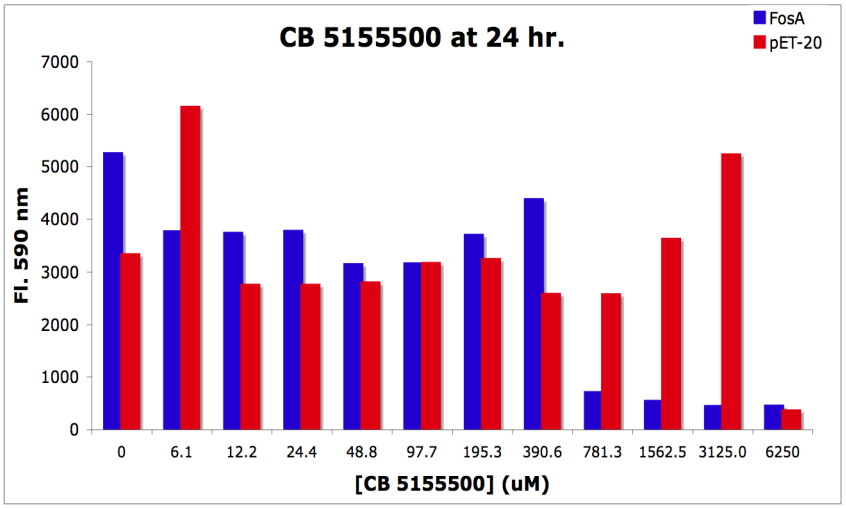

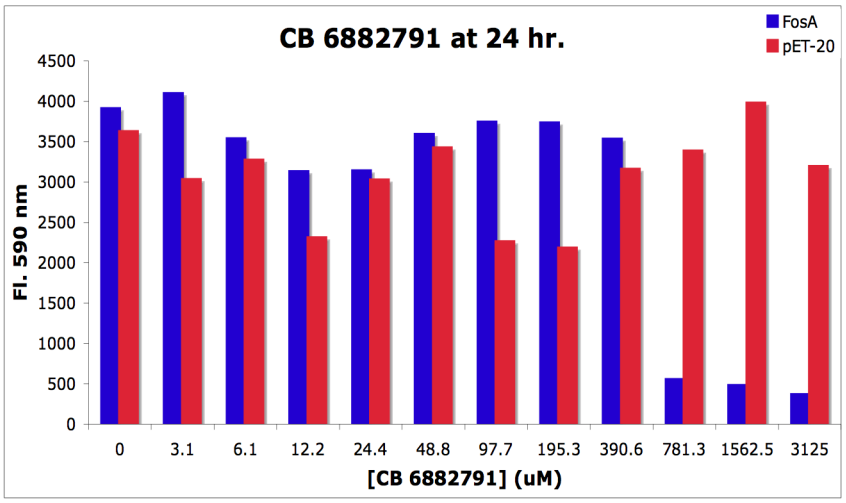

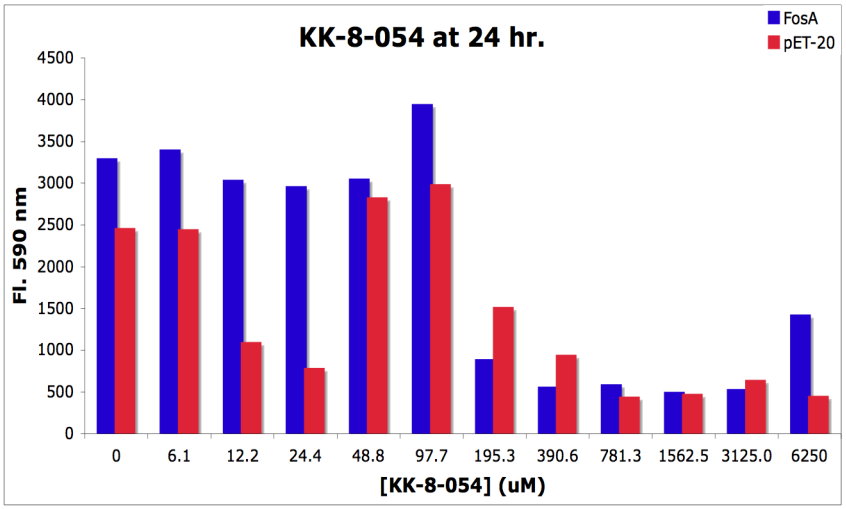

Figure 56: Comparison of the Fl. 590 nm for the Pa1129 FosA and empty pET-20 cells after 24 hr. of incubation at 37 ºC. A) CB 5155500. B) CB 6882791. C) KK-8-054.

Discussion

This assay is designed to be a quick assay to screen for inhibitors specific to the FosA enzyme (Figure 57). The assay, as developed, demonstrates good sensitivity and has a theoretically small chance of false negative results. Using glutathione as the limiting reagent at a 50x molar concentration to the compounds being tested ensures that, even should any compounds in the screen bind with GSH, the reaction will still run. Any compounds that react with GSH would probably not be good drug candidates, so the loss of these compounds is minimal.

This assay system is easily corrected for any false positive results that would occur due to the inherent fluorescence of the compounds in the library by simply taking plate readings both before and after the addition of the fluorophore. Also, should any compounds react with the fluorophore, a secondary reaction run in the absence of GSH can confirm whether any signal produced by the reaction is due to genuine inhibition of the FosA reaction.

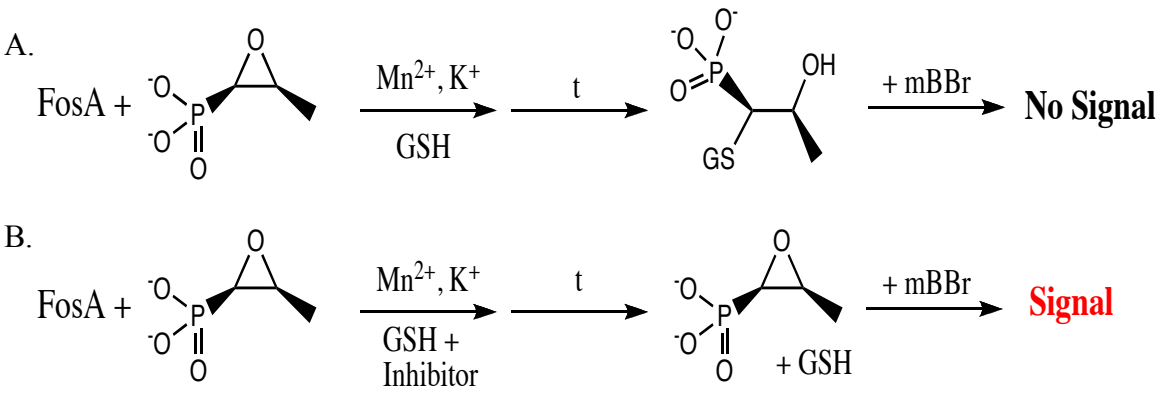

Figure 57: Cartoon depiction of the FosA assay. A) With no inhibitor present all GSH is tied up as product. The addition of mBBr will then give no fluorescent signal. B) If an inhibitor is present, the formation of product will be hindered leaving a pool of GSH to react with the mBBr when added, yielding the fluorescent GS-mB product.

This assay has undergone several method changes to get to one that works properly. The first version of this assay identified 104 hits out of 3200 compounds screened. However, the confirmation screen only confirmed one hit out of those 104 and that one confirmation was actually four analogs of a compound no longer commercially available, CB 5838696. In essence, this gives a confirmation rate of less than 1% for this assay. A very generous threshold for confirmation would be about 50%, so this version of the assay proved to be extremely error prone.

Several steps in the assay were changed around and some were eliminated to create the second version. The number of hits identified dropped to only two compounds when using the exact same 3200 compounds as the first screen. Both of these were confirmed, a 100% confirmation rate. The lower number of false positives was due to three major changes. One was the method of hit picking – switching to the population analysis. A population analysis distributes error over the entire population of compounds and removes any plate-to-plate variability. Two other changes were also instrumental in the success of this second version of the Pf controlled assay.

The fewer number of liquid handling steps in the second version of the Pf controlled assay helped to reduce the overall error as less compound and enzyme manipulation is required. The more significant changes, however, most likely had to do with changing from polystyrene to polypropylene plates and using methanol instead of acetonitrile for the mBBr. According to the chemical stability information on the Greiner Bio-One website, PS plates are very unstable in AcCN. The plates used in the first version of the assay were holding a solution of 17% AcCN for 30 min, which could lead to severe scoring of the plates as the PS starts to dissolve. Polypropylene plates are also

unstable in AcCN, so a different mBBr solvent was needed. Monobromobimane is really only soluble in AcCN, DMSO, and methanol for the purposes of this assay. DMSO forms a complex with mBBr slowly over time, so storage in DMSO is not possible. Polypropylene plates are, however, stable in methanol, so this combination of plate type and solvent was used for the second version of the assay. This should reduce any error that would come from the chemical instability of the plates and solvents. The results from the second version of the assay were highly satisfactory.

The only drawback to this version of the assay was the continued necessity of adding Pf manually as the positive control. The manual addition of controls slows down the overall process and creates a situation where the controls do not act as process controls since they do not undergo the same liquid handling steps. Since Pf is not soluble in DMSO, it cannot be added to the reaction plates using the Labcyte Echo. This makes Pf a less than ideal positive control for this assay. However, as will be discussed later, the presence of high concentrations of zinc in some of the confirmed hits allowed for the creation of a final assay that eliminates this concern.

Zinc chloride is soluble in DMSO and can, therefore, be used as a positive control for this assay. Zinc is a much better inhibitor of FosA than Pf is, so less compound needs to be used. Zinc is also much cheaper than Pf, which lowers the operating cost for a large-scale screen. Adding the controls with the Echo speeds up the assay process and gives a much tighter distribution of fluorescence for the entire population of controls over the course of a screen. A comparison of the overall Z' for the second version of the Pf controlled assay and the zinc controlled assay shows that the Zn controlled assay is much more able to differentiate inhibited and uninhibited reactions. In fact the Z' for the Pf

assay was only 0.43 due to a large standard deviation in the positive controls. The Z' for the Zn screen was 0.77.

The zinc assay uses a higher than IC_{50} concentration to completely inhibit the reaction. This is done so that all data points from the compounds being screened will be within the boundaries of the controls. This was not the case in the second version of the Pf controlled screen where one compound was a much better inhibitor and fell outside of the control boundaries. Using zinc creates more space between the positive and negative controls and actually helped to identify more confirmed hits when screening the same 3200 compounds. The zinc version of the assay has found, to date, nine hits out of 4800 compounds, six of which were confirmed, and one that was not able to be identified.

Only getting six confirmed hits out of 4800 compounds, a 0.167% hit rate, may seem relatively low. However, when the entire Vanderbilt Collection of compounds is screened, containing around 160,000 compounds, we should expect to get around 267 hits. While only around 200 or so of these may be confirmed, this would be a more than sufficient start in the search for new inhibitors. The best compounds could then be selected for modification from a medicinal chemistry approach to develop more potent and bioactive inhibitors to FosA.

Confirmed Hits

The compounds that were confirmed as hits were subjected to more testing to ascertain their IC_{50} values and to authenticate their ability to inhibit FosA. Many of the compounds tested have IC_{50} values much smaller than the model compound Pf, while others are about as potent and others are less so (Figure 58). All of this is to be expected from a properly functioning screen.

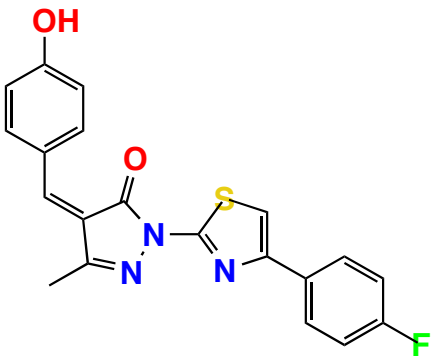

VCB0001205 P20
CB 5838696
IC_{50} = N.D.

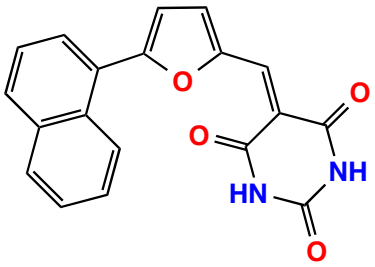

VCB0001181 O13
ChemBridge 5155620
IC_{50} = N.D.

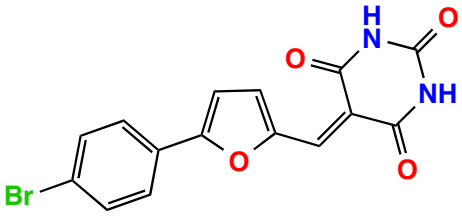

VCB0001181 I13
ChemBridge 5155500
IC_{50} = 15.1 ± 0.3 μM

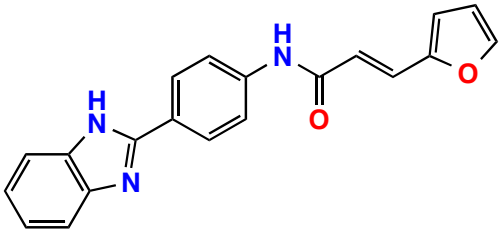

VCB0001208 K21
ChemBridge 5847158
IC_{50} = 17.9 ± 0.4 μM

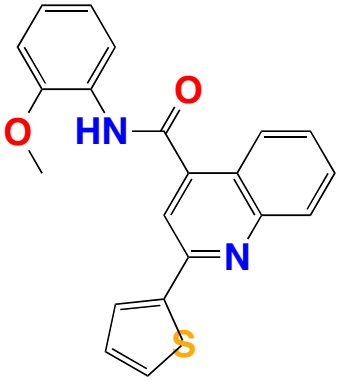

VCB0001000 E17
CB 6106988
IC_{50} = 74 ± 1 μM

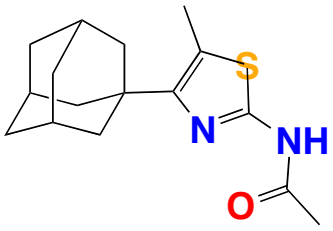

VCB0001011 H10
ChemDiv 1597-0070
IC_{50} = 28.8 ± 0.6 μM

Figure 58: All hits from the compound screens with the plate ID and well number from the Vanderbilt Collection, the ChemBridge or ChemDiv ID number and IC_{50} values.

Most of the secondary work to date has focused on CB 5838696 and its analogs since these compounds have a much lower IC_{50} than any of the others identified (Figure 59). The initial IC_{50} and K_d data for these compounds seemed to indicate that a structural scaffold had been found with excellent inhibitory capacity and very tight binding to FosA (all compound K_d values were lower than the native substrates fosfomycin and GSH). However, once these compounds were independently synthesized by the VCSC, they showed no activity against FosA.

Based on the limited information available from ChemBridge in regards to the synthesis of their compounds, it was proposed that the ChemBridge compounds were contaminated with zinc. Zinc is able to inhibit the closely related FosX enzyme from *Listeria monocytogenes* (Brown and Armstrong, unpublished), so it was hypothesized that it could also inhibit the FosA enzyme from *P. aeruginosa*.

To determine whether or not zinc might be present in the ChemBridge samples we further purified them by HPLC and re-ran the HTS assay. This purification led to the almost complete loss of activity by the compounds. A stoichiometric concentration of zinc was then added back to one compound, CB 5846450. This restored the purified compounds activity against FosA. In addition, the IC_{50} calculated for this solution was identical to pure zinc, within error. All of which pointed to zinc contamination being the reason for the activity seen in this family of compounds and would help explain why they all have very similar IC_{50} values despite the differences in their structures.

To determine the exact amount of zinc in these compounds, two were sent to Elemental Analysis, Inc. for zinc concentration determination. Elemental Analysis, Inc.

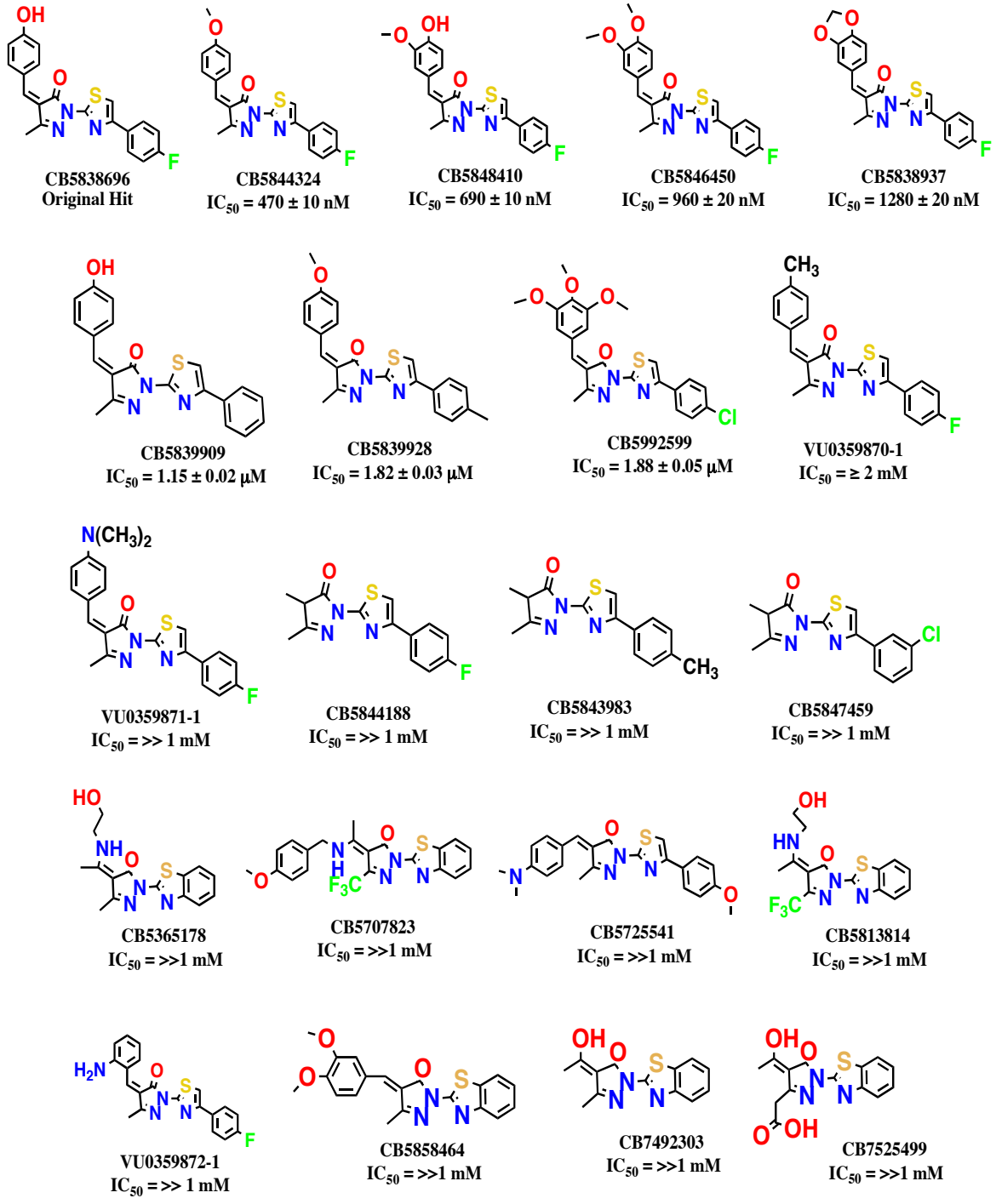

Figure 59: All derivations of CB 5838696 tested. All compound IDs beginning with CB were ordered from ChemBridge. The compound IDs beginning with VU were synthesized by the Vanderbilt Chemical Synthesis Core.

(Lexington, KY) used a technique called Neutron Activation Analysis (NAA) to determine the % zinc in the dry weight of compounds CB 5839909 and CB 5992599. This analysis irradiates the sample and then monitors the radioactive decay. Each element has a specific wavelength of decay and can be identified thusly. The amount of a specific element can then be quantitated by measuring the intensity of the gamma waves being emitted.[62] NAA analysis on CB 5839909 and CB 5992599 showed that a significant percentage of the dry weight of the compound was actually zinc. In fact, using these known concentrations and back calculating the IC_{50} for the zinc in the sample, an IC_{50} for both compounds was calculated that was very near the IC_{50} of zinc alone. This would suggest that the inhibitory ability of these compounds stems from their high zinc contamination and not from the compounds themselves. This also suggests that the differences seen for the IC_{50} values among the compounds is most likely due to the amount of zinc present, not from any structural differences between the compounds.

The final step was then to confirm that zinc could actually inhibit the FosA enzyme using another assay besides the HTS assay. This was done using the same HPLC based assay used in kinetics measurements of FosA because it directly measures the amount of product being formed. This analysis showed that zinc could indeed inhibit FosA, but at a much higher IC_{50} than the HTS assay suggests. It is not clear at this time why this discrepancy may exist since the conditions for both assays were identical aside from the quenching of enzymatic activity. However, it does offer conclusive evidence that Zn^{2+} is able to inhibit FosA and is the likely culprit in the activity noted for CB 5838696 and its analogs.

The other five confirmed hits have not been as extensively tested since so much focus was placed on CB 5838696 and its analogs. These compounds have been synthesized by the VCSC and shown to exhibit similar activity to the commercial purchased compounds. The lack of zinc in these samples and the difference in structure among these hits is interesting, but all of these compounds are relatively poor inhibitors and need to be optimized. Several derivations of the ChemBridge compounds have been ordered and tested (Figures 60 and 61). More needs to be done, however to begin to develop good SAR.

Resazurin Bioactivity Test

The test for bioactivity of any potential inhibitors is important. It does not do any good to develop an excellent enzyme inhibitor that cannot make it across the cell wall to reach its target, or is not very specific. This cell based assay is designed to determine whether or not *E. coli* transformed with a plasmid containing FosA with a leaky promoter will be more susceptible to fosfomycin in the presence of increasing concentrations of the inhibitors being tested. In addition, using *E. coli* transformed with empty vector (plasmid without resistance gene) can help determine whether or not the inhibitors being tested have any cytotoxic effects on their own. Other antibiotics, such as kanamycin can be used as a positive control.

The rate of cell growth for *E. coli* transformed with FosA begins to decline at about 500 μM fosfomycin (Figure 62). For this reason, this concentration was used in all tests of the four ChemBridge compounds from the HTS assay. At high concentrations, around 2-3 mM, there is some decrease in the growth rates for the FosA transformed *E. coli*. However, it is very probable that this was the result of excess zinc in the

compounds, not the compounds themselves, since the same effect was seen in transformed cells both with and without FosA.

When confirmed hits from the Zn-controlled screen and some of their derivatives were screened for their bioactivity, four compounds were found to demonstrate a concentration-dependent decrease in the growth rates of *E. coli* transformed with Pa1129 FosA (Figure 53). However, all four of these compounds show similar decreases in the growth rates of *E. coli* without the FosA enzyme indicating some potentially cytotoxic activity other than the FosA inhibition (Figure 54).

After 24 hours of incubation, however, only three of these compounds show any ability to slow the growth of *E. coli*. Compound CB 7226895 shows some ability to slow initial growth based on the 12 hr. curve, but this ability does not extend to longer time points. The same does not hold true for CB 5155500, CB 6882791, and kk-8-054. All three of these compounds are able to demonstrate long-term decreases in the growth of *E. coli*. The growth inhibition of *E. coli* can be monitored visually by noting the lack of color change of resazurin in the wells containing high concentrations of these compounds in Figure 55. The growth inhibition can also be monitored spectrofluorometrically with a λ_{ex} = 530 nm and a λ_{ex} = 590 nm. Compounds CB 5155500 and CB 6882791 show almost no growth for *E. coli* transformed with Pa1129 FosA above 780 μM of the compound. Interestingly, this same effect is not seen in plates with *E. coli* transformed with an empty pET-20 vector. The difference in growth rates between *E. coli* transformed with FosA or empty vector pET-20 is a good indication that the lack of growth of the cells with FosA is due solely to the inhibition of the FosA enzyme allowing the antibiotic fosfomycin to work as it is supposed to and not from a non-specific

interaction with other cell enzymes. There is no difference between transformed cells for the compound kk-8-054. While this compound is the most potent at inhibiting cell growth, it does so in cells both with and without FosA. This is a good indication that the ability of this compound to arrest cell growth is not due to its ability to inhibit FosA but from some other, non-specific, mechanism.

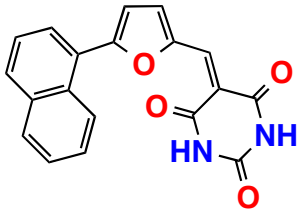

VCB0001181 O13
CB 5155620
IC_{50} = n.d.

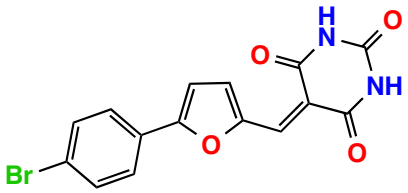

VCB0001181 I13
ChemBridge 5155500
IC_{50} = 15.1 ± 0.3 µM

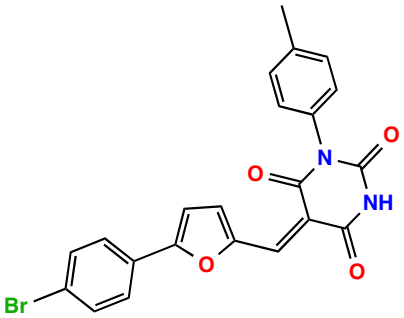

CB 5912931
IC_{50} = 11.4 ± 0.2 µM

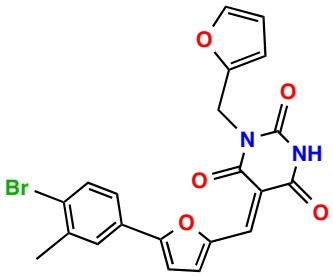

CB 6367287
IC_{50} = 13.5 ± 0.3 µM

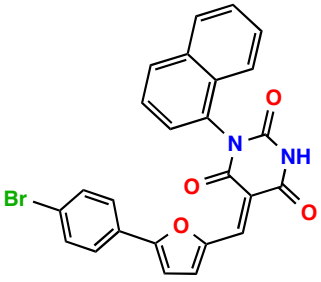

CB 7433453
IC_{50} = 9.1 ± 0.2 µM

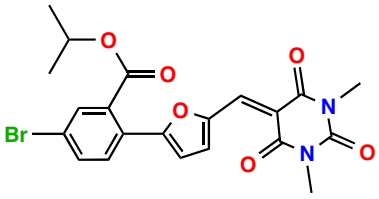

CB 6882791
IC_{50} = 122 ± 2 µM

Figure 60: Structure, ChemBridge ID, and IC_{50} of four derivatives of hit compounds CB 5155620 and 5155500.

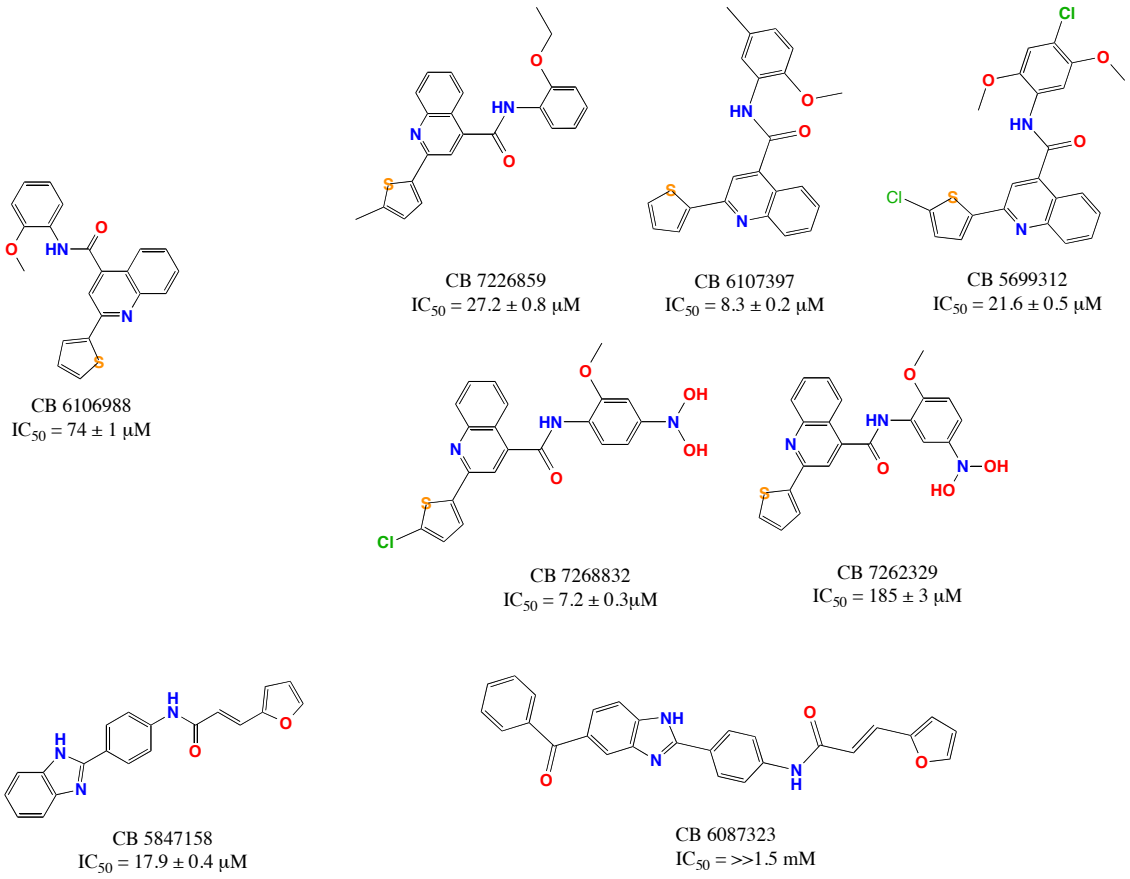

Figure 61: Structure, ChemBridge ID, and IC_{50} values for four derivatives of hit compound CB 6106988 and one derivative of hit compound CB 5847158.

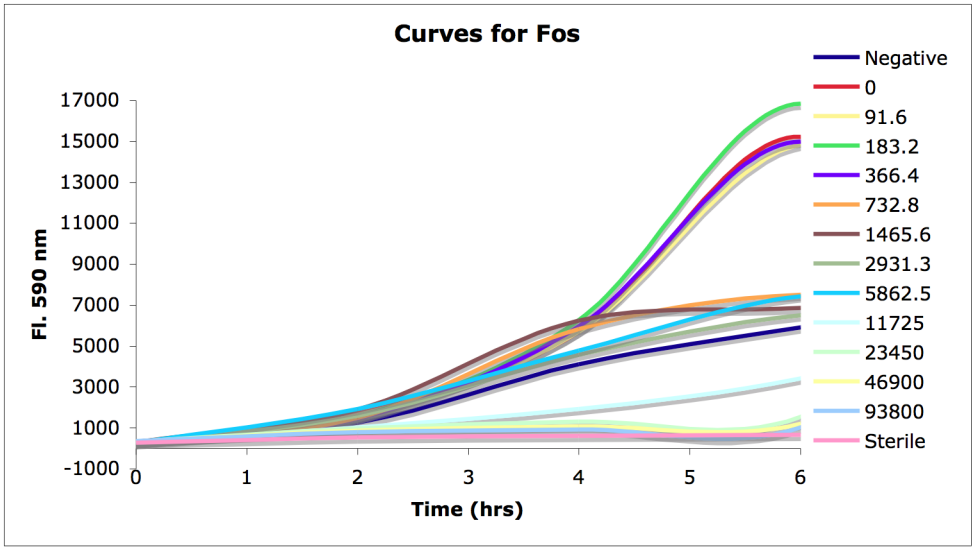

Figure 62: Resazurin growth curves for *E. coli* transformed with the Pa1129 FosA with increasing concentrations of fosfomycin. Concentrations in the legend are in micromolar.

CHAPTER VI

DEVELOPMENT OF A HIGH THROUGHPUT SCREEN FOR THE FOSX ENZYME FROM *Listeria monocytogenes*

Results

Assay with Fluorescent Boronic Acids

The product of the FosX reaction is a vicinal diol. Many assays have been published using fluorescent boronic acids to detect the vicinal diol of carbohydrates.[63,71-73] Initial experiments with 3-(dansylamino) phenyl boronic acid (DAPBA) in a fluorimeter showed no difference in the fluorescence signal with or without the product diol. Several different buffer conditions and concentration ratios of diol to fluorophore resulted in similar outcomes.

The compound 8-quinoline boronic acid (8-QBA) is reported to give a signal in proportion to the concentration of diol product present.[63] As such, it should make a good fluorophore for testing the FosX reaction. However, using molar equivalents of 8-QBA and purified diol again showed no difference in the fluorescence intensity in reactions with and without the diol present. The lack of sensitivity to the fos-diol product concentration indicates that this is not a viable method of assay development (Figure 18).

Adrenaline Based FosX Assay

A modified version of the adrenaline assay for the discovery of epoxide hydrolases was then developed to try and measure the concentration of the diol product indirectly (Figure 19).[64,74] As an absorbance based assay rather than a fluorometric one; the assay was done in clear 96-well plates. The reaction works by using sodium

periodate to oxidize the diol product formed, with the periodate and substrate/product in equal molar concentrations. Once this reaction is complete adrenaline is added and any remaining periodate will oxidize the adrenaline to adrenochrome. The absorbance of the adrenochrome can then be recorded spectrophotometrically. The more diol product that is formed in the enzymatic reaction, the less periodate left over to oxidize the adrenaline and the less adrenochrome formed.

Phosphonoformate was used as a model inhibitor with the *L. monocytogenes* FosX in the initial stages of developing this assay. Phosphonoformate is not a very good inhibitor of the FosX enzymes with an IC_{50} = ~25 mM. Also, this assay requires high micromolar to low millimolar concentrations of fosfomycin, periodate, and adrenaline. Since the compounds screened would only be 10 micromolar, a more sensitive assay was deemed necessary.

Gallocyanine Based FosX Assay

The assay sensitivity was greatly enhanced with the simple substitution of gallocyanine for adrenaline (Figure 20). The oxidation product of gallocyanine by sodium periodate is a fluorophore.[75] The concentration of fosfomycin used, therefore, is three times less with the gallocyanine-based assay and in the same range as that used in the FosA assay. The oxidized form of gallocyanine is able to be detected spectrofluorometrically, so black plates are used instead of clear, and sensitivity is greatly increased. The only problem that remained was to find a good model inhibitor for the assay. Again, phosphonoformate is a poor inhibitor of the *L. monocytogenes* FosX, which creates several problems, especially in liquid handling. In the search for new

inhibitors, several other small phosphonates were tested as well as several chelators and inactive metals (Figure 63).

The other small phosphonates tested were ethylphonsphonic acid (EPA), phosphonoacetic acid (PAA), 2-carboxyethylphosphonic acid (CEPA), ethyldiethoxyphosphinyl formate, Tris(trimethylsilyl) phosphite, ehtoxycarbonyl phosphate (ECP), and acetyl phosphonate. None of these showed any appreciable activity against the *L. monocytogenes* FosX. Metal chelators were then tested to see if they could inhibit the FosX reaction by either binding to the Mn^{2+} in the active site or pulling the metal out of the enzyme. The chelators tested were adenosine mono-, di-, and triphosphate (AMP, ADP, and ATP), EDTA, EGTA, ADA, citrate, HEDTA, BAPTA, and oxalate. Again, no appreciable activity was seen. The only thing that worked was the last ditch effort of trying inactive metal ions, such as zinc. In fact, zinc proved to be a good inhibitor of the *L. monocytogenes* FosX with an $IC_{50} = 3.06 \pm 0.08$ μM.

The gallocyanine assay seemed promising for the FosX enzymes; however, when DMSO was added to the reaction mixture no inhibition was seen. By process of elimination, it was determined that the DMSO was in fact reacting with the periodate so that there was never any remaining to react with the gallocyanine (Figure 64). The reaction of DMSO and periodate resulted in a baseline reaction that made it seem as if no inhibition was taking place.

PHOME FosX Assay

The compound PHOME can be used in HTS assays for the discovery of inhibitors to mammalian soluble epoxide hydrolases.[66] There is no similarity in the sequence or structure of the mammalian soluble epoxide hydrolases and the *L. monocytogenes* FosX.

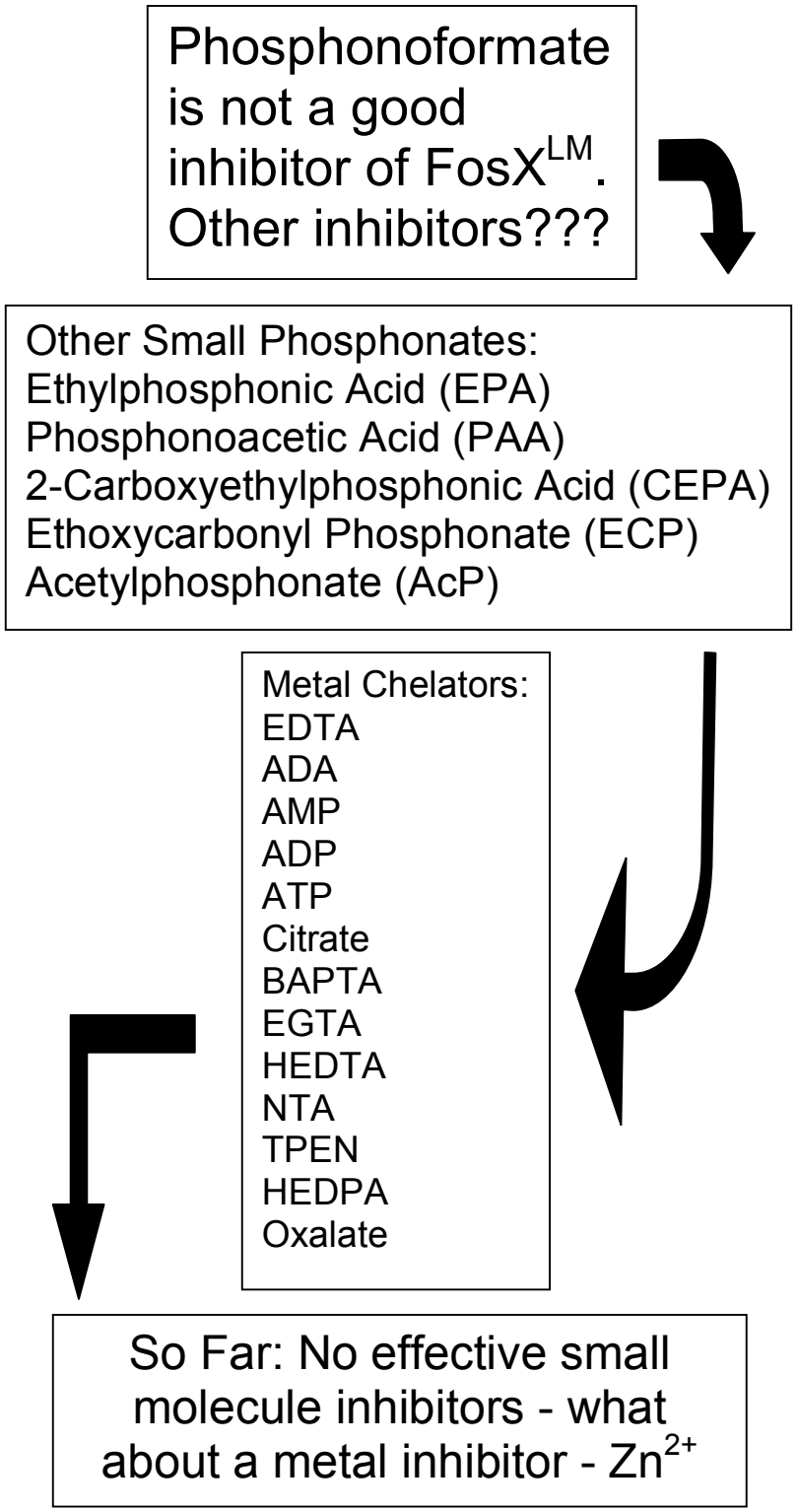

Figure 63: Flow-chart depicting the search for model inhibitors for the FosX gallocyanine-based assay. Zn^{2+} finally was chosen and found to have an IC_{50} = 3 μM.

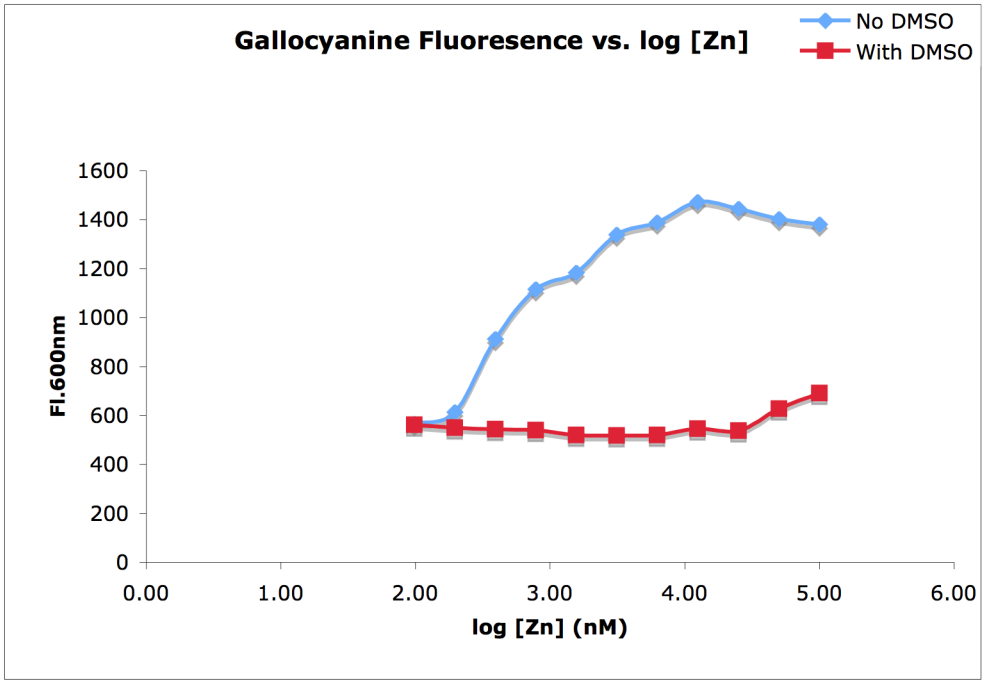

Figure 64: The gallocyanine assay shows a good increase in fluorescence with the addition of Zn in the absence of DMSO. However, the addition of DMSO completely diminishes the ability of this assay.

To test the reaction of PHOME with the *L. monocytogenes* FosX, a series of reactions was run using a 2x dilution of PHOME to determine the rate of the reaction catalyzed by FosX. The *L. monocytogenes* FosX was able to catalyze the reaction, but not well. The calculated k_{cat} = ~4 x 10^{-4} s^{-1} with a K_M = ~31 mM for a k_{cat}/K_M = 13 M^{-1} s^{-1}. This shows that while PHOME is a substrate for the FosX enzyme, it is not a good one. The k_{cat}/K_M for the human soluble epoxide hydrolase is on the order of 1 x 10^5 M^{-1} s^{-1}. This slow of a turnover for the FosX enzyme eliminates this as a viable HTS assay (Figure 65).

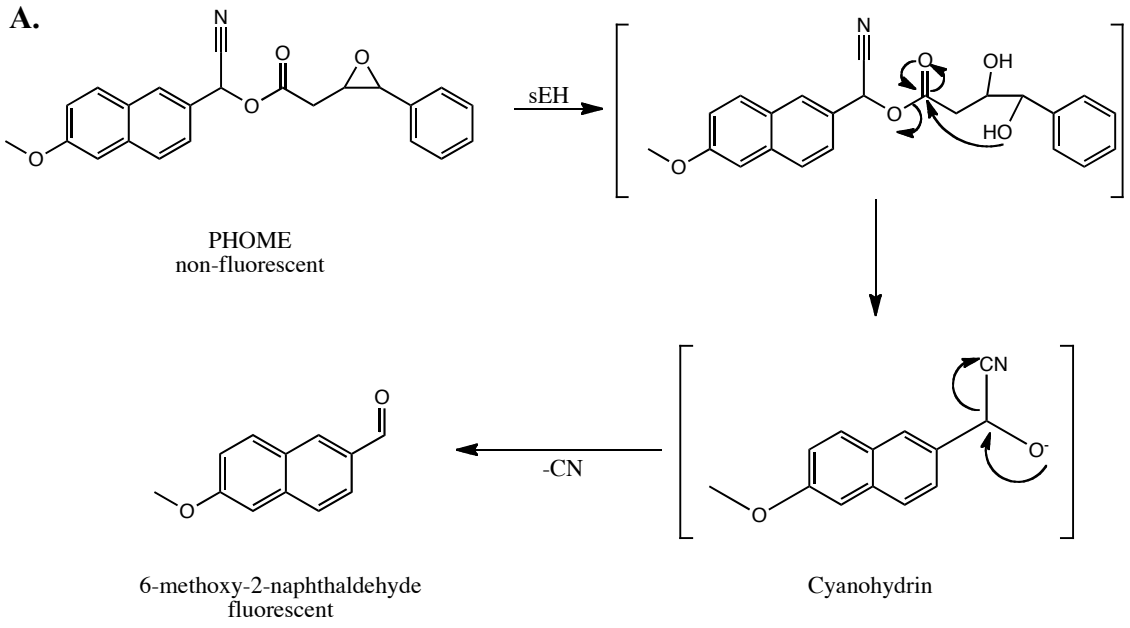

B.

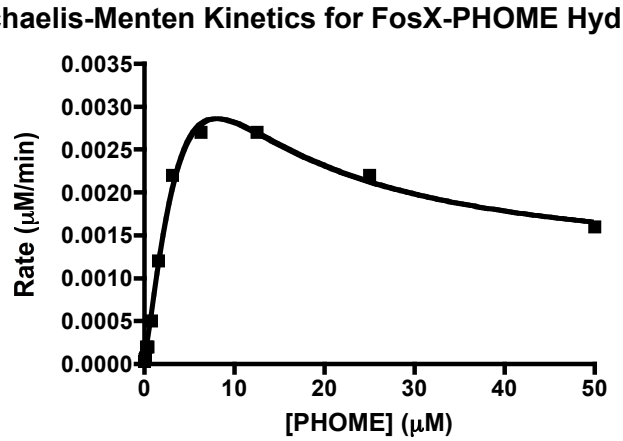

Figure 65: A) The reaction catalyzed by epoxide hydrolase with PHOME. The hydrolyzed product spontaneously decomposes to the fluorescent compound 6-methoxy-2-napthaldehyde. B) Michaelis-Menton kinetics for PHOME hydroxylation by the *L. monocytogenes* FosX. v_{max} = 0.02529 μM/min, k_{cat} = 0.02529 min^{-1} = 4.215 x 10^{-4} s^{-1}. K_M = 31.45 mM = 3.145 x 10^{-5} M. k_{cat}/K_M = 13.4 M^{-1} s^{-1}. Compare to human sEH: k_{cat}/K_M = 1.15 x 10^5 M^{-1} s^{-1}.

Discussion

The attempt at developing an HTS assay has now been abandoned since no viable assay was ever established. As a hydrolase enzyme, an assay similar to the FosA assay is not feasible since the other substrate is water, a ubiquitous molecule in an aqueous environment. All four of the potential assays tried failed for different reasons, but failed nonetheless.

The assay using fluorescent boronic acids seemed promising as this type of assay has been used for many years in the detection of carbohydrates. However, most of the fluorescent boronic acids on the market are designed for HPLC use, as there is no difference in the intensity of fluorescence for the bound and unbound boronic acid. In order for this type of assay to work for HTS there needs to be a strong difference between bound and unbound boronic acid to be able to accurately identify the presence of the product being formed. The compound 8-QBA does show a concentration-dependent signal with fructose, but did not show a concentration-dependent signal with fos-diol.

The periodate based assays seemed more promising, but the reaction of DMSO and periodate proved to invalidate the assay. The adrenaline-based assay required far too much substrate for an HTS assay. Having 1.5 mM fosfomycin as compared to 10 μM of the test compounds would immediately eliminate any weak inhibitors and possibly any average to moderate ones as well since the compounds would have to really out compete fosfomycin to show up in the assay. Replacing the adrenaline with gallocyanine allows for the use of much less fosfomycin, a concentration on par with that used in the FosA assay. Again, this assay works well as long as DMSO is not added. The FosX enzyme is not inhibited very well by phosphonoformate, so a search for a new model inhibitor

turned up zinc. Zinc inhibits the enzyme well, but once DMSO is added, the signal is lost. Even the small amount of DMSO in the reaction, 0.1%, is equivalent to about 18 mM DMSO – more than enough to react with all of the periodate in the reaction system.

One last effort was made to modify an assay used for mammalian soluble epoxide hydrolases. This assay uses the compound PHOME which, when hydroxylated, spontaneously decomposes to 6-methoxy-2-napthaldehyde. The production of the napthaldehyde can be measured spectrofluorometrically. Interestingly, FosX can catalyze this reaction despite having no sequence or structural similarity to the mammalian soluble epoxide hydrolases. However, FosX catalyzes the reaction about 10,000 times less efficiently than the human hydrolase. With a low efficiency any compound inhibiting this reaction wouldn't necessarily be inhibiting the natural reaction of the FosX enzymes. In addition, such a slow reaction rate would lead to many hits of very weakly binding inhibitors and leave too many compounds to confirm and recheck. This is just not an efficient enough reaction for HTS.

No further work was done to develop an assay using the *L. monocytogenes* FosX.

CHAPTER VII

CONCLUSION

As the rising tide of antibiotic resistant infections continues to inundate clinics around the world, the imperative to find solutions becomes more pressing. One clinically valid method of fighting this tide is to make old antibiotics useful again. The use of inhibitors to enzymatically catalyzed antibiotic resistance has been commercially successful in combinations of β-lactam antibiotics, such as amoxicillin, and β-lactamase inhibitors, like clavulanic acid. A similar combination of antibiotic and resistance inhibitor should be, therefore, a viable tactic to take against other forms of enzymatically derived resistance.

The antibiotic fosfomycin has been little used over the years despite its broad-spectrum activity and lack of significant side effects. In fact, recent analysis has shown that fosfomycin alone is able to achieve cure in 80% of infections when used. Other reports have shown that fosfomycin would be a good alternative to more established antibiotics, such as linezolid, against Vancomycin Resistant Enterococci (VRE).[76]

The main reason for the lack of fosfomycin use is the amount of resistance that has been mounted against it. Of the five major methods of resistance derived by bacteria four have been specifically found in relation to fosfomycin. Two of these, enzymatic degradation and modification, should be able to be counteracted with novel therapeutics. It is for this reason that an HTS campaign has been mounted against fosfomycin resistance.

For the purposes of the HTS assay the well-studied enzyme FosA from *P. aeruginosa* was used. The structural and functional elements of this enzyme have been largely discerned through crystallographic and computational analysis. The docking and analysis of the GSH binding site helped elucidate this final piece of the puzzle and completed the picture of FosA. The docked structure of GSH in FosA also helped to give a keen insight into the possible route of evolution of these very robust inhibition enzymes from less robust progenitors. Still, all of this structural analysis was necessary to better understand the rise of antibiotic resistance.

Phosphonoformate, an anti-viral compound, is known to inhibit FosA, but its antimicrobial activity was not due to specific inhibition of FosA. Still, the knowledge of this inhibition gave a great starting point for developing HTS assays. After several false starts a viable HTS assay has now been established. The final assay uses Zn as a positive control, however, because it is a more potent inhibitor and much cheaper than Pf, lowering the overall cost of running a large screen. Small screens have identified six confirmed inhibitors of the FosA enzyme from a mere 4800 compounds to date. The assay works quickly using the purified enzyme and hits were identified at a rate of 0.19% and hits were confirmed at a rate of 75%.

Subsequent analysis of hits from the compound screens revealed one compound whose close structural analogs had IC_{50} values less than or equal to 1 μM. In all, seven compounds were purchased from ChemBridge and found to be very active at inhibiting FosA. Further testing revealed that the inhibitory activity of these compounds was due to a high level of zinc contamination.

Not much work has been done yet on the other confirmed hits because they are much weaker inhibitors of FosA. These compounds may be metal chelators, which are often rejected as drug lead compounds, so it will be a challenge to get around this. Still, it is a good start and bodes well for the future discovery of new compounds.

An assay to test the bioactivity of these compounds has also been developed. This will be important, as the ability of an inhibitor to cross the cell membrane will be vital to its success. Using *E. coli* transformed with expression plasmids either with or without FosA it will be possible to test compounds for their bioactivity and also for their specificity. The combination of bioactivity and specificity will be of utmost importance in the development of novel drug compounds.

Future Directions

More work will be needed to understand the details of the evolution of robust fosfomycin resistance from less robust progenitors. Future work in this area will focus on DNA shuffling of the *M. loti* FosX to better FosX enzymes and directed evolution of the *M. loti* FosX to make a better FosA.

The HTS assay is ready for a larger screen and that will be done in the near future. This screen should also work with the FosB enzymes since they also use small thiols. This may prove attractive for studies of the *S. aereus* FosB, for example. More work will also be done to optimize the activity of the inhibitors discovered to date to make them more effective, bioactive, and specific.

APPENDIX

NMR DATA FROM CHEMBRIDGE AND KK-5-SERIES OF COMPOUNDS

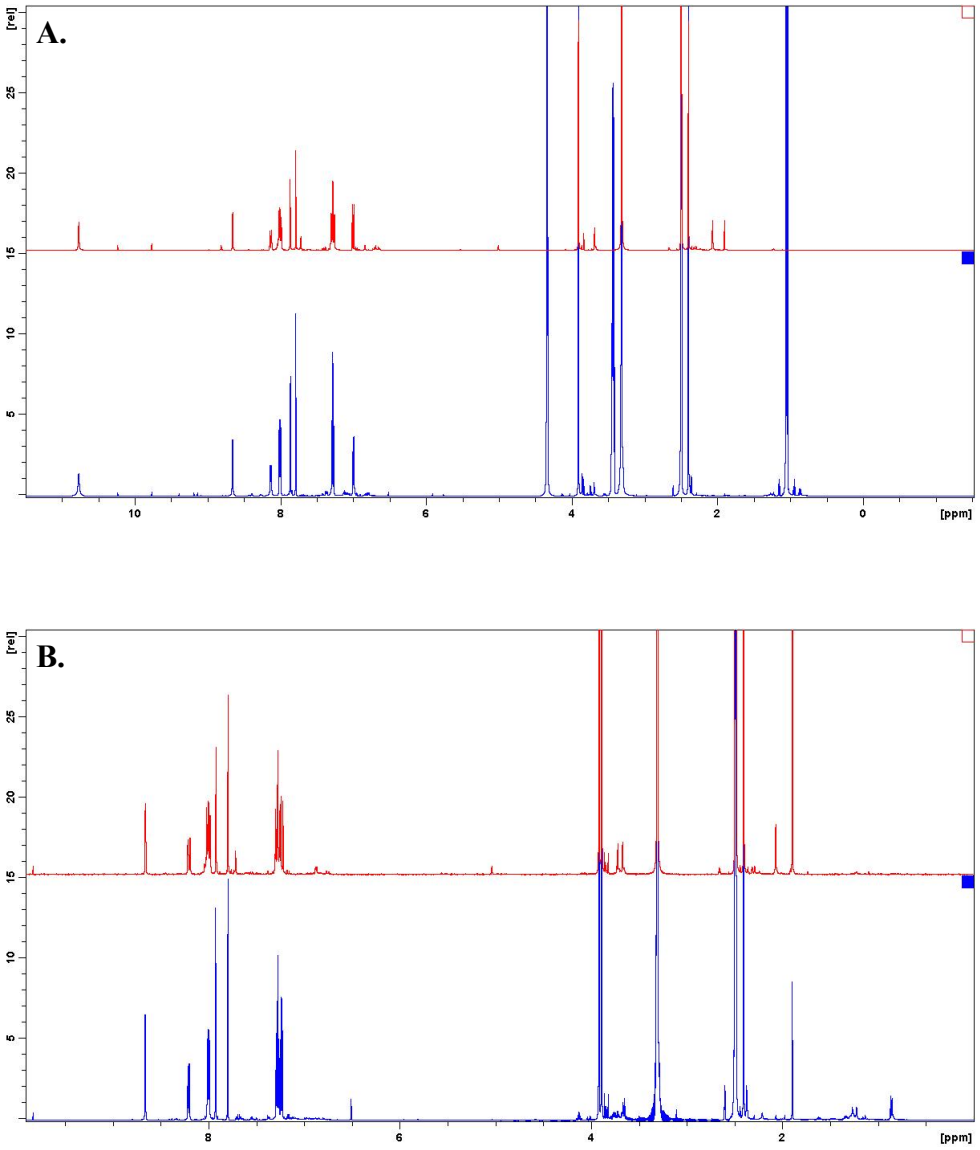

Figure 66: A) Comparison of the ^{1}H NMR spectra from kk-5-141-2 (same as kk-5-095-4) in red and CB 5848410 in blue. B) Comparison of the ^{1}H NMR spectra from kk-5-141-1 (same as kk-5-095-3) in red and CB 5846450 in blue. All data shown in this appendix was collected at 600 MHz in d_6- DMSO. See Methods for details.

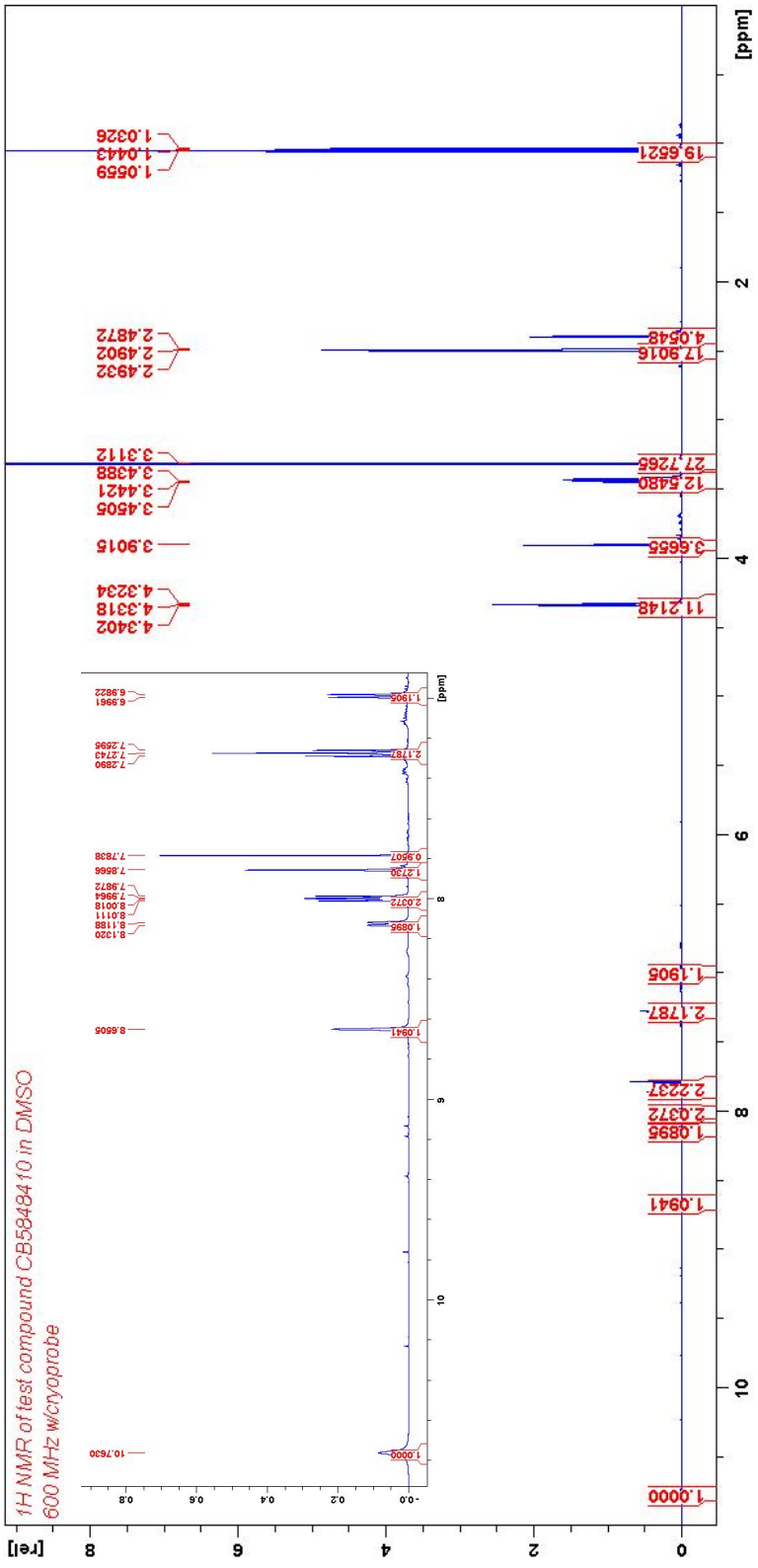

Figure 67: [1]H NMR for CB 5848410 with aromatic region inset.

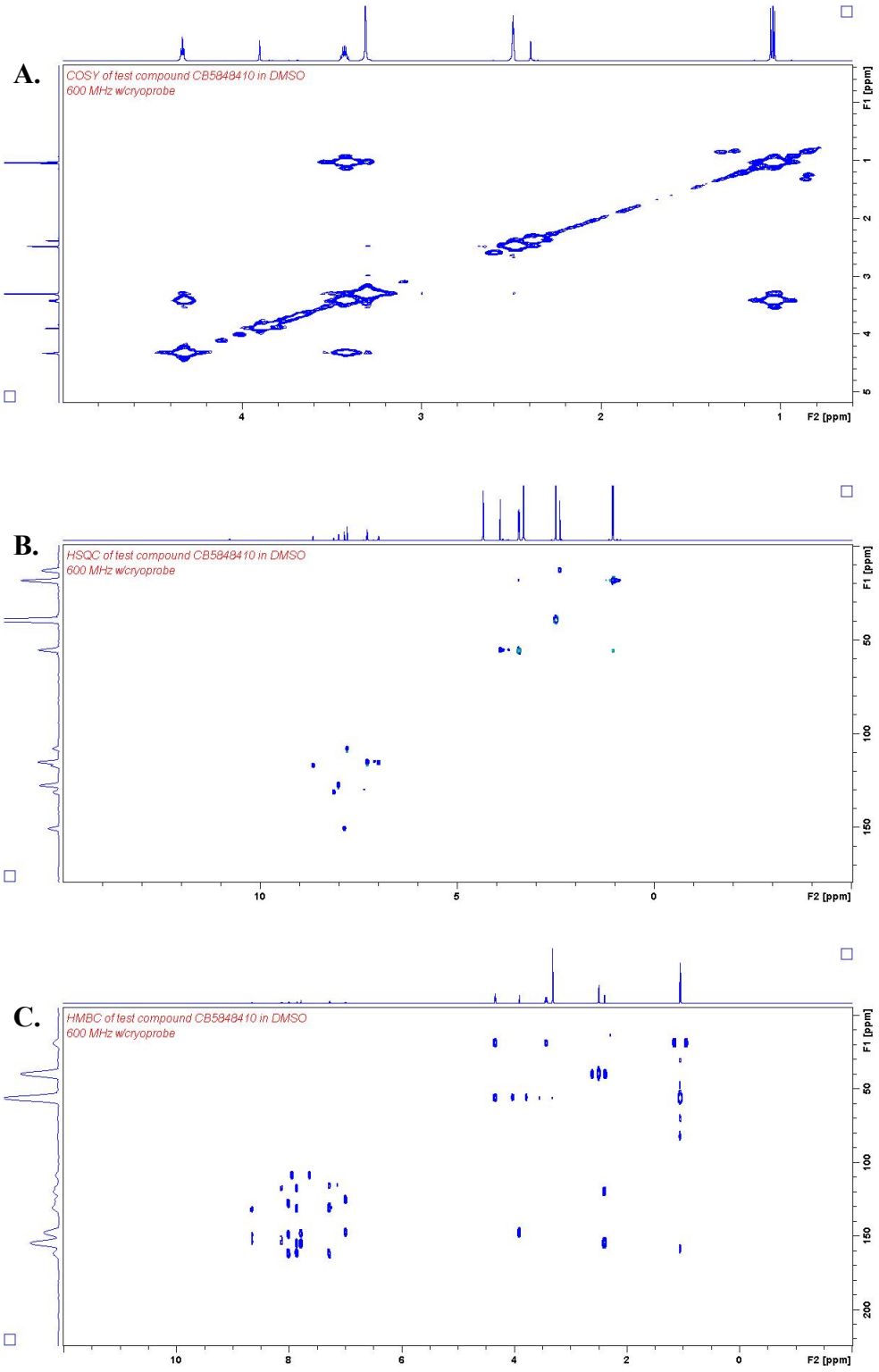

Figure 68: A) COSY spectrum for CB 5848410. B) HSQC spectrum for CB 5848410. C) HMBC spectrum for CB 5848410.

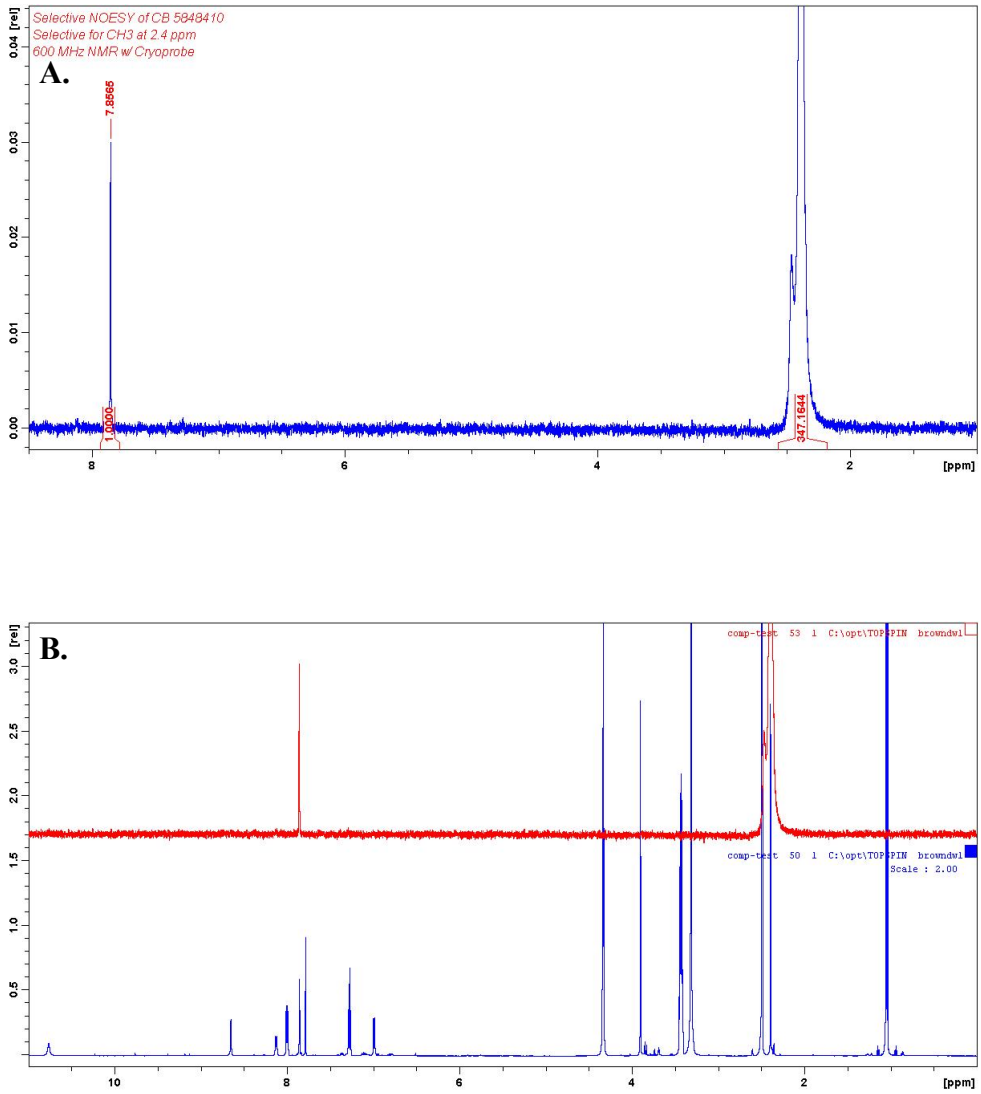

Figure 69: A) Selective NOESY experiment targeting interactions with the methyl group a δ2.4 ppm showing an interaction with a single proton at δ7.86 ppm (see Figure 75). B) Comparison of the selective NOESY experiment, red, with the full 1H spectrum, blue.

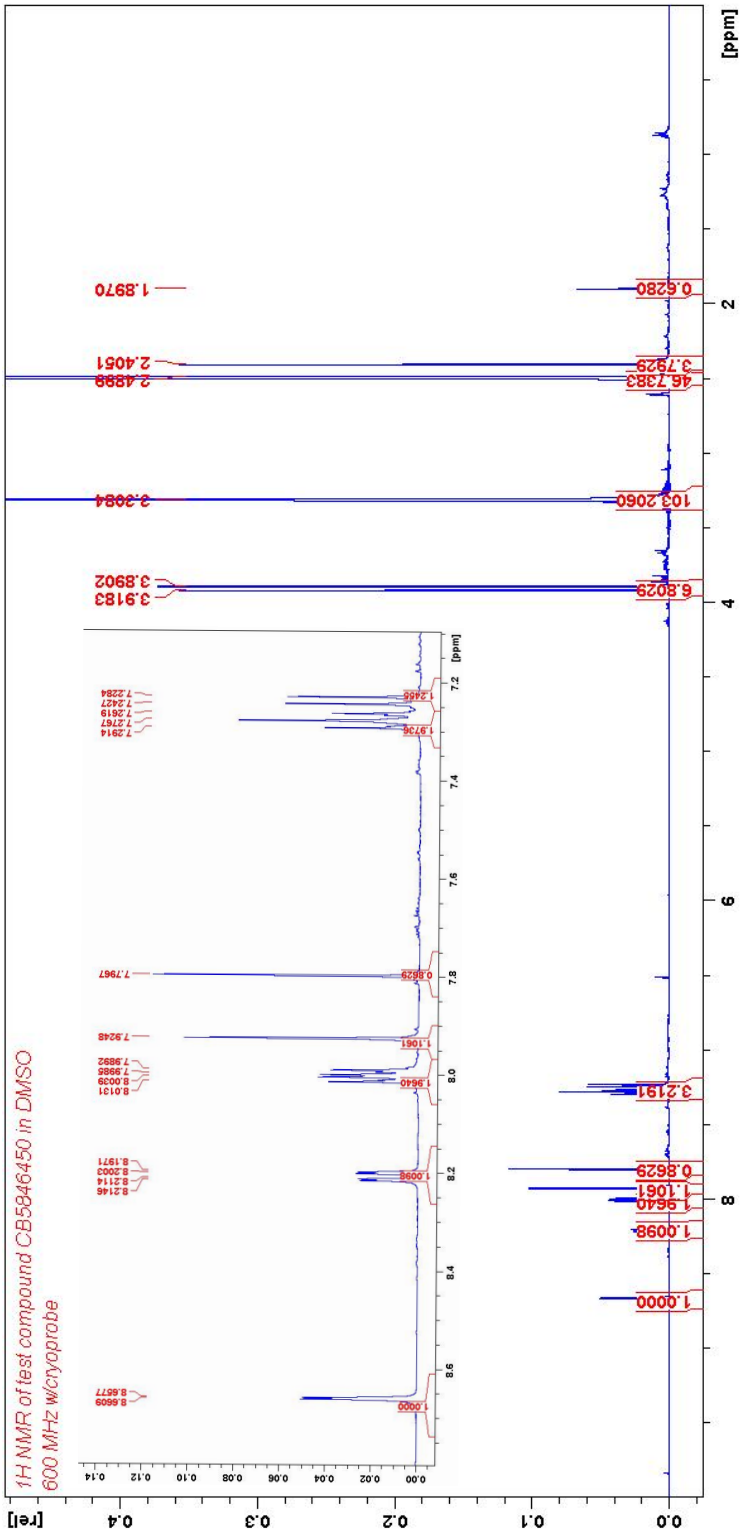

Figure 70: ^{1}H NMR for CB 5846450 with aromatic region inset.

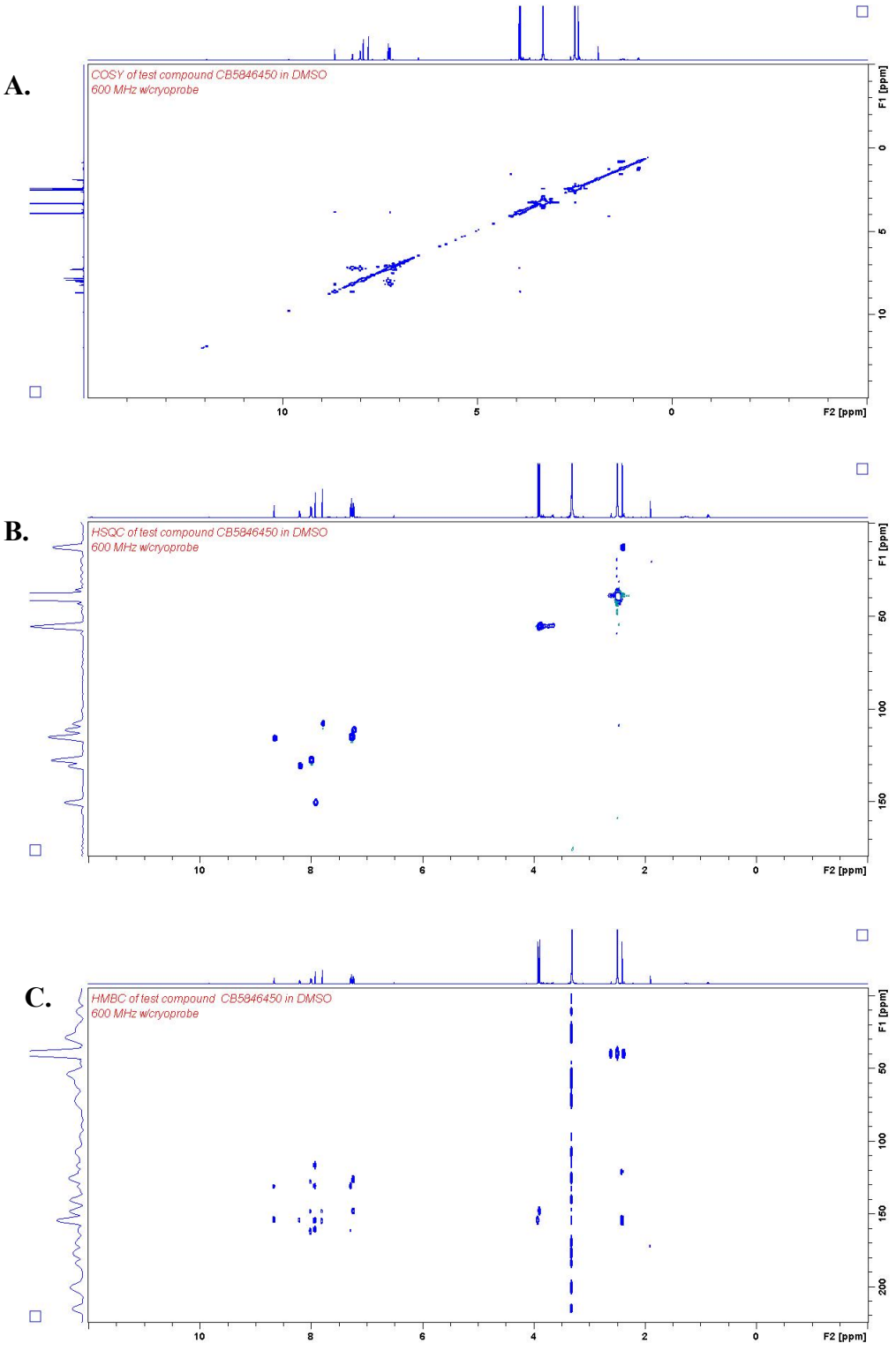

Figure 71: A) COSY spectrum for CB 5846450. B) HSQC spectrum for CB 5846450. C) HMBC spectrum for CB 5846450.

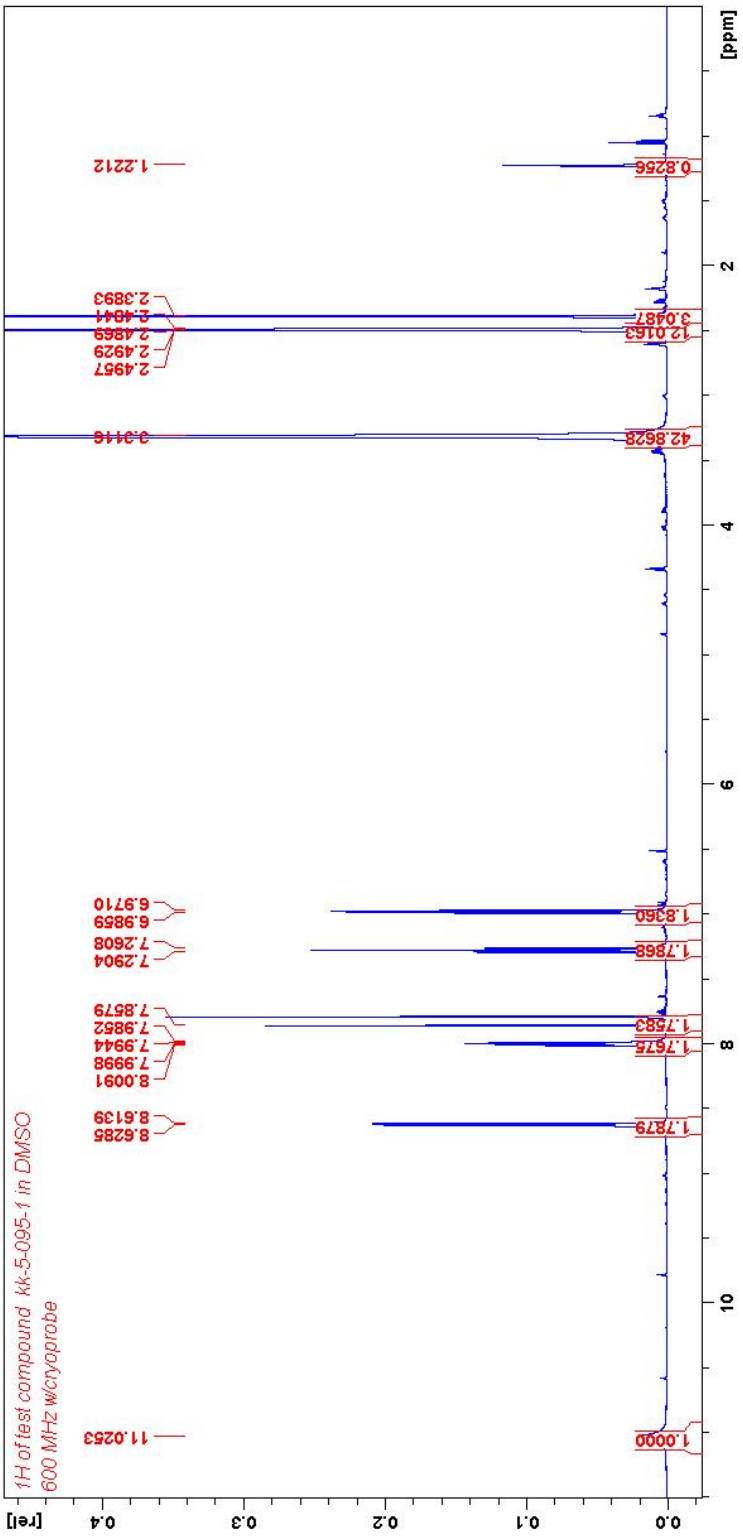

Figure 72: ^{1}H NMR for kk-5-095-1 (equivalent to CB 5838696).

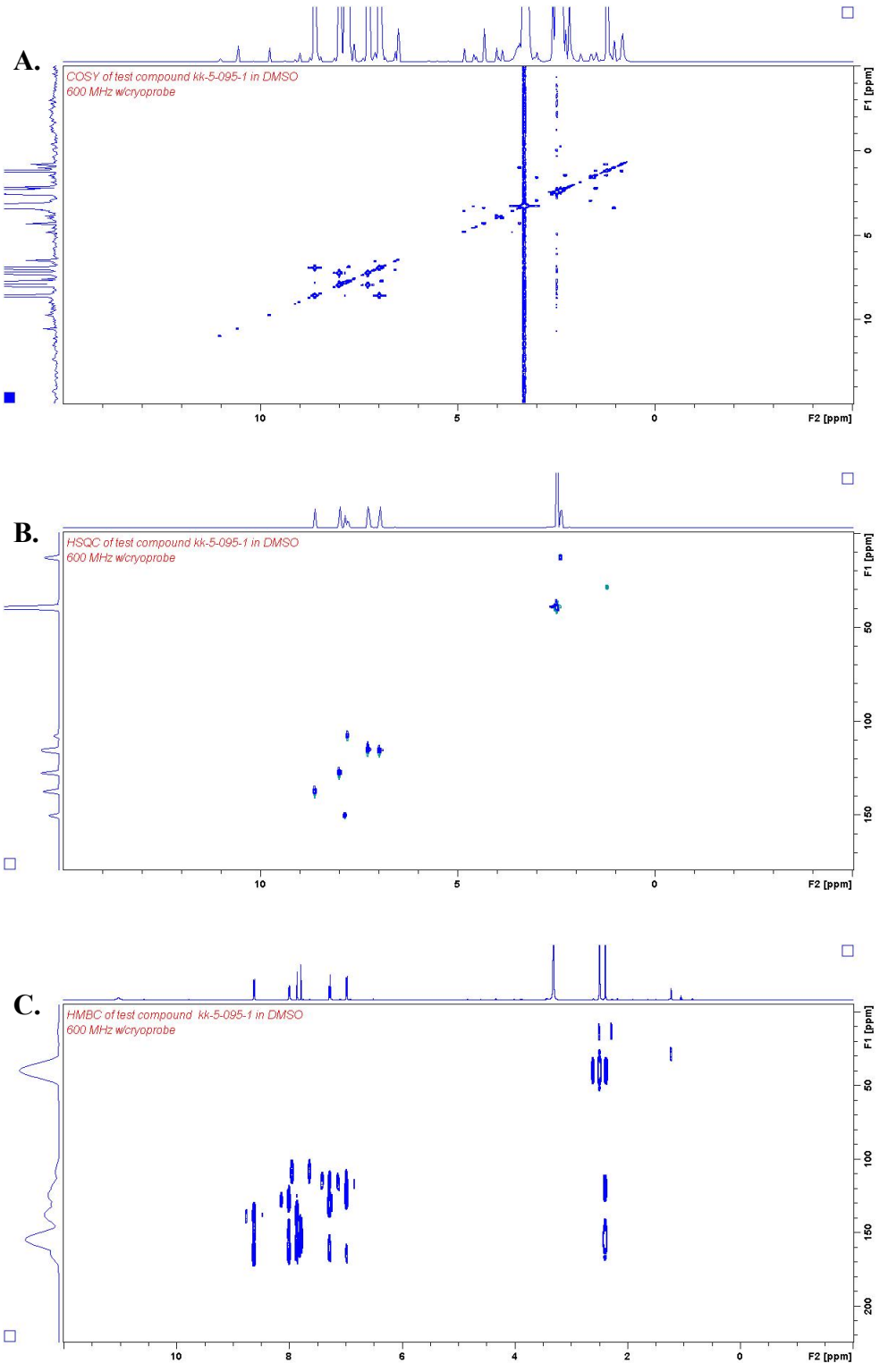

Figure 73: A) COSY spectrum for kk-5-095-1. B) HSQC spectrum for kk-5-095-1. C) HMBC spectrum for kk-5-095-1.

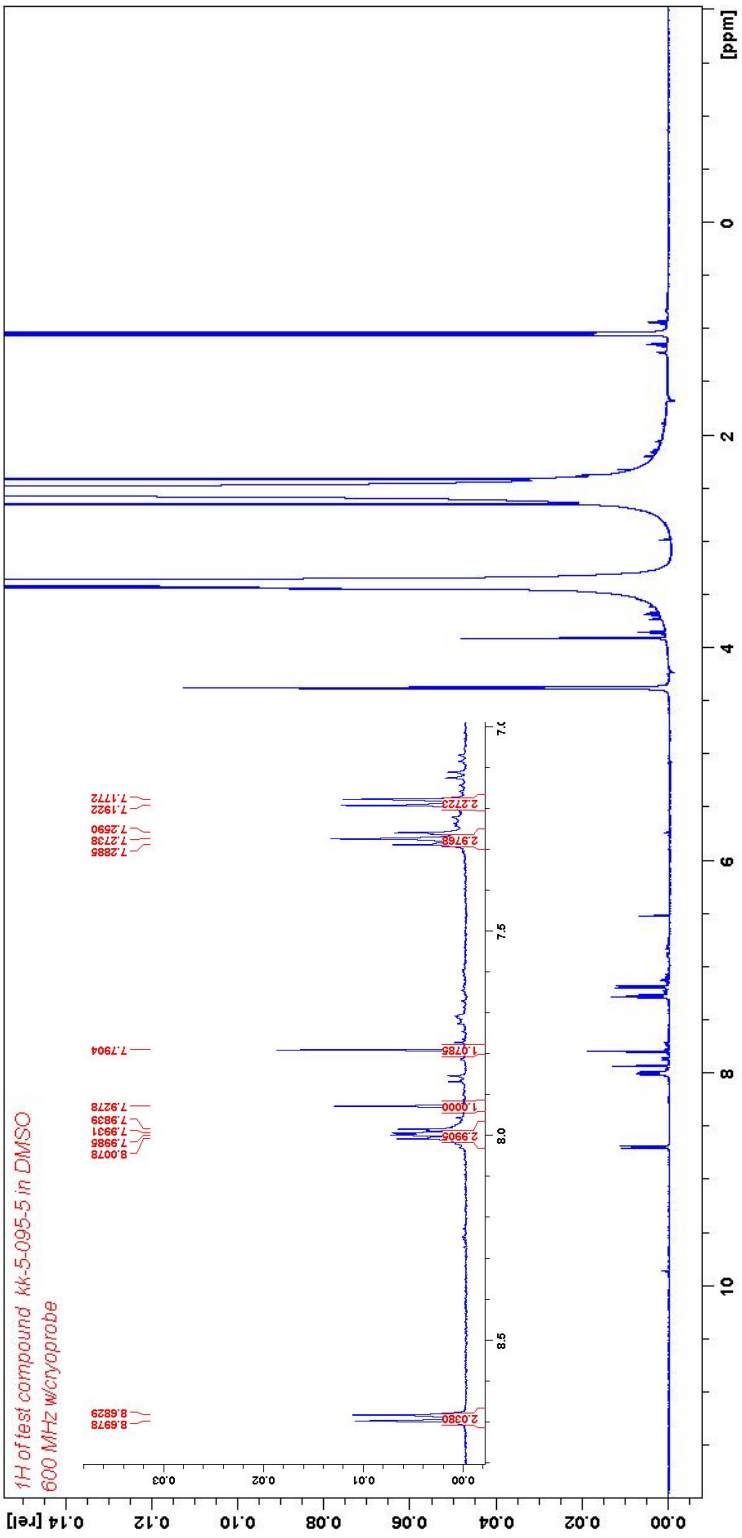

Figure 74: ^{1}H NMR of kk-5-095-5 (equivalent to CB 5844324) with aromatic region inset.

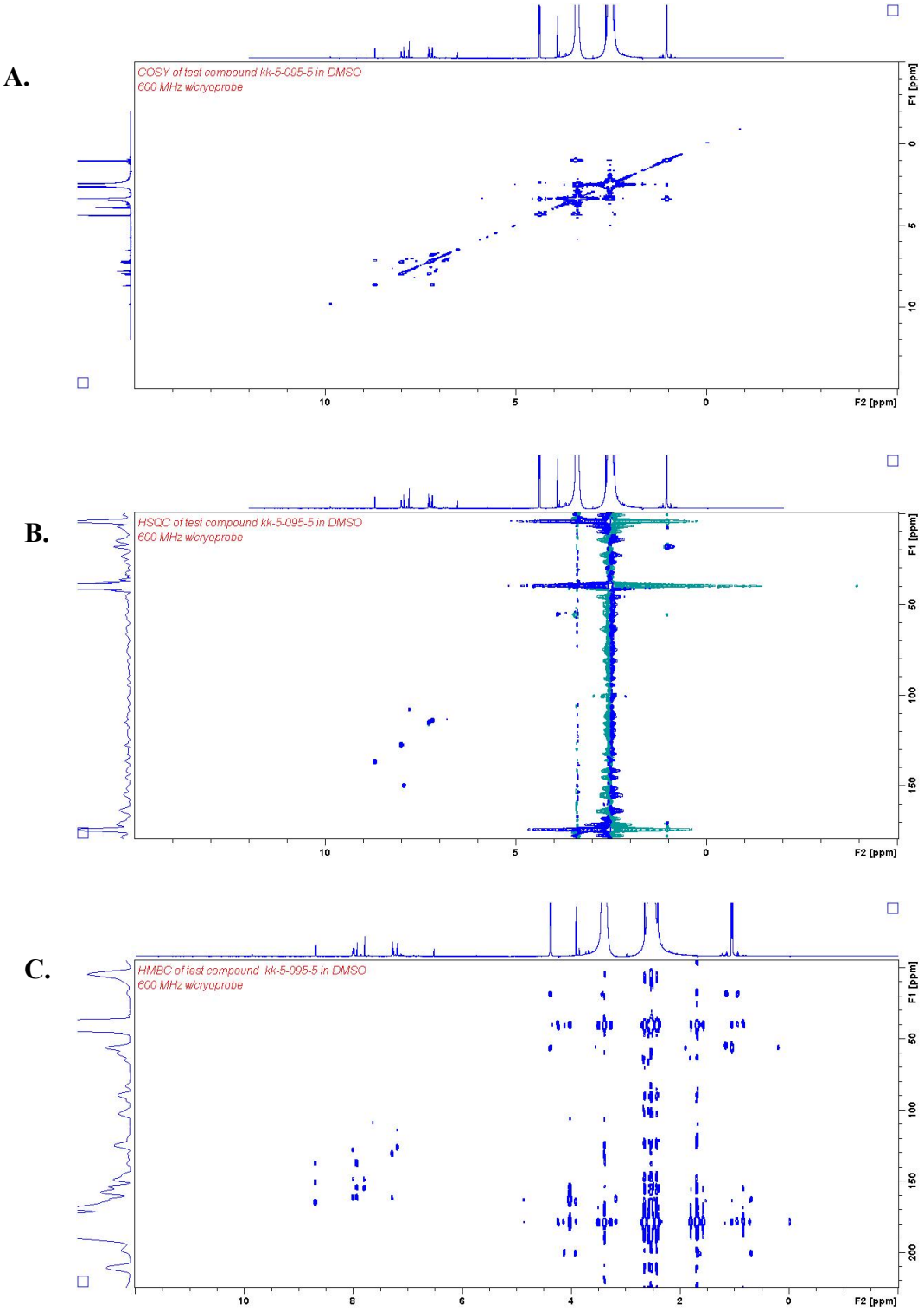

Figure 75: A) COSY spectrum for kk-5-095-5. B) HSQC spectrum for kk-5-095-5. C) HMBC spectrum for kk-5-095-5.

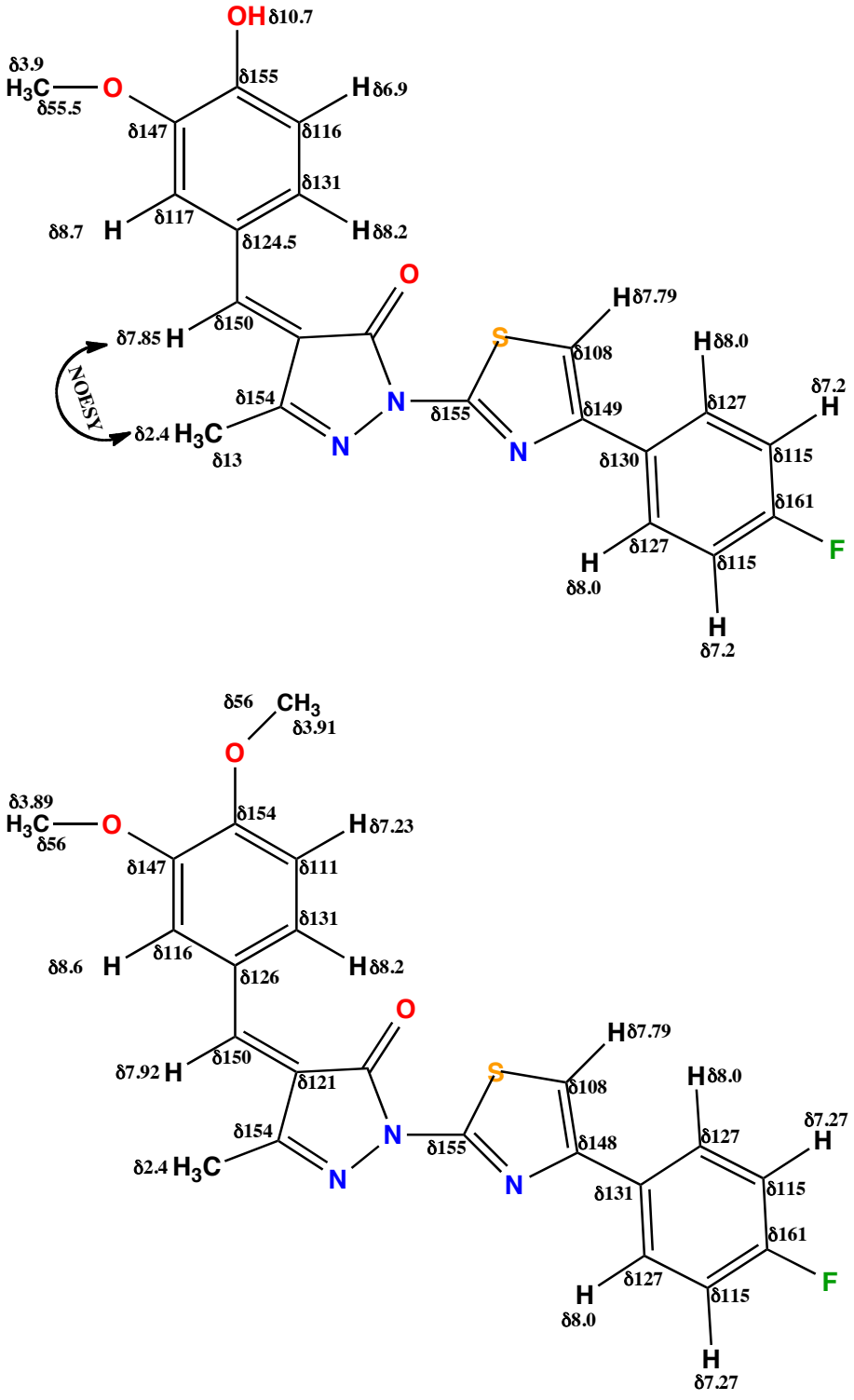

Figure 76: A) Chemical shift data for CB 5848410. The double-sided arrow labeled NOESY indicates the key interaction from the selective NOESY experiment that confirmed the stereochemistry of the double bond between the two rings. B) Chemical shift data for CB 5846450.

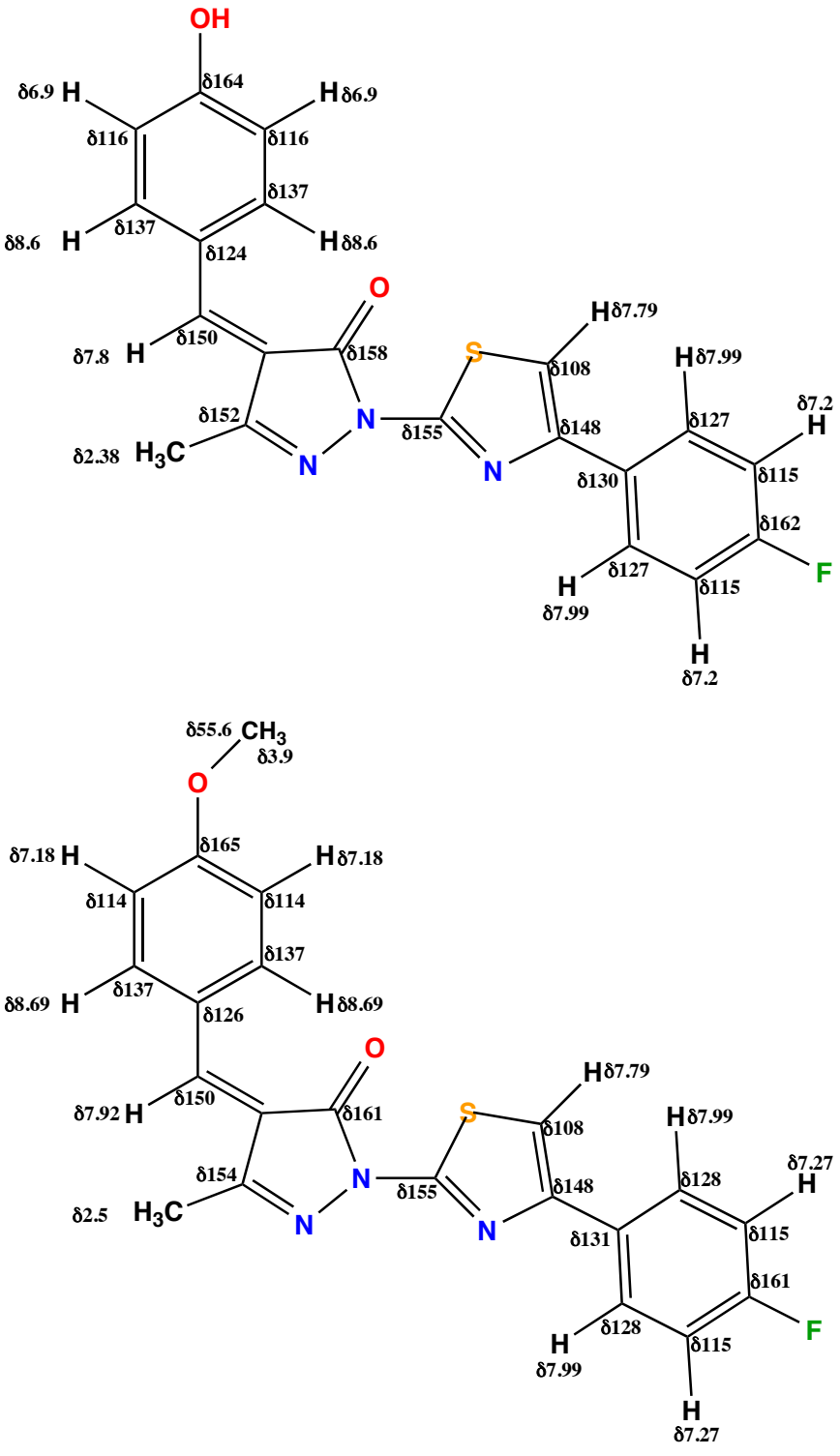

Figure 77: A) Chemical Shift Data for kk-5-095-1 (equivalent to CB 5838696). B) Chemical Shift Data for kk-5-095-5 (equivalent to CB 5844324).

References

(1) Fleming, A. *Brit. J. Exp. Path.* **1929**, *10*, 226-236.
(2) Demain, A. L.; Elander, R. P. *Antonie van Leeuwenhoek* **1999**, *75*, 5-19.
(3) Bush, K. *Clin. Micobiol. Infec.* **2004**, *10*, 10-17.
(4) Powers, J. H. *Clin. Micobiol. Infec.* **2004**, *10*, 23-31.
(5) Fernandes, P. *Nat. Biotechnol.* **2006**, *24*, 1497-1503.
(6) Katz, M. L.; Mueller, L. V.; Polyakov, M.; Weinstock, S. F. *Nat. Biotechnol.* **2006**, *24*, 1529-1531.
(7) Wang, J.; Soisson, S. M.; Young, K.; Shoop, W.; Kodali, S.; Galgoci, A.; Painter, R.; Parthasarathy, G.; Tang, Y. S.; R., C.; Ha, S.; Dorso, K.; Motyl, M.; Jayasuriya, H.; Ondeyka, J.; Herath, K.; Zhang, C.; Hernandez, L.; Allocco, J.; Basilio, A.; Tormo, J. R.; Genilloud, O.; Vicente, F.; Pelaez, F.; Colwell, L.; Lee, S. H.; Michael, B.; Felcetto, T.; Gill, C.; Silver, L. L.; Hermes, J. D.; Bartizal, K.; Barrett, J.; Schmatz, D.; Becker, J. W.; Cully, D.; Singh, S. B. *Nature* **2006**, *441*, 358-361.
(8) Fox, J. L. *Nat. Biotechnol.* **2006**, *24*, 1521-1528.
(9) Walsh, C. *Nat. Rev. Microbiol.* **2003**, *1*, 65-70.
(10) Christoffersen, R. E. *Nat. Biotechnol.* **2006**, *24*, 1512-1514.
(11) Hall, B. G. *Nat. Rev. Microbiol.* **2004**, *2*, 430-435.
(12) Levy, S. B.; Marshall, B. *Nat. Med.* **2004**, *10*, S122-S129.
(13) Tomasz, A. *Science* **2006**, *311*, 342-343.
(14) D'Costa, V. M.; McGrann, K. M.; Hughes, D. W.; Wright, G. D. *Science* **2006**, *311*, 374-377.
(15) Dantas, G.; Sommer, M. O. A.; Oluwasegun, R. D.; Church, G. M. *Science* **2008**, *320*, 100-103.
(16) Harbarth, S. *Curr. Opin. Crit. Care* **2007**, *13*, 554-556.
(17) Payne, D. J.; Gwynn, M. N.; Holmes, D. J.; Pompliano, D. L. *Nat. Rev. Drug Disc.* **2006**, *6*, 29-40.
(18) Baum, E. Z.; Montenegro, D. A.; Licata, L.; Turchi, I.; Webb, G. C.; Foleno, B. D.; Bush, K. *Antimicrob. Agents Ch.* **2001**, *45*, 3182-3188.
(19) Lujan, S. A.; Guogas, L. M.; Ragonese, H.; Matson, S. W.; Redinbo, M. R. *P. Natl. Acad. Sci.* **2007**, *104*, 12282-12287.
(20) Lock, R. L.; Harry, E. J. *Nat. Rev. Drug Disc.* **2008**, *7*, 324-338.
(21) Smith, P. A.; Romesberg, F. E. *Nat. Chem. Biol.* **2007**, *3*, 549-556.
(22) Lomovskaya, O.; Bostian, K. A. *Biochem. Pharmacol.* **2006**, *71*, 910-918.
(23) Avison, M. B. *Genome Biol.* **2005**, *6*, 243.1-243.4.
(24) Miller, L. A.; Ratnam, K.; Payne, D. J. *Curr. Opin. in Pharmacol.* **2001**, *1*, 451-458.
(25) Ball, P. *Int. J. Antimicrob. Agents* **2007**, *30S*, S113-S117.
(26) Hendlin, D.; Stapley, E. O.; Jackson, M.; Wallick, H.; Miller, A. K.; Wolf, F. J.; Miller, T. W.; Chaiet, L.; Kahan, F. M.; Foltz, E. L.; Woodruff, H. B. *Science* **1969**, *166*, 122-123.
(27) Christen.Bg; Leanza, W. J.; Beattie, T. R.; Patchett, A. A.; Arison, B. H.; Ormond, R. E.; Kuehl, F. A.; Alberssc.G; Jardetzk.O *Science* **1969**, *166*, 123-124.

(28) Kahan, F. M.; Kahan, J. S.; Cassidy, P. J.; Kropp, H. *Ann. NY Acad. Sci.* **1974**, *235*, 364-386.
(29) Marquardt, J. L.; Brown, E. D.; Lane, W. S.; Haley, T. M.; Ichikawa, Y.; Wong, C. H.; Walsh, C. T. *Biochemistry* **1994**, *33*, 10646-10651.
(30) Kim, D. H.; Lees, W. J.; Kempsell, K. E.; Lane, W. S.; Duncan, K.; Walsh, C. T. *Biochemistry* **1996**, *35*, 4923-4928.
(31) Garcialobo, J. M.; Ortiz, J. M. *J. Bacteriol.* **1982**, *151*, 477-479.
(32) Leon, J.; Garcialobo, J. M.; Ortiz, J. M. *Antimicrob. Agents Ch.* **1982**, *21*, 608-612.
(33) Llaneza, J.; Villar, C. J.; Salas, J. A.; Suarez, J. E.; Mendoza, M. C.; Hardisson, C. *Antimicrob. Agents Ch.* **1985**, *28*, 163-164.
(34) Arca, P.; Rico, M.; Brana, A. F.; Villar, C. J.; Hardisson, C.; Suarez, J. E. *Antimicrob. Agents Ch.* **1988**, *32*, 1552-1556.
(35) Arca, P.; Hardisson, C.; Suarez, J. E. *Antimicrob. Agents Ch.* **1990**, *34*, 844-848.
(36) Suarez, J. E.; Mendoza, M. C. *Antimicrob. Agents Ch.* **1991**, *35*, 791-795.
(37) Bernat, B. A.; Laughlin, L. T.; Armstrong, R. N. *Biochemistry* **1997**, *36*, 3050-3055.
(38) Bernat, B. A.; Laughlin, L. T.; Armstrong, R. N. *Biochemistry* **1999**, *38*, 7462-7469.
(39) Bernat, B. A.; Laughlin, L. T.; Armstrong, R. N. *J. Org. Chem.* **1998**, *63*, 3778-3780.
(40) Rife, C. L.; Pharris, R. E.; Newcomer, M. E.; Armstrong, R. N. *J. Am. Chem. Soc.* **2002**, *124*, 11001-11003.
(41) Cao, M.; Bernat, B. A.; Wang, Z. P.; Armstrong, R. N.; Helmann, J. D. *J. Bacteriol.* **2001**, *183*, 2380-2383.
(42) Newton, G. L.; Rawat, M.; La Clair, J. J.; Jothivasan, V. K.; Budiarto, T.; Hamilton, C. J.; Claiborne, A.; Helmann, J. D.; Fahay, R. C. *Nat. Chem. Biol.* **2009**, *5*, 625-627.
(43) Fillgrove, K. L.; Pakhomova, S.; Newcomer, M. E.; Armstrong, R. N. *J. Am. Chem. Soc.* **2003**, *125*, 15730-15731.
(44) Fillgrove, K. L.; Pakhomova, S.; Schaab, M. R.; Newcomer, M. E.; Armstrong, R. N. *Biochemistry* **2007**, *46*, 8110-8120.
(45) O'Brien, P. J.; Herschlag, D. *Chem. Biol.* **1999**, *6*, R91-R105.
(46) Laughlin, L. T.; Bernat, B. A.; Armstrong, R. N. *Chem-Biol. Interact.* **1998**, *112*, 41-50.
(47) Park, H.-S.; Nam, S.-H.; Lee, J. K.; Yoon, C. N.; Mannervik, B.; Benkovic, S. J.; Kim, H.-S. *Science* **2006**, *311*, 535-538.
(48) Stemmer, W. P. C. *Proc. Nat. Acad. Sci.* **1994**, *91*, 10747-10751.
(49) Rigsby, R. E.; Rife, C. L.; Fillgrove, K. L.; Newcomer, M. E.; Armstrong, R. N. *Biochemistry* **2004**, *43*, 13666-13673.
(50) Inglese, J.; Johnson, R. L.; Simeonov, A.; Xia, M.; Zheng, W.; Austin, C. P.; Auld, D. S. *Nat. Chem. Biol.* **2007**, *3*, 466-479.
(51) Inglese, J.; Shamu, C. E.; Guy, K. *Nat. Chem. Biol.* **2007**, *3*, 438-441.
(52) Coma, I.; Clark, L.; Diez, E.; Harper, G.; Herranz, J.; Hofmann, G.; Lennon, M.; Richmond, N.; Valmaseda, M.; Macarron, R. *J. Biomol. Screen.* **2009**, *14*, 66-76.

(53) Falagas, M. E.; Giannopoulou, K. P.; Kokolakis, G. N.; Rafailidis, P. I. *Rev. Anti-Infect. Agents* **2008**, *46*, 1069-1077.
(54) Beharry, Z.; Palzkill, T. *J. Biol. Chem.* **2005**, *280*, 17786-17791.
(55) Rigsby, R. E.; Brown, D. W.; Dawson, E.; Lybrand, T. P.; Armstrong, R. N. *Arch. Biochem. Biophys.* **2007**, *464*, 277-283.
(56) Brown, D. W.; Schaab, M. R.; Birmingham, W. R.; Armstrong, R. N. *Biochemistry* **2009**.
(57) Sarker, S. D.; Nahar, L.; Kumarasamy, Y. *Methods* **2007**, *42*, 321-324.
(58) Rigsby, R. E.; Fillgrove, K. L.; Beihoffer, L. A.; Armstrong, R. N. *Method. Enzymol.* **2005**, *401*, 367-379.
(59) Copeland, R. A. *Enzymes*; Wiley-VCH, 2000.
(60) Zhang, J. H.; Chung, T. D. Y.; Oldenburg, K. R. *J. Biomol. Screen.* **1999**, *4*, 67-73.
(61) Kubista, M.; Sjoback, R.; Eriksson, S.; Albinsson, B. *Analyst* **1994**, *119*, 417-419.
(62) Elemental Analysis, Inc.
(63) Wang, B. H.; Yang, W. Q.; Yan, J.; Springsteen, G.; Deeter, S. *Abstr. Pap. Am. Chem. S.* **2003**, *225*, U296-U296.
(64) Wahler, D.; Jean-Louis, R. *Angew. Chem. Int. Edit.* **2002**, *41*, 1229-1232.
(65) Cedrone, F.; Bhatnagar, T.; Baratti, J. C. *Biotechnol. Lett.* **2005**, *27*, 1921-1927.
(66) Wolf, N. M.; Morisseau, C.; Jones, P. D.; Hock, B.; Hammock, B. D. *Anal. Biochem.* **2006**, *355*, 71-80.
(67) Armstrong, R. N. *Chem. Res. Toxicol.* **1997**, *10*, 2-18.
(68) Kosower, N. S.; Kosower, E. M. *Method. Enzymol.* **1987**, *143*, 76-84.
(69) Fahey, R. C.; Newton, G. L. *Method. Enzymol.* **1987**, *143*, 85-96.
(70) Kosower, E. M.; Kosower, N. S. In *Biothiols, Pt A* 1995; Vol. 251, p 133-148.
(71) Cao, H. S.; Heagy, M. D. *J. Fluoresc.* **2004**, *14*, 569-584.
(72) Kawanishi, T.; Romey, M. A.; Zhu, P. C.; Holody, M. Z.; Shinkai, S. *J. Fluoresc.* **2004**, *14*, 499-512.
(73) Luis, G. P.; Granda, M.; Badia, R.; Diaz-Garcia, M. E. *Analyst* **1998**, *123*, 155-158.
(74) Mateo, C.; Arhcelas, A.; Furstoss, R. *Anal. Biochem.* **2003**, *314*, 135-141.
(75) Ensafi, A. A.; Dehahgi, G. B. *Spectrochim. Acta A* **2001**, *57*, 1739-1743.
(76) Maviglia, R.; Nestorini, R.; Pennisi, M. A. *Curr. Drug Targets* **2009**, *10*, 895-905.